

# Exploiting Additives for Directing the Adsorption and Organization of Colloid Particles at Fluid Interfaces

Jacopo Vialetto\* and Manos Anyfantakis\*



Cite This: <https://doi.org/10.1021/acs.langmuir.1c01029>



Read Online

ACCESS |



Metrics & More

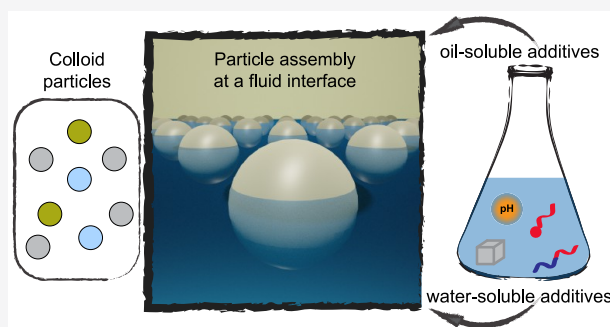


Article Recommendations



Supporting Information

**ABSTRACT:** The self-assembly of colloids at fluid interfaces is a well-studied research field both for gaining fundamental insights and for material fabrication. The fluid interface allows the confinement of particles in two dimensions and may act as a template for guiding their organization into soft and reconfigurable structures. Additives (e.g., surfactants, salts, and polymers) in the colloidal suspension are routinely used as a practical and effective tool to drive particle adsorption and tune their interfacial organization. However, some phenomena lying at the heart of the accumulation and self-assembly of particles at fluid interfaces remain poorly understood. This Feature Article aims to critically analyze the mechanisms involved in the adsorption and self-organization of micro- and nanoparticles at various fluid interfaces. In particular, we address the role of additives in both promoting the adsorption of particles from the bulk suspension to the fluid interface and in mediating the interactions between interfacial particles. We emphasize how different types of additives play a crucial role in controlling the interactions between suspended particles and the fluid interface as well as the interactions between adsorbed particles, thus dictating the final self-assembled structure. We also critically summarize the main experimental protocols developed for the complete adsorption of particles initially suspended in the bulk. Furthermore, we highlight some special properties (e.g., reconfigurability upon external stimulation and dissipative self-assembly) and the application potential of structures formed by colloid self-organization at fluid interfaces mediated/promoted by additives. We believe our contribution serves both as a practical roadmap to scientists coming from other fields and as a valuable information resource for all researchers interested in this exciting research field.



## INTRODUCTION

Because of its remarkable progress over the last decades, colloid synthesis is currently able to make particles with precisely engineered physical and chemical properties.<sup>1</sup> However, the key step toward exploiting these particles in advanced functional materials is to go beyond the single-particle level and drive their controlled organization in the bulk of host materials and at various types of interfaces. This is because of the unique properties exhibited by colloid particles organized at the nano- or microscale, which may arise from collective effects due to the interactions between neighboring particles or from intriguing structural features resulting from their hierarchical organization.<sup>1</sup>

Of particular interest is the colloid self-assembly at the interface formed between two immiscible fluids 1 and 2, where 2 can be either a gas or a liquid (e.g., air or oil), whereas 1 must be a liquid (typically water). This is an extensively studied yet still highly active research field for several reasons. From a fundamental perspective, the classic utility of colloids is to serve as the micrometer-scale analogue of atoms.<sup>1</sup> The fluid interface easily ensures the two-dimensional (2D) confinement of colloids, and it is exploited to study, directly and in real time, physical phenomena occurring in two dimensions using

methods as simple as optical microscopy.<sup>2</sup> Besides exploring fundamental phenomena such as crystallization and glass transition, the physics of 2D colloidal systems at fluid interfaces is particularly interesting because of the wealth of interactions involved.<sup>3,4</sup> In addition to forces governing the interactions between particles suspended in a solvent, particles at fluid interfaces are subject to forces that arise *because of* the presence of the interface. These forces depend on both the chemical and geometrical characteristics of the particles and the physical properties of the fluid phases. From a more practical viewpoint, particle assembly at fluid interfaces allows for manufacturing materials with remarkable physical and chemical properties (and hence functionality) that can be tailored on demand. A significant advantage of interfacial assembly compared to common top-down patterning strategies is that it is a

Received: April 15, 2021

Revised: June 17, 2021

Table 1. Overview of Formulations (Colloid Particles + Additives) Used to Form 2D Particle Assemblies at Fluid Interfaces<sup>a</sup>

additives	building blocks	transport mechanism	notes	ref
salts	metal NPs	centrifugation	oil phase denser than water	11
		emulsification	salts can be dissolved in water or in the organic phase	6, 16–18
	PS (few $\mu\text{m}$ )	diffusion	air–water interface	19, 20
pH	metal NPs	centrifugation	pH-dependent ionizable surface groups	11
	anionic (1.9 $\mu\text{m}$ ) or cationic (2.6–0.4 $\mu\text{m}$ ) PS	solvent evaporation or emulsification		14, 21
	PS (5 $\mu\text{m}$ )	sedimentation or diffusion	surfactant may (high $C_s$ ) or may not (low $C_s$ ) modify particle surface properties	9, 22
surfactants	silica (2 $\mu\text{m}$ to 300 nm)	sedimentation		12
	metal NPs	sedimentation or emulsification		12, 23
	PS (500 nm)	solvent evaporation	surfactants modify NP properties	24
	silica or PS NPs	diffusion, emulsification, or foam formation		25–28
polymers	anionic NPs	diffusion	formation of NP–polymer complexes at the fluid interface	29, 30
alcohols	Au NPs	diffusion + flows	alkane–water interface	31, 32
	Pt (3 nm), silica (200 nm)	sonication		33
lipids	DNA-coated NPs	diffusion	unclear if NPs adsorb onto the interface	13
others	Au NPs	diffusion + evaporation or emulsification	reactions involving Au NP ligands	32, 34–36

<sup>a</sup>The particle diameters are listed in parentheses. PS, polystyrene; NPs, nanoparticles having diameters from a few nanometers to 100 nm; and  $C_s$ , surfactant concentration.

straightforward yet precise, reproducible, cost-effective, and scalable way<sup>5</sup> of obtaining elaborate functional structures, including reversible plasmonic mirrors<sup>6</sup> and bijels,<sup>7</sup> for photonics and catalysis applications, respectively.

Both the plethora of interactions that govern colloid self-assembly at fluid interfaces and the practical advantages of this strategy for engineering advanced materials mentioned above are direct consequences of two physical effects that are *unique* to particles adsorbed at fluid interfaces. First, particles with radius  $R_p$  larger than about 5 nm have adsorption energies  $E_{\text{ads}}$  that can reach  $\sim 10^3 k_B T$  ( $k_B$ , Boltzmann's constant;  $T$ , absolute temperature).<sup>8</sup> As a result, particle adsorption is irreversible under normal laboratory conditions and the interfacial particles may be considered to be “locked” in 2D: although they can freely move in the plane of the interface, their motion in the direction perpendicular to the interface is not allowed. What is more interesting, and a distinctive feature of fluid interfaces, is that colloid structures formed there can be dynamically tuned. Indeed, the lateral mobility of particles allows one to rearrange them upon external stimulation, creating novel materials that can be reconfigured via tuning interparticle interactions/organization. Such a strategy is powerful for achieving a long-sought goal in materials science: the creation of materials, the structure and hence the functionality of which can be reconfigured on demand.<sup>6,9</sup>

Besides the particles and the solvent, a third component commonly present in suspensions is additives, which are routinely used as a practical tool to drive particle adsorption at a fluid interface and tune their subsequent organization. Here we call any substance that is present in the colloidal suspension, other than the solvent and the particles, an additive. Usually, additives are deliberately introduced into a colloid for various purposes: for instance, surfactants are frequently used to ensure the stability of the suspensions against aggregation or sodium azide is added as a bacteriostatic preservative. Importantly, in some cases additives can unintentionally be part of the suspension composition (e.g., in the form of unreacted monomers from the synthesis). In either case, additives can have a dramatic effect on both the interactions between

suspended particles and the fluid interface, which can lead to particle adsorption, and between adsorbed particles, which will eventually define the structure of the formed colloid assembly. Because of this, the introduction of additives into ordinary suspensions can provide perhaps the most straightforward way of achieving self-organization without the need for more complicated materials and/or methods. While this strategy is well developed for producing foams and emulsions,<sup>10</sup> it is now also gaining much attention for the fabrication of 2D materials with controlled particle arrangements.<sup>9,11,12</sup> For many practical applications, such materials formed at a fluid interface are then transferred to a solid substrate. Although we do not focus on this rich field of study here, we refer to several relevant examples of this important process throughout this paper.

This Feature Article is organized as follows. We begin by discussing the transport mechanisms that bring particles into the proximity of a fluid interface and then describe various experimental procedures that are used to efficiently accumulate particles at interfaces. We then analyze the fundamental phenomenon of the interaction between a particle that is suspended in a good solvent and the interface the latter makes with a second immiscible fluid. After briefly describing the types of forces at work, we specifically investigate the influence of various additives (e.g., electrolytes, surfactants, and lipids) on the particle–interface interaction. We highlight the case in which this interaction is favorable because this is the driving force for particle adsorption at the fluid interface and thus the occurrence of a true 2D colloidal system. In the second part, we briefly discuss the interactions between interfacial particles, which is the basic phenomenon that defines the phase behavior of the 2D colloidal system. We emphasize how different additives modulate the particle properties and interparticle interactions, thus dictating the structural properties of the final self-assembled structure. The final part is concerned with the special properties and the application potential of structures formed by 2D colloid organization promoted or mediated by additives. We first discuss chemical stimulation: how the system composition can be modulated to achieve the desired interactions. We then highlight an interesting alternative:

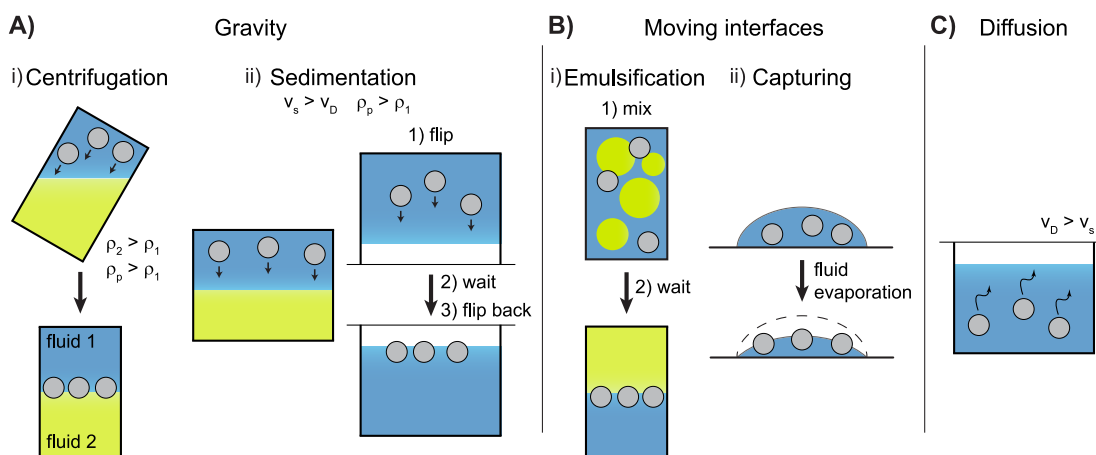


**Figure 1.** Main methods and mechanisms for transporting particles from the bulk of a suspension to the fluid interface it forms with another immiscible fluid. (A) Gravity-driven transport methods: centrifugation and sedimentation. Alternatively, if  $\rho_1 > \rho_p$ , then buoyancy can drive particle motion toward an upper fluid surface. ( $\rho_1 > \rho_2$ ). (B) Transport methods based on the creation and/or motion of fluid interfaces that capture the dispersed particles: emulsification and a descending air–water interface due to solvent evaporation. (C) Particle movement toward an interface due to diffusion.

exploiting stimuli-responsive additives (e.g., photosensitive surfactants) to convert an otherwise inert colloidal dispersion to an externally controlled system. Although our main focus is on macroscopically flat rather than strongly curved fluid interfaces (of practical interest for applications involving long-range-ordered structures), in some instances we highlight the results from the rich literature<sup>10</sup> on foams and emulsions to illustrate the relevant physical mechanisms at work.

## ■ INTERACTIONS OF PARTICLES WITH A FLUID INTERFACE AND THE INFLUENCE OF ADDITIVES

A prerequisite for realizing a 2D colloidal system at a fluid interface, regardless of the exact type and properties of the particles and the fluids involved, is that the particles are able to (i) be transported to the interface and (ii) penetrate the interface and adsorb there. We analyze the influence of additives on both of these steps for a plethora of representative systems that have been investigated so far (Table 1). Various transport mechanisms are able to bring particles near the fluid interface (step (i)). These can be spontaneous processes, such as Brownian motion, sedimentation, and buoyancy, or induced externally by supplying energy to the system via processes such as centrifugation and emulsification (Figure 1) or by applying electric fields (SI). Additives in colloids are usually present in such low concentrations that they practically do not affect the transport mechanisms. However, the situation is different when additives are surface-active; in this case, Marangoni flows that are caused by surface tension gradients at the fluid interface can cause convective flows in the bulk of the suspensions. Any type of hydrodynamic flow, if strong enough, may influence or even induce particle transport to the interface.

Once the transport step (i) is achieved and particles are brought near the interface, the two will interact. Depending on the net interaction potential, the particles can be repelled from or attached at the interface. A purely 2D colloid system contains particles that can move only in the plane along the interface (i.e., in  $x$ ,  $y$ ) and not perpendicular to it. Such systems are realized when particles are *adsorbed* at fluid interfaces. Most often, the term “particle adsorption” is used to describe particles that penetrate the fluid interface, therefore making a finite contact angle with it;<sup>8</sup> we also adopt this terminology here. This is qualitatively different from particles that sit on liquid–solid

interfaces<sup>1</sup> or even at fluid interfaces but without being immersed in both phases.<sup>13</sup> Additives play a dramatic role in mediating the net interaction potential between the particles and the fluid interface. This may be achieved by reducing or eliminating energy barriers that prohibit the two coming close enough through either particle surface modification or the promotion of favorable particle–interface interaction without changing the particle properties. We note that, in several papers where particles are employed as foam or emulsion stabilizers, a precise understanding of the effect of additives in suspension is confounded by the experimental procedure adopted to mix the fluids. Indeed, the adsorption barrier can be overcome by providing an additional hydrodynamic force (through turbulent mixing) that pushes the particles toward the interface. The strength of mixing allows particle adsorption in cases where weaker or absent mixing fails to produce a Pickering emulsion.<sup>14</sup> In this article, we put emphasis on the case where particle adsorption at the fluid interface takes place spontaneously, without the use of external forces. Notably, the way that particles are brought to the interface affects their adsorption behavior and hence their self-organization.<sup>15</sup> We concentrate on flat interfaces as model systems to understand how both adsorption and organization are influenced by added chemicals. However, we frequently use examples from the literature on the mature field of foams and emulsions to better illustrate the mechanisms at work.

### Mechanisms That Transport Particles to the Interface.

Various experimental configurations exploit gravity for driving particles toward a fluid interface. In a dilute suspension, each particle is essentially isolated from the others and its terminal velocity is given by Stokes’ law,<sup>37</sup> which considers the balance between the gravitational force and the viscous drag. For a single spherical particle of radius  $R_p$  and density  $\rho_p$ , the Stokes velocity  $V_{St}$  is

$$V_{St} = \frac{2R_p(\rho_p - \rho_1)g}{9\eta} \quad (1)$$

where  $g$  is the gravitational acceleration and  $\eta$  is the dynamic viscosity of the solvent. The particles will move downward when their density is higher than that of the solvent, while they will move upward in the opposite case ( $\rho_p < \rho_1$ ). If a suspension forms an interface with a second immiscible fluid ( $\rho_2$ ), then gravity can transport particles to the interface when (Figure 1A)

- both densities of the particle and the second phase exceed that of the solvent ( $\rho_2 > \rho_1$  and  $\rho_p > \rho_1$ ),
- the particle density is lower than that of the solvent, and
- the particle density is higher than that of the solvent but the solution is flipped upside-down.

Equation 1 shows that the effectiveness of gravity in bringing particles to the interface is increased when (i) the density mismatch between the particle and the solvent is increased, (ii) the particle size increases, and (iii) the solvent viscosity decreases. In conclusion, gravity, via sedimentation, and buoyancy are efficient driving forces for the interfacial accumulation of particles, provided they overcome diffusion.

Diffusion is an ever-present physical phenomenon in suspensions and perhaps is the most exploited transport mechanism for driving small particles to a fluid interface. Contrary to gravity, diffusion becomes more important with decreasing particle size. A simple way to quantify the competition between gravity and diffusion is to calculate the Péclet number for particle transport,  $Pe$ , given by

$$Pe = \frac{R_p V_{St}}{D} \quad (2)$$

where  $D$  is the diffusion coefficient. This dimensionless number indicates the relative importance of particle motion due to gravity and particle transport due to diffusion at a length scale on the order of  $R_p$ . To illustrate its use, we apply it to the well-studied example of aqueous suspensions of PS particles, where  $\rho_1 = 0.997 \text{ g}\cdot\text{cm}^{-3}$ ,  $\rho_p = 1.055 \text{ g}\cdot\text{cm}^{-3}$ , and  $\eta = 8.90 \times 10^{-4} \text{ Pa}\cdot\text{s}$  at  $T = 298 \text{ K}$ . Assuming that the hydrodynamic radius is equal to  $R_p$ , we find that  $Pe = 1$  for particles with  $R_p \approx 12 \text{ nm}$ . This calculation tells us that water-suspended PS particles with  $R_p$  from a few nanometers to  $\sim 50 \text{ nm}$  will be mostly transported by diffusion and that gravity is insignificant. Instead, for  $R_p \gg 50 \text{ nm}$ , sedimentation will dominate and the particles will precipitate to the bottom within a time that can be estimated by eq 1.

**Gravity-Driven Transport Mechanisms.** Anyfantakis et al. devised a simple method to induce particle transport from the bulk to the air–water interface by exploiting sedimentation.<sup>22</sup> They prepared mixtures of anionic micro- or nanoparticles (PS or silica) with small amounts of ordinary cationic surfactants (dodecyltrimethylammonium bromide, DTAB, or hexadecyltrimethylammonium bromide, CTAB) in cylindrical chambers. Then, they inverted the chamber and left it in this position for a time adequate to allow particles to reach the air–water interface by sedimentation (eq 1). Thanks to the small diameter of the chamber (7 mm), the suspension was held in place by capillary forces that overcame the liquid weight. In the next step, the chamber was inverted back to its initial position and gravity brought the particles to the center of the fluid interface due to the concave meniscus shape. This is a practical and efficient way to bring all suspended particles near the air–water interface. Furthermore, it was also efficient in transporting smaller particles (diameters down to  $D_p = 100 \text{ nm}$ ) made from various materials (metals, silica) to the interface, provided that the flipping time was chosen accordingly.<sup>12</sup> However, the major drawback remains that only small sample cells can be used.

When the density mismatch between the particles and the solvent is small or if the particles are too small to sediment within the time scale of the experiment, centrifugation may be used to speed up particle movement toward the interface. Turek et al. employed centrifugation to drive the adsorption of Au NPs ( $D_p$

$= 16 \text{ nm}$ ) dispersed in aqueous suspensions at the interface with 1,2-dichloroethane (DCE). This allowed the authors to subsequently tune their self-assembly into monolayers with controlled interparticle spacing.<sup>11</sup> This experimental approach is a simple, fast, and efficient way to transport NPs to the fluid interface. However, if aqueous suspensions are to be used, then the oil phase, besides being immiscible with water, must be denser than it. These requirements could be fulfilled also for other solvents that contain heavy atoms, but this remains to be demonstrated. Nevertheless, such solvents are generally toxic, harmful, and costly if one considers their large-scale use.

Buoyancy is another force that can efficiently bring particles into the vicinity of a fluid interface. Surprisingly, experiments exploiting this transport mechanism are rare, which may be attributed to inorganic particles having densities that cannot be outweighed by conventional solvents. However, the condition  $\rho_1 > \rho_p$  required for buoyancy to push particles toward the interface of liquid 1 with an immiscible fluid 2 can be satisfied for polymeric particles. Common strategies for increasing the density of water, such as the addition of salt or other solutes such as glycerol, are typically not applicable if one wishes to control particle adsorption and organization at a fluid interface. This is due to problems such as the destabilization of the suspension and the viscosity increase (that in turn decreases  $V_{St}$ ). Wang et al. overcame this problem by dispersing PS particles in heavy water ( $\rho = 1.10 \text{ g}\cdot\text{cm}^{-3}$  at  $T = 298 \text{ K}$ ). When this dispersion was capped with hexadecane, the PS particles spontaneously moved toward the oil–water interface due to buoyancy. This clever solution was used to determine if the PS particles were adsorbed at the fluid interface. After particle migration to the interface,  $D_2O$  was replaced with  $H_2O$ : adsorbed particles stayed at the interface, whereas nonadsorbed ones sedimented to the bottom.<sup>14</sup>

**Diffusion-Driven Transport Mechanisms.** In an early study, Williams and Berg<sup>19</sup> identified diffusion as the main transport mechanism responsible for PS particle migration to the interface of air with aqueous NaCl solutions. Although the authors noted that the geometry of their sample cell, combined with their effort to diminish evaporation, was effective at minimizing convective flows, they mentioned that irreproducibility in the measured rates of particle adsorption may be attributed to noneliminated convection.<sup>19</sup> In subsequent investigations of particle adsorption at the air–water interface, Abdel-Fattah and El-Genk<sup>20,38</sup> used a similar experimental setup that was optimized to minimize convective flows. In all of these studies, NaCl was used to enable particle adsorption (PS,  $D_p = 1.01 \mu\text{m}$ ) to the fluid interface, which is not expected to affect the diffusion coefficient of the particles at the concentrations used (0 to 1 M). Although electrolytes at these concentrations reduce the surface tension of the air–water interface (by  $\sim 1$  to  $2 \text{ mN}\cdot\text{m}^{-1}$ , enough to cause Marangoni flows that can drag particles), these authors did not report such an effect.<sup>19,20,38</sup> When micrometer-sized particles are used, substantial sedimentation should be expected, despite the authors noting it as insignificant. Therefore, diffusion may be considered to be an inefficient transport mechanism for large particles.

Diffusion is routinely used as an efficient transport mechanism for suspensions of NPs; several such examples are reported throughout this Feature Article. Indeed, for small particles diffusion alone can be sufficient for complete coverage of the interface within the time scale of the experiment. For example, Duan et al. observed that the addition of toluene to aqueous suspensions of Au ( $D_p = 5\text{--}12 \text{ nm}$ ) and Ag ( $D_p = 10\text{--}40 \text{ nm}$ )

NPs caused their spontaneous transport and self-assembly into monolayers at the toluene–water interface. The efficiency of Brownian motion to bring the particles to the interface can be explained by the small NP size. Additional energy input by gentle shaking of the samples was found to accelerate the process.<sup>39</sup> In a follow-up study, Li et al. used a slightly modified version of the above method to adsorb Pt ( $D_p = 3.3$  nm) and SiO<sub>2</sub> NPs ( $D_p = 200$  nm) at a toluene–water interface. These authors employed gentle sonication to accelerate the interfacial assembly of NPs in the presence of ethanol.<sup>33</sup> The mechanisms that transported NPs to the fluid interface and the influence of ethanol on them have not been discussed. For example, Marangoni flows driven by interfacial tension gradients should be present, which could also lead to convection inside the liquid phases. Furthermore, the reported formation of small bubbles during ethanol addition<sup>33</sup> could facilitate NP transport to the toluene–water interface as bubbles ascended toward the oil phase due to buoyancy. The observation that the rate of ethanol injection was crucial in defining the structure of the resulting NP monolayer<sup>33</sup> might be related to the above effects. Finally, one must note that ethanol is miscible with toluene; therefore, flows associated with mixing could also drive NPs toward the oil phase. This may be supported by the conclusion of Li et al. that the presence of toluene, before the addition of ethanol, should be considered to be a key factor in the formation of these assemblies.<sup>33</sup> Furthermore, sonication, which is often used in processes involving particle adsorption, such as foam formation,<sup>26</sup> might affect particle transport to the interface. We conjecture that all of these effects might facilitate the interfacial accumulation of NPs, especially in the case of the relatively heavy SiO<sub>2</sub> NPs used.<sup>33</sup>

#### *Transport Mechanisms Involving Moving Fluid Interfaces.*

Bigioni et al. followed in real time the self-assembly of dodecanethiol-ligated Au NPs ( $D_p = 6$  nm) at the top surface of a drying toluene sessile drop containing excess dodecanethiol. During evaporation, islands of Au NPs formed at the free interface of the drop, which later merged to form a macroscopic NP layer that spanned the entire air–toluene interface. The kinetics of solvent evaporation had a strong impact on the self-assembly process: no monolayer was formed when the evaporation rate was slowed down substantially. Quick evaporation was instead a key requirement for the process because it ensured that the descending fluid interface was able to efficiently segregate NPs in its proximity. The authors developed a simple model based on two parameters, the NP flux toward the fluid interface and the interfacial diffusion length that NPs could cover, which was able to capture the kinetics and the energetics of the drying-mediated NP self-assembly phenomenon.<sup>34</sup> The authors also highlighted the importance of controlling the interaction between particles and the fluid interface if one wished to fabricate ordered monolayers (Figure 4B). This often-overlooked concept is discussed in the next section. Anyfantakis et al. observed a similar phenomenon in drying drops of aqueous suspensions of anionic PS particles ( $D_p = 500$  nm) mixed with cationic surfactants. At intermediate surfactant concentrations, surfactant adsorption onto the particles increased their affinity for the air–water interface. Under this condition, upon water evaporation, the fluid interface descended toward the supporting solid substrate and all particles in contact with the interface adsorbed onto it. As a result, upon further water loss, all particles were gradually accumulated at the fluid interface. Upon complete evaporation, the particle-laden interface was deposited on the substrate, leading to uniform deposits.<sup>24</sup> The authors

estimated that diffusion could account only for a small number of particles reaching the interface within the time scale of the experiment. They suggested that this “sweeping” mechanism was instead the dominant effect. Such a mechanism is frequently observed in drying suspensions, provided that the motion of the fluid interface is faster than particle motion due to diffusion, as confirmed by subsequent studies.<sup>40</sup>

Apart from the examples of a descending fluid interface due to solvent evaporation, an external supply of energy can be used to promote particle–interface contacts. This can be achieved by increasing the interfacial area through the creation of drops or bubbles, which are then mixed in solution to collect suspended particles. In a subsequent study by the Edel group, Cecchini et al. devised another simple method to transport NPs to the oil–water interface and create NP arrays for multiphase trace analyte detection.<sup>17</sup> By briefly yet vigorously shaking a tube containing an aqueous Au NP suspension and DCE, an unstable emulsion with the NPs attached at the liquid interface was formed. After shaking, the poorly stabilized emulsion quickly separated into the two single phases, with the NPs remaining self-assembled at the planar oil–water interface formed. This emulsification process accelerated the diffusion-controlled transport of NPs to the liquid interface by reducing the average distance between the two.<sup>17</sup> A similar emulsification process has also been used by the Bell group to adsorb various types of NPs<sup>5,16</sup> to the liquid interface, as discussed later. Their experimental protocol was based on vigorously shaking an aqueous NP suspension in contact with an immiscible oil, in the presence of a small amount of salts that had hydrophobic ions with charge opposite to that of the NPs. This led to the formation of unstable, NP-decorated emulsion drops, the coalescence of which resulted in an NP film at the planar macroscopic liquid interface.<sup>16</sup> Interestingly, such a pseudoemulsification method does not demand the use of organic liquids with specific density values (as for centrifugation<sup>11</sup>). This was demonstrated by using common solvents, which served as the oil phase.<sup>16</sup> It is worth noting that the reports from both the Edel<sup>17</sup> and Bell<sup>5,16</sup> groups do not contain details of the emulsification process or information about the nature of the unstable emulsions. We believe that further investigation will lead to valuable insights into the accumulation of NPs on the (resulting) planar liquid interface, which is an integral part of this practically useful self-assembly method that does not require any special equipment.

Lin et al. recently demonstrated a highly efficient strategy for forming assemblies at oil–water interfaces that is applicable to a broad range of NPs, provided they can be dispersed in halogenated solvents.<sup>41</sup> Their strategy consisted of first dispersing the NPs in a solvent denser than water (e.g., dichloromethane, DCM). Particle adsorption onto the interface was then achieved by vigorous mechanical shaking that led to the formation of unstable oil drops in the aqueous phase. Upon phase separation, a random, non-close-packed monolayer was formed at the fluid interface. In a second step, a second oil that was lighter than water (e.g., hexane) was added to the system, which led to the transfer of NPs from the bottom to the top oil–water interface and to the compression of the NPs into a dense monolayer. These were attributed to the emergence of Marangoni stresses that resulted from the surface tension ( $\gamma$ ) gradient between the two oil–water interfaces.<sup>41</sup> A value of  $\Delta\gamma \geq 7.8$  mN·m<sup>-1</sup> between the two oil–water interfaces was required to promote climbing of the NPs and compression into a close-packed monolayer. Interestingly, this study highlights the advantages of combining multiple transport mechanisms

(emulsification and flows) for the interfacial assembly of NPs in a simple, generic, and cost-effective fashion.

**Interactions between Suspended Particles and the Interface.** Colloid particles tend to adsorb at fluid interfaces, and this is one of the main reasons for their efficiency in stabilizing such interfaces. This tendency may be understood by considering the thermodynamics of adsorption. The energy of a fluid interface is reduced when a particle adsorbs onto it because a portion of the fluid–fluid interface (typically of high interfacial tension) is replaced by a particle–fluid interface (normally of lower interfacial tension).<sup>8,42</sup> Therefore, particle adsorption is energetically favorable. This energy reduction  $\Delta E$  is directly proportional to the surface area of the fluid interface replaced by the particle; it is thus proportional to  $R_p$  and contact angle  $\theta$ , as described by

$$\Delta E = E_{\text{ads}} = \pi R_p^2 \gamma (1 \pm \cos \theta)^2 \quad (3)$$

We may consider that  $\Delta E$  is the amount of energy required to remove (i.e., desorb) an adsorbed particle from the fluid interface. Note that the sign inside the parentheses is negative (respectively positive) for particle desorption to phase 2 (respectively 1).<sup>8</sup> It can be seen from eq 3 that the highest  $\Delta E$  (i.e., the most efficient stabilization) is obtained for intermediate  $\theta$  values with a maximum for  $\theta = 90^\circ$  and for  $R_p$  larger than a few nanometers.<sup>8</sup> In this Feature Article, we focus mostly on cases in which particles, if they pierce the interface, remain irreversibly adsorbed. While thermodynamics can explain why particles are strongly attached at fluid interfaces, the process of adsorption is somewhat more complex and may be hindered in many colloidal systems. When a suspended particle reaches the fluid interface, it must overcome an energy barrier that prevents its adsorption.<sup>42,43</sup> This adsorption barrier stems from the total interaction potential between the particle and the fluid interface, which results from several contributions (e.g., van der Waals (vdW), electrostatic interactions, and image charge effects (Figure 2)).

van der Waals interactions have a substantial impact on a colloidal system because they are always present and can be of significant strength at both small and large distances. The vdW

interaction energy between a spherical particle of radius  $R_p$  and a flat surface can be expressed as the product of a geometrical factor and the Hamaker constant  $A$ , which describes the integrated molecular interactions

$$W_{\text{vdW}} = -\frac{AR_p}{6d} \quad (4)$$

where  $d$  is the distance between the particle edge and the surface. This general expression is valid regardless of the theoretical approach used to compute  $A$  (SI).<sup>44</sup> If one considers the vdW interaction of an object made from material 3 ( $A = A_{33}$ ) with another object of material 2 ( $A_{22}$ ), both suspended in a medium of material 1 ( $A_{11}$ ), then the following expression, proposed by Hamaker, can be used to calculate the effective Hamaker constant  $A_{312}$  that describes this interaction:<sup>37</sup>

$$A_{312} = (\sqrt{A_{33}} - \sqrt{A_{11}})(\sqrt{A_{22}} - \sqrt{A_{11}}) \quad (5)$$

In the common case of two particles of the same material suspended in a solvent, the vdW interaction is attractive because the corresponding Hamaker constant is always positive. However, the situation is different when a particle interacts with a fluid interface. As both the simple (eq 5) and the more elaborate expressions (SI) indicate,  $A_{312}$  can be either negative or positive, corresponding respectively to vdW repulsion or attraction, depending on the dielectric properties of the three media. To illustrate this in a direct way, we apply eq 5 to the commonly studied system of PS particles (material 3,  $A_{33} \approx 6.58 \times 10^{-20}$  J) dispersed in water (material 1,  $A_{11} \approx 3.70 \times 10^{-20}$  J). By using  $A_{33} = A_{22}$ , we find  $A_{312} = 0.42 \times 10^{-20}$  J; this positive value indicates that the two particles will be attracted to each other. If we now consider a single PS particle in water, interacting with air (material 2,  $A_{22} \approx 0$ ), then we obtain  $A_{312} = -1.25 \times 10^{-20}$  J. Hence, the colloid particle experiences a repulsive vdW force from the air–water interface.

Electrostatic interactions between a fluid interface and a suspended particle emerge because both the particle surface and the fluid interface can carry electric charges. Various mechanisms are responsible for charging the surface of a particle, such as the ionization of functional end groups, ion exchange between the particle surface and the surrounding solvent, and the adsorption of charged molecules. Some of these mechanisms can also cause charging of the fluid interface. In fact, several experimental studies have shown that both air–water and oil–water interfaces are negatively charged, although the existence and origin of this charge are still a matter of debate.<sup>45</sup> Studies on the stability of thin water films on substrates coated with polyelectrolytes carrying negative or positive charge have shown that in the latter case rapid film rupture was observed, indicating the presence of a negative charge.<sup>46</sup> Electrophoretic mobility measurements in pure (i.e., surfactant-free) oil drops dispersed in water showed that the oil–water interface is negatively charged as well.<sup>47</sup> Finally, by following the deprotonation of a carboxylic acid by the nebulization of its aqueous solution and analyzing the surface of the resulting droplets by electrospray ionization mass spectrometry, hydroxide ions on the surface of water were detected.<sup>48</sup>

The theoretical description of the electrostatic interactions between dispersed particles is available in textbooks,<sup>37,44</sup> and it will be discussed here only briefly. The electrostatic interaction between two approaching particles is essentially described by the interaction between their surrounding electric double layers. This is well-established for the case of two interacting objects of

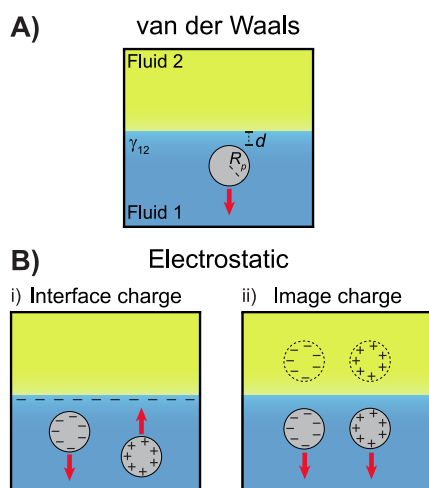


**Figure 2.** Main interactions between a suspended particle and a fluid (air–water or oil–water) interface. (A) van der Waals repulsive interaction. (B) Electrostatic interactions depending on the particle charge. (i) Interaction between charged particles and a charged fluid interface. (ii) Electrostatic interactions between charged particles and the image charge formed in the apolar phase.

the same geometry, with identical surface charge (or potential). The electrostatic interaction between a charged particle and a charged interface does not fall into the above category, and the required electrostatic conditions at the interface are not always precisely known.<sup>49</sup> Wang et al. used the linear superposition approximation to calculate the electric double layer potential accounting for the interaction of a particle with an oil–water interface. In this case, the energy of interaction arises from the exact solution to the linearized Poisson–Boltzmann equation, assuming the boundary condition of charge regulating surfaces, and is given by<sup>14</sup>

$$W_{\text{EDL}} = 2\varepsilon_0\varepsilon_1\kappa\psi_3\psi_2e^{-\kappa d} \quad (6)$$

where  $\varepsilon_0$  is the vacuum permittivity,  $\varepsilon_1$  is the dielectric constant of water,  $\kappa^{-1}$  is the Debye length, and  $\psi_3$  and  $\psi_2$  are the surface potentials of the particle and the oil phase, respectively.

A special case of electrostatic interaction between a particle and a fluid interface arises due to image charge effects, which are significant when the two fluids have a large difference in their dielectric constants. A particle that is suspended in fluid 1 and carries a charge  $q$  will interact with a fluid interface at a distance  $d$ , as if there is an image charge  $q'$  at distance  $2d$ . The latter can be described by<sup>14,44</sup>

$$q' = q \frac{\varepsilon_1 - \varepsilon_2}{\varepsilon_1 + \varepsilon_2} \quad (7)$$

For the most common case of charged particles dispersed in an aqueous phase ( $\varepsilon_1$ ) and interacting with an interface formed with air or oil ( $\varepsilon_2$ ),  $\varepsilon_1 > \varepsilon_2$  and the image charge interaction is repulsive. Note that this interaction will always be repulsive, regardless of the actual charge of the particle (Figure 2B). As in the case of real charges, it can be screened by increasing the electrolyte concentration. Interestingly, if the particle is suspended in the fluid of lower dielectric constant, then the sign of the image charge is opposite to that of the particle and the resulting interaction is attractive. Williams and Berg<sup>19,49</sup> considered the interactions between PS particles and the air–water interface to be a case of sphere–half space interaction. They assumed that the air phase was a perfect dielectric and that the air–water interface had no charge, which is the equivalent of the interaction of the electric double layer of the particle with its image across the interface. On the basis of this image charge interaction, the calculated potential was

$$V_{\text{el(im)}} = \left( \frac{64\pi R_p n_0 k_B T V_0^2}{\kappa^2} \right) e^{-2\kappa d} \quad (8)$$

where  $n_0$  is the electrolyte concentration (in  $\text{m}^{-3}$ ),  $V_0 = \frac{e^A - 1}{e^A + 1}$ , and  $A = \frac{zeV_{\text{Stern}}}{2k_B T}$ . Here,  $z$ ,  $e$ , and  $V_{\text{Stern}}$  are the ionic charge, the electron charge, and the Stern potential, respectively.<sup>49</sup> In a remarkable experiment, Chaikin and co-workers<sup>50</sup> studied the interaction of PMMA particles dispersed in a mixture of cyclohexyl bromide and *cis*-decalin with the interface formed with water. The particles were grafted with poly(12-hydroxystearic acid), and the macroscopic contact angle at a PMMA surface was found to be close to  $180^\circ$ . Although the particles were not adsorbed, the image charge effect at the fluid interface pulled the particles to the phase boundary, forming a permanently bound monolayer of almost nonwetting particles. Interestingly, this system allowed for decoupling wetting and

electrostatic effects at work in the interaction between particles and the fluid interface.

Other forces can also contribute to the total interaction potential between a particle and a fluid interface. These include structural forces that emerge due to the structuring of solvent molecules between the interacting surfaces and the hydrodynamic drainage of the liquid film that separates the interacting surfaces (SI). As a last remark, we here consider only the case in which a single particle interacts with a fluid interface free of adsorbed particles. It is important to clarify that once particles have already adsorbed at the interface, interactions between suspended particles and interfacial particles also occur.<sup>43</sup> Notably, when particles are stabilized with polymer brushes or consist of cross-linked polymers partially soluble in one of the two fluids (e.g., microgels),<sup>51,52</sup> they may spontaneously overcome the energy barrier and adsorb at the interface, even in the absence of introduced additives. Similar to the linear polymers that constitute them, these particles significantly decrease the interfacial energy upon adsorption. This is a direct consequence of their softness and deformability; stretching and spreading of the polymer chains in the plane of the interface render the adsorbed state thermodynamically more favorable than the bulk dispersion and drive their adsorption onto the fluid surface.

To summarize, in typical experiments in which particles are well stabilized in the aqueous phase, the adsorption of such particles at fluid interfaces is usually prevented. It is for this reason that, in both basic research and industrial applications, various types of additives are added to one or both of the constituent fluids. Additives allow the particles to overcome adsorption barriers and promote their attachment to a fluid interface. This may be achieved via the additive-induced *in situ* modification of the particle surface. Alternatively, additives can mediate the particle–fluid interface interaction, leaving the particle surface properties unaffected (usually termed *in situ* promotion).<sup>53</sup> In the following sections, we explain how additives can accomplish the above by illustrating examples of the relevant literature.

**Additive-Enhanced Particle Adsorption to the Interface through Particle Surface Modification.** The *in situ* surface modification of particles refers to the alteration of their surface properties due to interactions with additives introduced into the system. When suspensions form a fluid interface with a second immiscible fluid, this is typically achieved by dissolving a surface-active additive in either fluid. The particle–additive complexation can lead to a drastic change in the particle surface charge and/or wettability with respect to both fluid phases. As analyzed above, these properties dictate the interaction potential between the particles and the interface, and proper tuning of this potential by choosing the appropriate type and concentration of additive results in overcoming adsorption barriers.

**Case of Surfactants.** Using surfactants to promote particle adsorption onto a fluid interface has a long history that largely stems from froth flotation, a process used by the mining industry to recover minerals containing valuable materials from gangue (the commercially unimportant part of an ore deposit).<sup>53</sup> For this purpose, surfactants are added to the aqueous slurry of mineral particles, which is then aerated to form a froth. The particles adsorb to the bubbles and ascend to the top surface of the slurry, where they are accumulated continuously. In this way, particles are efficiently separated from the suspension. Early experiments correlated the adsorption of surfactant onto hydrophilic particles with an increase in  $\theta$  and hence an

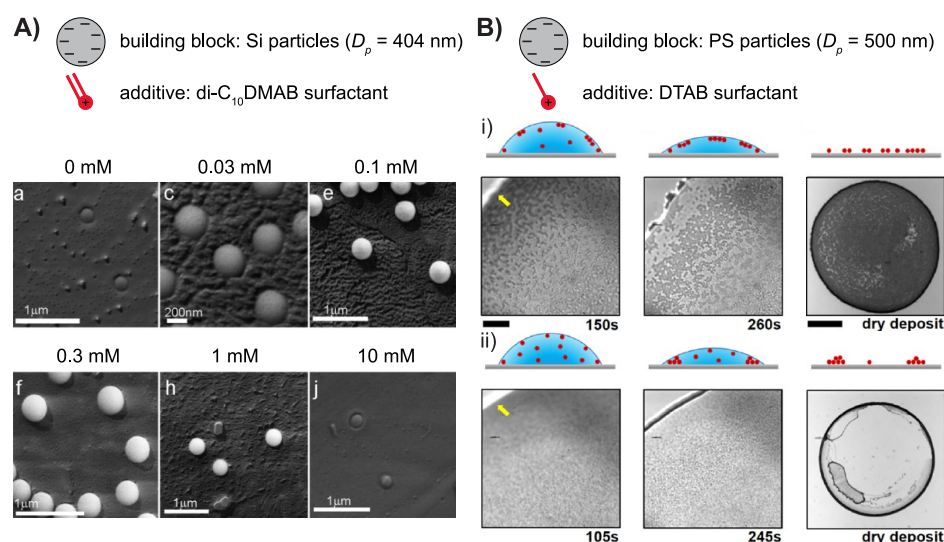


**Figure 3.** Additive-enhanced particle adsorption at a fluid interface via particle surface modification by surfactant addition. (A) FreSCa cryo-SEM images of Si NPs adsorbed at the decane–water interface at different concentrations of di- $C_{10}$ DMAB cationic surfactant. The visible portion of the NPs was originally exposed to decane. Adapted with permission from ref 58. Copyright 2013 American Chemical Society. (B) Images during the evaporation of a drop containing anionic PS particles with (top row, (i)) and without (bottom row, (ii)) 0.025 mM DTAB. The focal plane was kept at the free surface of the drop. In the presence of surfactant, particles accumulate at the fluid interface and form interconnected clusters: this leads to a homogeneous pattern after drying. Without surfactant, particles do not adsorb at the interface and the final deposit is dictated by the coffee-ring effect. Scale bars: 50  $\mu\text{m}$  (left) and 500  $\mu\text{m}$  (right). Adapted with permission from ref 24. Copyright 2015 American Chemical Society.

enhancement in flotation recovery (i.e., adsorption of particles to the forming fluid interface). This demonstrated how the *in situ* hydrophobization affects the interfacial phenomena involved.<sup>53</sup> Interestingly, such particle hydrophobization and consequent separation can be done selectively, as exemplified by the case of suspensions containing galena and quartz particles. In this example,<sup>53</sup> oleic acid is used as the surfactant that enables the collection of particles at the air–water interface. Oleic acid adsorbs on galena, making its surface more hydrophobic, whereas it does not adsorb on glass. Consequently, only particles of galena are collected in the froth.

The ability of surfactant/particle mixtures to stabilize foams and emulsions has been studied by numerous researchers focusing both on its fundamental aspects<sup>26–28,54–56</sup> and its practical importance.<sup>7,57</sup> In most cases, aqueous suspensions of charge-stabilized micro- or nanoparticles in contact with another immiscible phase are explored due to their high relevance in applications. As mentioned earlier, in the common case of anionic particles, the surface charge prevents the particles from adsorbing onto a fluid interface. If the particle manages to overcome this barrier (e.g., via copious energy supply to the system)<sup>25,26</sup> and adsorb onto the fluid interface, then its wettability will come into the picture, manifested by the contact angle that it makes with the interface. If the particle is very hydrophilic ( $\theta \rightarrow 0^\circ$ ), then  $E_{\text{ads}}$  will be comparable to  $k_B T$ , according to eq 3. The physical meaning of this is that the thermal energy is enough to cause particle desorption from the interface. Typically, surfactants are added to modify the wettability and/or charge of the particles, rendering their surface more hydrophobic and thus allowing them to strongly adsorb (i.e.,  $E_{\text{ads}} \gg k_B T$ ) onto the fluid interface in question.<sup>28,58</sup> Such surface modifications are usually a consequence of the electrostatic adsorption of surfactant onto the particle (physisorption). Depending on the relative surfactant/particle concentration, this effect can lead to different surfactant structures assembled onto the particle surface, which in turn

yields particles with varying surface activity (and thus varying stabilization efficiency).

Binks et al.<sup>25</sup> investigated the stabilization of dodecane/water emulsions by mixtures of anionic, hydrophilic  $\text{SiO}_2$  NPs ( $D_p = 15$  nm) and the cationic surfactant CTAB. The authors showed that the addition of CTAB in a suspension of strongly charged NPs (at pH 9) led to the electrostatic adsorption of single surfactant molecules onto the particles, and a surfactant monolayer could form. As a result, the initially well-stabilized NPs became progressively less charged and more hydrophobic. With increasing surfactant concentration ( $C_s$ ), further adsorption onto the NPs took place via hydrophobic interactions between the apolar chains. This resulted in the formation of a surfactant bilayer on the particle surface, which eventually became hydrophilic again because of the exposure of the charged headgroups to the aqueous phase. The above phenomena had a profound influence on both the stability of the suspensions and the ability of NPs to stabilize emulsions. In the absence of CTAB, the well-stabilized NPs could not stabilize oil/water (O/W) emulsions. However, upon CTAB addition, surfactants and NPs acted synergistically and were efficient in stabilizing the emulsions. The most efficient stabilization occurred at intermediate  $C_s$  (for constant NP concentration), which led to the conclusion that the most stable emulsions were prepared utilizing the most unstable suspensions. Cryo-SEM imaging confirmed the presence of large NP flocs at the fluid interface.<sup>25</sup> In a follow-up study from the same group, similar phenomena were at work during the double phase inversion of the dodecane/water emulsion that was stabilized by anionic silica NPs and a dichain cationic surfactant. The first inversion from O/W to W/O emulsions was attributed to the surfactant-driven hydrophobization of NPs and subsequent flocculation, whereas the second W/O to O/W inversion took place because NPs became charged and hydrophilic again due to the formation of a surfactant bilayer on their surface.<sup>54</sup> The correlation between  $C_s$  and the resulting particle hydrophobicity was later evidenced by direct measurements of the contact angle of silica NPs using



freeze-fracture shadow-casting (FreSCa) cryo-SEM (Figure 3A).<sup>58</sup> These indeed showed that particles were hydrophilic at low  $C_s$ , hydrophobic at intermediate  $C_s$ , and again hydrophilic upon further surfactant addition. The synergism between NPs and oppositely charged surfactants may be also exploited to prepare stable air-in-water foams.<sup>26</sup> Similar to emulsions, foams were the most stable at intermediate surfactant concentrations. The authors linked the maximum foam stability to NPs being strongly flocculated, which also corresponded to low surface charge and maximum hydrophobicity.

The general picture of surfactant-induced particle charge neutralization and subsequent flocculation has been observed in a plethora of oppositely charged surfactant/particle mixtures, regardless of their exact physical and chemical properties. Maestro et al. employed ellipsometry to explore the arrangement of silica NPs at the air–water interface in the presence of cationic surfactants of different hydrophobicity (DTAB and CTAB).<sup>28</sup> They developed a model to understand the structure of the adsorbed NPs, which was controlled by the balance between electrostatic and hydrophobic interactions between the surfactants and the oppositely charged NPs. The contact angle of the NPs at the fluid interface was calculated, and the authors found that  $\theta$  strongly depended on  $C_s$ . For both DTAB and CTAB,  $\theta$  reached its maximum value at intermediate  $C_s$ , corresponding to the maximum NP affinity for the fluid interface.<sup>28</sup> Further studies on the same system evidenced how adding CTAB to silica NP suspensions caused both an increase in  $\theta$  and an increased affinity of the NP–surfactant complexes for the fluid interface. This in turn caused an increase in the effective number of adsorbed particles, and consequently the average NP separation in the monolayer decreased (as evidenced by *in situ* atomic force microscopy and grazing incidence small-angle X-ray scattering).<sup>59</sup> In the majority of these works, salt (typically 1 mM NaCl) was added to the aqueous phase to promote particle–surfactant and particle–interface attractions. This complicates the elucidation of the effect of surfactants alone on the interaction between particles and the fluid interface and among interfacial particles.

The influence of electrostatic surfactant adsorption on particle wettability (and thus  $\theta$ ) is not the same for NPs made from different materials. Deleurence et al. studied the stabilization of air–water interfaces (in foams) by mixtures of anionic yet hydrophobic particles (PS with sulfate surface groups) and cationic surfactants.<sup>27</sup> A similar picture of surfactant-driven particle neutralization yielding flocculation, followed by charge reversal with increasing  $C_s$ , was revealed. However, contrary to mixtures of hydrophilic silica NPs with similar surfactants, the particle charge could be changed over a broad range (including neutralization) without a strong change in  $\theta$ . This was attributed to the hydrophobic nature of the bare particle, and this provided the means to decouple the effects of the surface charge and wettability of the NPs on the adsorption behavior. The authors concluded that a key parameter dictating the foam properties was the flocculation state of the suspension rather than the electrostatic charge of the NPs alone.<sup>27</sup> This is in agreement with results from a very different system, mixtures of PS NPs with proteins (Figure 11D).<sup>60</sup> Neutralization due to protein adsorption on the NP surface was not always sufficient to cause NP adsorption at the air–water interface of a drying sessile drop. Instead, when adsorbed proteins reorganized to expose their hydrophobic moieties to the aqueous phase, NP adsorbed to the interface regardless of the value of the global electrostatic charge of the NPs.<sup>60</sup>

A similar phenomenon was exploited to control the morphology of deposits obtained by drying sessile drops containing mixtures of PS NPs with ionic surfactants (Figure 3B).<sup>24</sup> The authors have shown that the surfactant-mediated interactions between the NPs and the free interface of the drop, and not hydrodynamic flows driven by surface tension gradients, primarily defined how NPs were deposited on the supporting solid substrate. For like-charged surfactant/NP mixtures, most NPs were deposited near the drop edge. This was due to the coffee-ring effect (CRE),<sup>61</sup> which refers to the emergence of a convective flow of solvent in sessile drops that are partially wetting a solid surface. This flow results from the combined action of surface tension, contact line pinning, and the gradient in the evaporation rate across the free surface of the drop. The flow direction is from the center of the drop toward its edge, and it is usually strong enough to transport most particles to the contact line. The situation was dramatically different when NPs were mixed with oppositely charged surfactants. Three different cases were identified, depending on the initial surfactant concentration within the drop. At low  $C_s$  ( $\sim 10^{-3}$ – $10^{-4} \times$  CMC (critical micellar concentration)), limited or no surfactant adsorption onto the particles left their surface properties unaffected. At high  $C_s$  ( $\sim 10^{-1} \times$  CMC), the formation of bilayers on the particles rendered them hydrophilic, but their charge was opposite to that of the bare NPs. In both of these extreme cases, the well-charged and hydrophilic NPs were deposited at the drop edge upon drying, due to the CRE. The most interesting results were observed for intermediate  $C_s$  ( $\sim 10^{-2} \times$  CMC). In this case, the adsorbed surfactants formed a monolayer on the NP surface, which rendered them hydrophobic and reduced their charge down to complete neutralization. This in turn led to favorable interactions between the surfactant-decorated NPs and the free surface of the drop; as a result, almost all NPs were adsorbed onto the air–water interface during evaporation (Figure 3B). After complete drying, the interfacial NP assembly was deposited on the substrate, overcoming the CRE and resulting in uniform deposits.<sup>24</sup>

There are numerous works on surfactant-induced modification of the surface of particles and their consequent behavior at fluid interfaces, and here we only briefly presented a few representative examples. This rich body of literature clearly shows that surfactant/particle mixtures are a powerful means of stabilizing various types of fluid interfaces. The advantages of this pathway is that it is applicable to a broad range of surfactants and particles, and the concentration of the surface-active species is a simple yet robust control parameter to tune the particle–interface interactions. However, in these systems, the promotion of particle adsorption on the interface is inherently linked to particle flocculation that leads to the destabilization of the suspensions, both in the bulk and at the fluid interface. This is a direct consequence of the relatively high surfactant concentration regimes (around the CMC) where particle neutralization and/or hydrophobization takes place. This may be a serious limitation in applications in which one wishes not only to drive the attachment of particles onto a fluid interface but also to *control* their organization, for example, to create functional and/or responsive 2D assemblies. In such cases, destabilization of the suspension (especially at the interface) must be avoided because it strongly hinders the control of particle organization.

**Other Additives That Modify the Particle Surface Properties.** Adding cosolvents to the aqueous phase is another efficient method to destabilize particles and promote their adsorption at fluid interfaces. Reincke et al. observed the spontaneous

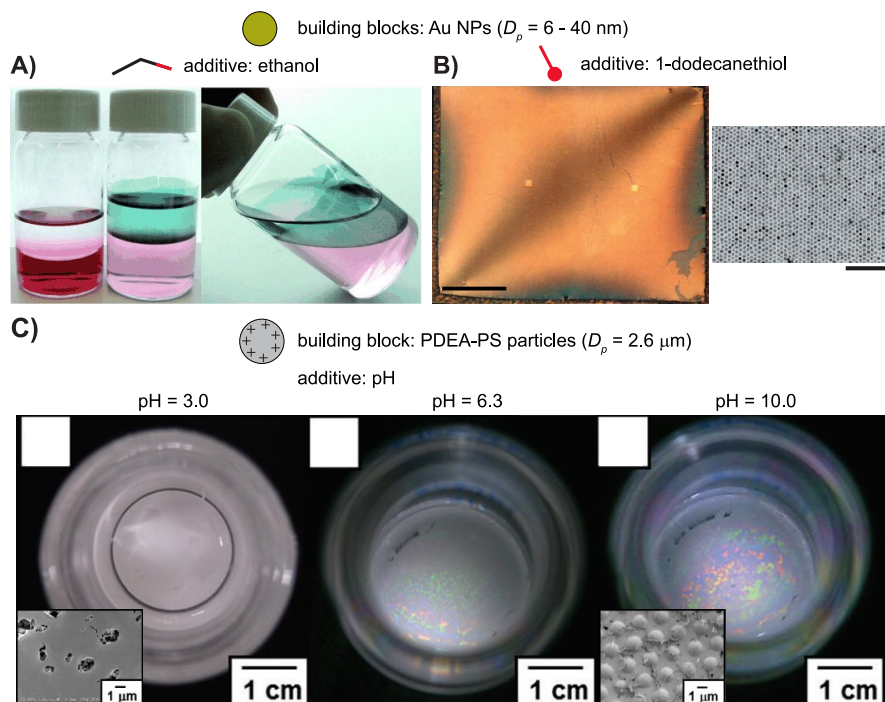


**Figure 4.** Additive-enhanced particle adsorption onto the interface through particle surface modification: the case of other additives. (A) Ethanol-induced adsorption of Au NPs at the heptane–water interface. (Left) A vial containing an aqueous NP suspension covered with heptane. (Middle and right) The sample after ethanol addition to the aqueous phase. An NP monolayer is formed at the fluid interface and extends up to the heptane–glass interface. Adapted with permission from ref 31. Copyright 2004 John Wiley and Sons. (B) (Left) A monolayer of Au NPs formed at the toluene–air interface in the presence of excess dodecanethiol. Scale bar: 100 nm. (Right) TEM image of the monolayer. Scale bar: 100 nm. Adapted with permission from ref 34. Copyright 2006 Springer Nature. (C) Effect of pH on the adsorption of PDEA–PS particles at the air–water interface during the drying of a concentrated suspension. Top-view photographs of the suspensions. (Insets) SEM images of the air–water interface after it was polymerized upon exposure to ethyl 2-cyanoacrylate vapor. At pH 3.0, the particles do not adsorb at the interface and the film is devoid of particles. At pH 10.0, the particles adsorb and form a crystalline layer at the interface. Reproduced from ref 21 with permission from the Royal Society of Chemistry.

formation of monolayers of negatively charged Au NPs ( $D_p$  from 8 to 40 nm) at the water–heptane interface after the addition of ethanol to the aqueous phase (Figure 4A).<sup>31</sup> Particle adsorption was attributed to a decrease in the particle surface charge density. This was caused by the displacement of citrate or gold chloride anions from the gold surface by ethanol molecules. A similar method was later used to adsorb Au ( $D_p = 18$  nm), Pt ( $D_p = 3.3$  nm), and SiO<sub>2</sub> NPs ( $D_p = 200$  nm) at a fluid interface.<sup>35</sup> After ethanol was used as an “inducer” to trap NPs at the interface between water and toluene, most of the latter was removed, decreasing the contact area between the organic and the aqueous phase. As a result, the initially loosely packed NP monolayer was compressed into a close-packed assembly.<sup>33</sup> In addition to particle destabilization in the aqueous phase due to the addition of ethanol, Park’s group<sup>32</sup> employed another additive (a long-chain alkanethiol soluble in the oil phase) to further control the particle organization at the fluid interface, as described later.

In their study of the self-assembly of dodecanethiol-functionalized Au NPs at the free surface of an evaporating toluene sessile drop, Bigioni et al. observed that an excess of (free) dodecanethiol was required to ensure an attraction between the NPs and the air–toluene interface.<sup>34</sup> This attractive interaction, combined with the increased particle concentration under the descending interface, led to a saturated 2D suspension at the fluid interface. This in turn resulted in the 2D nucleation and growth of NP islands into an exceptionally uniform, millimeter-sized monolayer comprising close-packed NPs (Figure 4B). Although their experiments could not elucidate

the details of the underlying mechanism, a clear correlation between the key role of the excess thiols in controlling particle–interface interactions and the growth of 2D particle islands was evidenced. Finally, upon complete evaporation, the NP film was deposited on the supporting solid surface.

The group of Girault developed a different method to adsorb Au NPs onto fluid interfaces based on an *in situ* electrochemical reaction which led to the destabilization of the particles.<sup>35</sup> The system was composed of an aqueous suspension of citrate-capped Au NPs, which was emulsified with DCE containing the lipophilic electron-donating molecule tetrathiafulvalene (TTF). Charge-transfer reactions between neutral TTF and Au NPs resulted in the formation of TTF<sup>•+</sup>, which then coated the surface of the NPs. Notably, the more reduced NPs could induce the removal of anionic citrate ligands electrostatically, further facilitating the absorption of TTF<sup>•+</sup>. Vigorous shaking of the sample allowed the authors to break the fluid interface into droplets, hence increasing the fluid surface area and consequently yielding a significant increase in the capturing of Au NPs. The surface charge of the particles coated with TTF<sup>•+</sup> was much lower than that of the pristine particles, and particle aggregation both in the bulk and at the interface was observed. Vigorous shaking, or alternatively ultrasonication, prevented the formation of large aggregates in the bulk prior to particle adsorption at the fluid interface. Nonetheless, the films coating the oil drops comprised dense multilayers of aggregated particles. Successively, as we describe later, the authors developed different protocols, in terms of organic solvent and

additives used, to produce particle monolayers with the desired optical responses.

When using particles with pH-responsive dissociable groups, varying the pH of the aqueous phase is another means to tune the particle–fluid interface and particle–particle interactions. Studies of foam stabilization have shown a correlation between the surface charge of the particles and their ability to adsorb at fluid interfaces. It was found that positively charged PS particles easily adsorbed at the air–water interface at pH values where their surface remains positively charged. On the contrary, negatively charged PS particles with sulfate surface groups, being anionic over the whole pH range investigated, did not form any noticeable foam.<sup>62</sup> Anionic particles with pH-dependent surface groups (PS latex stabilized by poly(acrylic acid)) were good stabilizers upon charge suppression or inversion at pH values below the isoelectric point.<sup>63</sup> It should be noted that these experiments included the addition of salt (usually 0.1 M NaCl) in the samples, which also decreased the adsorption barrier. A later work by Sekido et al. reported a similar effect of pH in adsorbing pH-responsive PS particles at the air–water interface, this time in the absence of externally applied forces.<sup>21</sup> The authors investigated the effect of pH on the dried structures of suspensions of poly[2-(diethyl-amino)ethyl methacrylate] (PDEA)-stabilized PS particles. At low pH, PDEA was protonated and positively charged. Under these conditions, the particles were well dispersed and did not adsorb at the air–water interface during drying. Increasing the pH caused a decrease in the particle charge, up to the point that flocculation and the formation of a 3D colloidal gel occurred at pH 10.0. Under these conditions, although most particles sedimented to the bottom, an iridescent color at the air–water interface was observed. SEM images of the solidified fluid interface, after the polymerization of ethyl 2-cyanoacrylate to trap the adsorbed particles, indeed revealed a crystalline close-packed structure (Figure 4C).

**Polymeric Surfactants.** Russell and co-workers developed another strategy that made use of oppositely charged additive/particle mixtures to control the adsorption of anionic NPs at an oil–water interface. They added NH<sub>2</sub>-terminated poly(dimethylsiloxane) (PDMS) chains to the oil phase to control the interfacial adsorption of COOH-functionalized PS or silica NPs dispersed in the aqueous phase.<sup>29,30</sup> These two components present in the different liquids attracted each other due to their opposite charge. This ultimately drove the adsorption of particles at the interface and the formation of an NP skin. This system and its applications are described in detail in the last section of this paper. Whereas the electrostatic attractions between NPs and surfactants were responsible for NP adsorption at the interface, the electrostatic interparticle repulsion in the aqueous phase controlled the number of NPs reaching the interface. Consequently, a second additive (NaCl) in water was used to further control the number of adsorbed particles. Increasing the electrolyte concentration lowered the repulsion between like-charged particles and induced an increase in the density of NPs at the fluid interface.<sup>64</sup>

**Additive-Enhanced Particle Promotion to the Interface without Particle Modification.** In this section, we discuss the effect of the main additives used to drive the interfacial adsorption of particles *without* altering their surface properties. Contrary to the *in situ* modification discussed above, this pathway for facilitating adsorption is based on the modulation of particle–interface interactions by other mechanisms, such as the screening of electrostatic repulsions. We

specifically focus on electrolytes soluble in water or in the organic phase and surface-active molecules.

**Water-Soluble Salts.** Non-surface-active additives, such as hydrophilic electrolytes, can drastically reduce adsorption barriers and facilitate particle adsorption at fluid interfaces. This approach is nowadays used by several research groups for a variety of particles composed of different materials (i.e., metals, polymers)<sup>11,64</sup> and with different surface properties (with anionic or cationic groups or chemically grafted polymers).<sup>65</sup>

Early experiments using thoroughly cleaned, surfactant-free anionic PS microparticles showed a strong influence of added NaCl on the particle–interface interaction.<sup>19</sup> At low salt concentrations, the rate of particle arrival at the interface was low, whereas at higher salt concentrations, the number of particles reaching the interface increased.<sup>19</sup> The authors' calculations indicated that the repulsive vdW interactions between the suspended particles and the air–water interface were short-ranged. The corresponding potential (eq 4) became lower than  $k_B T$  for particle–interface separations larger than  $\sim 40$  nm, making this contribution insignificant. On the contrary, the electrostatic particle–interface repulsion (eq 8) was both long-ranged and of significant strength. Hence, the above trends were attributed to strong and screened electrostatic particle–interface repulsion for respectively low and high ionic strengths. Interestingly, to explain the enhanced adsorption flux of particles compared to that predicted by the DLVO theory, the authors proposed the action of a long-range, hydrophobic attraction between the particles and the fluid interface that could overcome vdW and electrostatic repulsions. In a following study, Abdel-Fattah and El-Genk quantified the adsorption of PS particles at the air–water interface in the presence of NaCl.<sup>20</sup> For all NaCl concentrations examined (0–1 M), the same qualitative picture emerged: the number of adsorbed particles increased exponentially with time until it reached a plateau. The adsorption process was described by two parameters, the asymptotic particle surface coverage and the characteristic adsorption time. The asymptotic surface coverage first sharply increased with increasing ionic strength, reaching a maximum (corresponding to about half of the total number of particles) before it decreased slowly upon a further increase in NaCl concentration. The characteristic adsorption time showed the opposite trend: it first decreased before reaching a minimum (corresponding to the maximum surface coverage), after which it increased again with increasing ionic strength. The authors concluded that at zero and low salt concentrations, a finite adsorption energy barrier limited the accessibility of the fluid interface to the suspended particles. Increasing the NaCl concentration to 0.05 M (where maximum particle adsorption occurred) reduced the height of the adsorption barrier, facilitating the adsorption of a large number of single particles onto the interface. Upon further NaCl addition, however, the competing effect of particle aggregation in the bulk became more pronounced, leading to a decrease in the number of interfacial particles.<sup>20</sup> The authors later developed a model that confirmed that particle adsorption was limited by the accessibility of the fluid interface to suspended particles. The interface accessibility depended on the total energy barrier between particles and the interface (called the “sorption barrier”) and that between suspended particles in the bulk (“coagulation barrier”). These barrier heights were calculated using DLVO theory after considering a solvation zone around the particles and the air–water interface in the interparticle and particle–interface forces.<sup>38</sup>

Wang et al. investigated the efficiency of positively ( $D_p = 400$  nm) and negatively ( $D_p = 1.9 \mu\text{m}$ ) charged PS particles in stabilizing hexadecane in water emulsions at different pH values and NaCl concentrations.<sup>14</sup> The authors wanted to clarify whether the electrostatic repulsion from the negative fluid interface was the main component of the adsorption barrier. For high surface charge and weak electrostatic screening (i.e., low salt content), neither anionic nor cationic particles adsorbed at the oil–water interface. This corresponded to low pH for amidine-functionalized PS particles and high pH for carboxylated-functionalized ones. At high NaCl concentrations, anionic particles always adsorbed at the interface. Stable W/O and O/W Pickering emulsions were obtained for particles with low and high surface charge, respectively. The situation was different when cationic particles at high salt content were considered: stable O/W emulsions could be formed only for moderately to highly charged particles. However, even under such conditions of strong electrostatic screening, a regime of limited cationic particle adsorption, leading to emulsions with very poor short-term stability, was revealed. This led the authors to propose that the repulsion between the particles and the oil–water interface was due to not only the negative charge of the interface but also the electrostatic interaction between the charged particle and an image charge of the same particle in the oil phase (eq 7). Similar to the electrostatic forces between charged particles, the electrostatic image charge force could be screened and was hence strongly impacted by the pH of the suspension and by the addition of electrolytes.

The precise value of the negative charge at the surface of water under various experimental conditions is usually unknown, and an accurate theoretical description of the electrostatic interactions between particles and the interface is still lacking. Recently, Kang et al.<sup>66</sup> measured the adsorption probability of anionic PS particles onto the decane–water interface using optical tweezers. A single particle was first translated toward the interface, and then it was moved back to the bulk aqueous phase. When the particle adsorbed at the interface, the optical force was not strong enough to cause desorption, and the adsorption event could be visualized. The authors quantified the adsorption probability of particles as a function of the ionic strength of the water phase. They estimated the force required for a particle to overcome the repulsion from the interface and adsorb at it and found that the adsorption probability increased (and the required force decreased) upon increasing the ionic strength. They also found that, in their experiments, the electrostatic interaction between the like-charged particles and the fluid interface was the main component causing repulsion.

**Hydrophobic Electrolytes.** Besides ordinary hydrophilic electrolytes, salts that contain hydrophobic ions can also assist particles in overcoming adsorption barriers and attach to fluid interfaces.<sup>18</sup> Bell's group developed a strategy for promoting the adsorption and assembly of particles at oil–water interfaces based on using hydrophobic electrolytes (Figure 5A).<sup>16</sup> In an important work that helped to rationalize the effect of various additives that had been empirically used to realize colloid self-assembly at fluid interfaces, Xu et al. categorized additives into “modifiers” and “promoters”.<sup>16</sup> The former compounds change the surface properties of the particles (e.g., wettability and/or surface charge). Thus, by increasing  $\theta$ ,  $E_{\text{ads}}$  (eq 3) increases and the particle affinity for the fluid interface is enhanced. In contrast, promoters induce particle adsorption by modifying the electrostatic interactions between particles rather than by changing their hydrophobicity. The authors illustrated this

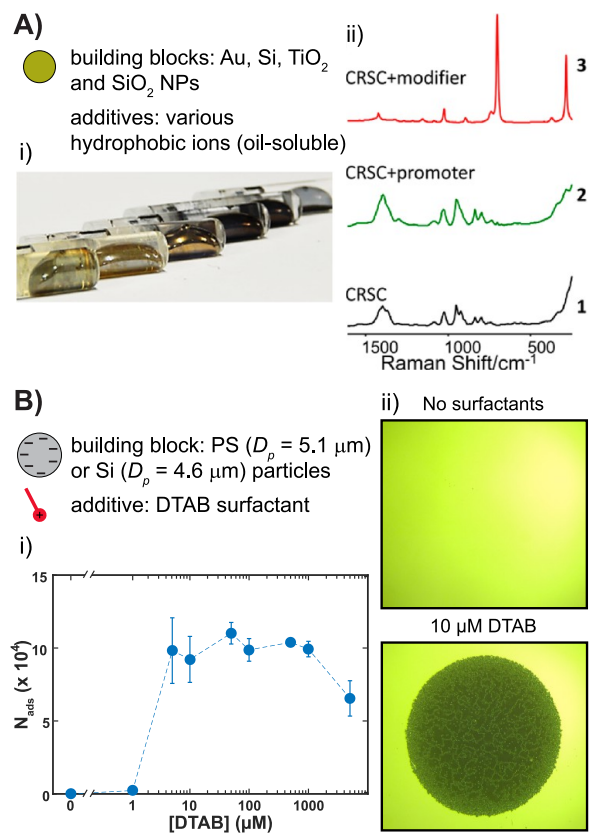


**Figure 5.** Particle adsorption onto a fluid interface promoted by additives. (A) Adsorption of anionic NPs at oil–water interfaces is promoted by the addition of oppositely charged, oil-soluble, hydrophobic ions in the organic phase. (i) Photograph of vials containing particle films at the fluid interface. (ii) SERS spectra of citrate-reduced silver NPs (CRSC, 1), NPs + TBA<sup>+</sup>NO<sub>3</sub><sup>-</sup> (2), and NPs + 1-pentanethiol (3). Adapted with permission from ref 16. Copyright 2016 American Chemical Society. (B) Adsorption of anionic PS particles at the air–water interface is promoted by the addition of minute amounts ( $\sim 10^{-4}$ – $10^{-3} \times \text{CMC}$ ) of DTAB surfactant. (i) Number of adsorbed particles versus DTAB concentration. (ii) Transmission micrographs of the air–water interface. In the absence of surfactant, particles do not adsorb at the interface. With 10  $\mu\text{M}$  DTAB, a 2D polycrystalline assembly is obtained. Scale bar: 1 mm. Adapted with permission from ref 22. Copyright 2018 American Chemical Society.

difference by using a simple method for preparing 2D assemblies by shaking an aqueous Au NP suspension with an immiscible oil (DCM) and a small amount of one of the two additive types. When 1-pentanethiol was used, a metal liquid-like film of Au NPs was formed at the oil–water interface. Surface-enhanced Raman scattering (SERS) showed that 1-pentanethiol was bound to the NPs (Figure 5A, (ii)); this increased their hydrophobicity and facilitated their adsorption at the interface, classifying this compound as a modifier. When tetrabutylammonium nitrate (TBA<sup>+</sup>NO<sub>3</sub><sup>-</sup>) was used instead of 1-pentanethiol, a similar metal film was formed, but no SERS signal of the hydrophobic salt was detected in the NP assembly (Figure 5A, (ii)). Since TBA<sup>+</sup>NO<sub>3</sub><sup>-</sup> left the surface properties of the NPs unaltered, it was termed a promoter.

The Bell group provided an extended list of promoters and modifiers and, importantly, clarified situations where substances reported as modifiers were in fact promoters.<sup>16</sup> They noted that chemically diverse compounds such as organic electrolytes, transition-metal complexes, and crown ethers might act as

promoters as long as one of their ions is hydrophobic. The adsorption and self-assembly of anionic (respectively cationic) NPs require a promoter having a hydrophobic cation (respectively anion). The requirement of a hydrophobic ion carrying a charge opposite to that of the NP suggested that the dominant interaction is that between the interfacial NPs and the oppositely charged ions in the oil phase. The authors explained the action of promoters by considering the balance between the interfacial energy reduction due to NP adsorption and the increased electrostatic interparticle repulsion due to their localization at the interface. For anionic NPs in the absence of promoter, the number of NPs adsorbed at the interface was low. When a hydrophobic salt was introduced, an interfacial potential and regions on each side of the interface rich in hydrophobic cations and hydrophilic anions were created. The promoter cations on the oil side screened the Coulomb repulsion from the portion of the negatively charged NP surface that resided in the oil. The reduction in interparticle electrostatic repulsion, in conjunction with vdW attraction, allowed interfacial NPs to pack closely, separated by a distance dictated by the balance between the two interactions. Because of its electrostatic screening nature, this mechanism was efficient in driving particle self-assembly in a plethora of systems, including NPs made from different metals<sup>5,16</sup> or inorganic materials such as silica and titanium oxide and fluid interfaces between water and various organic solvents.<sup>16</sup> It is worth noting that although the minimum amount of promoter should depend on the exact properties of each system, in practice a reasonable excess of hydrophobic salt (i.e., low enough to prevent aggregation) was found to be adequate in all of the studied cases.<sup>16</sup>

**Surfactants at Low Concentrations.** As analyzed earlier, using surface-active species at moderately high concentrations (i.e.,  $\sim$ CMC) is a practical and efficient way to induce the adsorption of particles at fluid interfaces. Interestingly, and perhaps surprisingly, much less is known about the interaction between particles and fluid interfaces in the presence of an ultralow ( $10^{-4}$ – $10^{-3} \times$  CMC) amount of surfactants, where the particle surface properties typically remain unaffected.

Anyfantakis et al. used a quantitative method, based on sedimentation, to transport various kinds of particles to the air–water interface and study their adsorption and self-organization phenomena.<sup>22</sup> When negatively charged microparticles that were carefully purified to remove any unwanted additives remaining from synthesis were brought near the air–water interface, no particle adsorption occurred. This was attributed to the repulsive particle–interface interaction arising from both electrostatic and vdW contributions. The situation changed when cationic surfactants such as DTAB and CTAB were added to the system in very low concentrations ( $C_s \approx \text{CMC} \times 10^{-4}$  to  $\text{CMC} \times 10^{-2}$ ), for which surface tension changes are negligible. Under these conditions, particles irreversibly adsorbed at the air–water interface, with the number of interfacial particles depending on  $C_s$ . For low  $C_s$  ( $1 \mu\text{M}$  for DTAB;  $\sim \text{CMC} \times 10^{-4}$ ), only a few particles accumulated at the surface. With increasing  $C_s$ , a dramatic increase in the number of adsorbed particles was observed (Figure 5B, (i)). This number remained roughly constant for an extended range of intermediate  $C_s$  ( $5$ – $1000 \mu\text{M}$ ) values before decreasing again at the highest  $C_s$  range ( $5 \text{ mM}$ ) explored. Notably, in the intermediate  $C_s$  range, the number of adsorbed particles was very close to the total number of particles in suspension, which means that almost *all* suspended particles could adsorb to the fluid interface. This a unique example of a method that requires no special equipment yet ensures absolute

particle adsorption efficiency. Whenever extensive adsorption occurred, particles made a low contact angle ( $\theta \approx 30^\circ$  as measured *in situ* by fast confocal microscopy) with the interface. Conversely, the particle surface charge remained essentially unaffected up to  $C_s = 100 \mu\text{M}$  and started decreasing only at higher  $C_s$ , when significant adsorption of surfactant onto the particles was evidenced. These results indicate that partial coverage of the particle surface with surfactant is *not* a requirement to promote complete particle adsorption from the bulk. The surfactant-induced particle adsorption at this ultralow concentration (especially for  $5$ – $100 \mu\text{M}$  for DTAB) was explained by an electrostatic shielding effect: the preferential adsorption of cationic surfactants onto the oppositely charged air–water interface diminished the electrostatic barrier for particle adsorption. A direct consequence was that the authors were able to further control particle organization into 2D polycrystalline structures, the organization of which was governed by the remaining electrostatic repulsion between like-charged particles (*vide infra*). The authors pointed out the qualitative analogy of this surfactant role to that of salts, which also mediate particle adsorption to a fluid interface. However, surfactants do this at concentrations that are about 3 orders of magnitude less than those of salts, acting essentially like “supersalts”. The above strategy was applicable to a plethora of systems including various anionic particles (silica and PS micro- and nanoparticles,<sup>22</sup> metal NPs of different surface chemistries and shapes<sup>12</sup>) and different cationic surfactants.<sup>9,22</sup> Additionally, it was exploited to form and systematically study a variety of 2D colloid assemblies, including photoresponsive 2D crystals (Figure 13C).<sup>9</sup>

A follow-up study further confirmed the general applicability of this strategy by showing that CTAB can induce the self-assembly of various negatively charged NPs (e.g., Au, Pt,  $\text{SiO}_2$ , and  $\text{TiO}_2$ ) into densely packed monolayers at water–oil interfaces.<sup>23</sup> Interestingly, these authors conclusively showed that in such an oppositely charged surfactant/NP mixture the surfactant has a dual role that depends on  $C_s$ . In the low- $C_s$  regime, surfactants promote the adsorption and self-assembly of particles at the interface without modifying the NP surface (as evidenced experimentally by the limited surfactant adsorption on the NPs). A mechanism similar to the case of hydrophobic salts was proposed, in which the cationic headgroups enter the oil phase and screen the charge of the portion of the NP immersed in oil. This, combined with screening by hydrophilic ions inherently present in the aqueous phase along with vdW interparticle attractions, led NPs to pack densely at the interface. Regardless of the exact microscopic mechanism, the authors pointed out that the action of CTAB at low  $C_s$  might explain earlier observations, such as the self-assembly of citrate-capped Au nanorods at liquid interfaces without the need of any additional additive.<sup>67</sup> This is because CTAB is commonly used in colloid synthesis and it is difficult to establish the exact amount of residual CTAB in a suspension. Conversely, in the high  $C_s$  regime, CTAB adsorbed on the NPs, rendering them neutral and hydrophobic. As expected, this surfactant-induced modification of the particle surface also led to NP assemblies at the fluid interface, which were nevertheless disordered (in contrast to the highly ordered 2D assemblies for low  $C_s$ ).<sup>23</sup>

The documented  $C_s$ -dependent dual action of CTAB for facilitating NP self-assembly at oil–water interfaces is important because it *bridges* the well-established picture of surfactant-induced hydrophobization that enables adsorption,<sup>10</sup> with the emergent picture of surfactant-driven particle adsorption

without surface alteration.<sup>22</sup> We believe that this overall picture is also true for surfactant-mediated particle adsorption at the air–water interface, as indicated by our studies.<sup>22,24</sup> It is worth noting that the scenario proposed by Bell's group to explain the promotion action of both hydrophobic salts<sup>16</sup> and CTAB at low  $C_s$ <sup>23</sup> is different from the explanation of surfactant-induced particle adsorption put forward by Baigl's group.<sup>12,22</sup> In the former case, the oppositely charged ions were responsible for reducing the particle–particle repulsion at the oil–water interface, and this in turn facilitated further adsorption of particles from the bulk. In the latter case instead, the influence of surfactants was attributed to the reduction of the adsorption barrier. This promoted the attraction between particles and the fluid interface. We want to point out that this step has been considered only occasionally, although it is a prerequisite for the well-addressed interaction of suspended particles with already-adsorbed particles. Both of these effects are significant and should be taken into account in future studies. Their relative importance should depend on the total number of particles and the fluid interface area available for adsorption as well as the physicochemical properties of the interface (air versus oil–water).

**Charged Lipids.** Srivastava et al. used *in situ* scattering techniques and *ex situ* SEM imaging to study the spontaneous self-assembly of Au NPs functionalized with single-stranded DNAs with nonhybridizing sequences ( $D_p = 8.5$  nm) at charged air–water interfaces coated with lipids.<sup>13</sup> Two types of fluid interfaces were explored, with different ratios of a neutral and a cationic lipid. With positively charged interfaces (due to adsorbed cationic lipids), the negatively charged NPs adsorbed at the interface via electrostatic attraction. This, combined with the electrostatic and steric repulsion between NPs, resulted in hexagonally packed NP monolayers. When the fluid interface was instead decorated solely by neutral lipids, no NP adsorption was detected; this indicated that the positive charge on the lipid layer was a prerequisite for the adsorption of the oppositely charged NPs. It is worth noting that although the authors highlighted that the confinement of the NPs at the lipid layer was strong due to the opposite charges,<sup>13</sup> the overall picture suggested that the NPs were sitting *below* the air–water interface without penetrating it. This differs qualitatively from most works covered in this Feature Article, where particle adsorption onto a fluid interface refers to the formation of a finite contact angle.

**Rational Choice of Additives for Particle Adsorption at Fluid Interfaces.** On the basis of the above discussion, two questions may arise: (i) Which transport mechanism is the most efficient for bringing colloid particles to a fluid interface? (ii) Which is the optimal additive choice for adsorbing particles at the interface? Our answer is no different from the most common scientific response: it depends on the system in question. The optimal choice of transport mechanism is largely influenced by the particle size as well as by the density difference with the solvent. Colloids for which  $Pe < 1$  are strongly affected by thermal motion, whereas sedimentation has a negligible impact on particle motion. Consequently, diffusion is an efficient way to accumulate such particles at a fluid interface; a further advantage is that this mechanism is spontaneous, so no special action is required from the experimentalist. The above condition is frequently met in practice when small particles are used.<sup>30,31</sup> For heavier particles where  $Pe \gg 1$ , transport mechanisms based on gravity are a good choice. Depending on the time scale of the experiment and the Stokes velocity of the particles, methods requiring no instruments, as simple as sedimentation,<sup>22</sup> or

realized using specific equipment such as ultracentrifugation<sup>11</sup> may be used. Other mechanisms that involve the motion of the fluid interface (e.g., in the case of drying suspensions<sup>34</sup>) or the creation of a new fluid interfacial area due to the external energy input (e.g., mixing or ultrasonication<sup>25,26</sup>) are efficient at accumulating particles at the interface, regardless of their features. The latter strategy must be considered carefully when planar monolayers are sought after because in the case of efficient particle adsorption, stable foams or emulsions may be obtained. Finally, one may notice that additives do not significantly influence the transport of particles to the fluid interface in most cases.

On the contrary, additives drastically affect particle–interface interactions via the numerous complex physical and chemical effects analyzed above. Therefore, choosing the right additive for a given application is a more delicate issue. We have described two major pathways by which additives induce particle adsorption: (i) by modifying the surface chemistry of the particles and (ii) by leaving the latter unaffected. Pathway (i) enhances particle adsorption typically through a modification of the wettability of the particles and/or a reduction of their surface charge. As a result, the particle adsorption energy is increased, making adsorption more energetically favorable. This pathway is very efficient at accumulating particles at various fluid interfaces, and it is extensively used in applications that require strong stabilization and mechanical robustness (e.g., particle-stabilized foams and emulsions) rather than precisely engineered structures (e.g., photonic crystals). This pathway typically leads to the destabilization of the colloids, and this may be highly problematic when precise control of the self-assembled structure is required. Additionally, extending this methodology to novel particles with different surface chemistries is not straightforward: each new colloid is essentially a new case.<sup>16</sup> With the much less explored pathway (ii), one can achieve extensive particle adsorption onto a fluid interface, essentially not affecting the suspension stability and leaving the particle properties unaltered. This offers several advantages compared to the use of additives that modify particle properties. First, a precise knowledge of the exact surface properties of the particles is not required because there is no specific chemical interaction between the additive and the surface groups of the particles. This can have the very practical advantage that, even ensuring a small additive excess (instead of an exact amount), can result in a successful outcome.<sup>23</sup> Second, the fact that the particles remain well stabilized (i.e., repulsive) allows the formation of highly ordered structures, the organization of which can be further tuned.<sup>12,18,36</sup>

From the above discussion, one realizes that the right choice of additive for particle adsorption depends on the specific application. If the degree of order of the resulting colloid assemblies is not important and the only requirement is extensive particle adsorption leading to efficient interface stability and robust mechanical properties, then pathway (i) may be followed. Alternatively, if highly ordered particle arrays are required, then pathway (ii) should be the right choice.

## ■ INFLUENCE OF ADDITIVES ON THE INTERACTIONS AND SELF-ORGANIZATION OF INTERFACIAL PARTICLES

As mentioned earlier, the first essential element for realizing colloid assembly at a fluid interface is that particles approach the interface (via a transport mechanism) and get immobilized there due to the combination of an attractive interaction and an overall favorable adsorption energy (i.e., for  $0^\circ < \theta < 180^\circ$ ). The second

essential element is that the interfacial particles rearrange in response to several forces acting on the system. These include forces that arise from the interaction potential between two individual particles in close proximity to each other. Moreover, other forces emerge when interfacial particle clusters approach each other. Here we use the word “clusters” to loosely refer to particle aggregation, regardless of whether it is reversible (flocculation) or irreversible (coagulation). Such clusters are caused by interparticle attraction and can be formed directly at the interface or can be the result of aggregation in the bulk prior to adsorption. The above forces may be described as inherent because they are a direct consequence of the properties of single particles or particle clusters, such as surface chemistry or weight, respectively. In addition to those, gravity, buoyancy, or applied external fields (e.g., optical, magnetic, and flow) can also exert forces on both single particles and particle clusters.

The total interaction potential between interfacial particles that determines their organization is complex;<sup>2,4</sup> therefore, the structure of the resulting colloid assembly cannot always be easily predicted. It is dependent on a delicate balance between a multitude of attractive and repulsive forces which act at different length scales (i.e., from a few nanometers up to several micrometers). The presence of the interface itself increases the complexity of the problem in comparison to the interactions usually considered in the bulk. Several forces acting in the bulk are also at work at fluid interfaces (e.g., vdW or electrostatic). However, the discontinuity between the two media fundamentally affects the theoretical models used to describe interparticle interactions. Therefore, their strength and dependence on various parameters, including the presence of additives, are altered with respect to the bulk and make the calculation of such interactions more complicated. Other forces, such as capillary or dipole–dipole interactions, are characteristic signatures of a fluid interface and have no analogue in the bulk. A detailed description of the interactions acting between interfacial particles is reported in several articles.<sup>2–4</sup> Here we discuss some of the most relevant interactions, putting emphasis on the use of additives to tune their magnitude to achieve the required particle organization.

**Overview of Interactions between Interfacial Particles.** The interactions between particles adsorbed at fluid interfaces can be broadly separated into attractive and repulsive. In this section, we use this categorization to briefly discuss the main forces directing particle assembly.

**Attractive Interactions.** An approximate treatment to estimate vdW interactions between two particles at a fluid interface is based on calculating an effective Hamaker constant ( $A_{\text{eff}}$ ) that depends on the fractional height  $f$  of the particles (material 3) immersed in medium 1.<sup>19</sup>

$$A_{\text{eff}} = A_{33} + f^2(3 - 2f)(A_{313} - A_{33}) \quad (9)$$

where  $f = (1 - \cos \theta)/2$  and  $A_{33}$  is the Hamaker constant for the particles in vacuum. The interaction between two spherical particles of radius  $R_p$  and surface-to-surface distance  $d$  is then given by<sup>44</sup>

$$W_{\text{vdW}} = -\frac{A_{\text{eff}}R_p}{12d} \quad (10)$$

The deformability of a fluid interface is responsible for attractive capillary interactions, which are a unique signature of the fluid interface itself. They arise from forces that can be divided into two types, the strength of which primarily depends on the

particle size.<sup>3</sup> One type of capillary force (called the lateral flotation force) stems from local deformations of the fluid interface around large (typically  $R_p > 5 \mu\text{m}$ ) floating particles, which creates a meniscus surrounding them (Figure 6A, (i)).

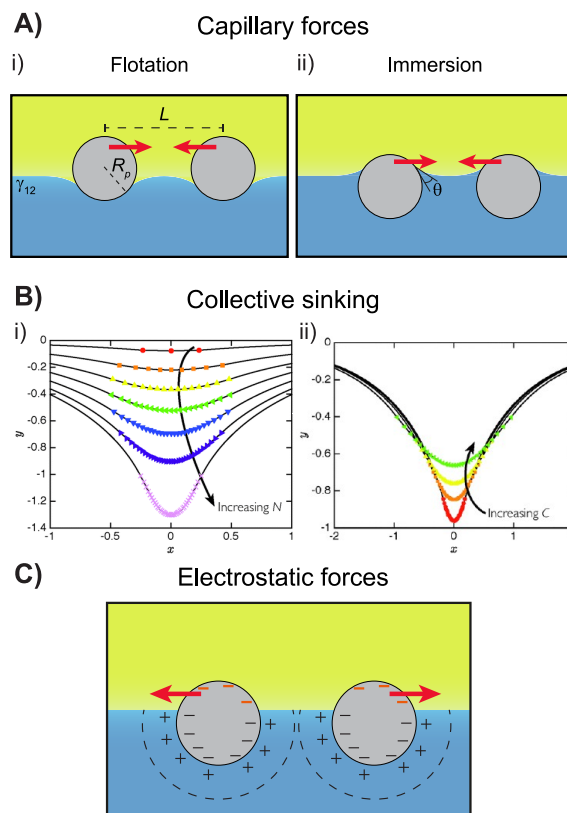


**Figure 6.** Key interactions between interfacial particles. (A) Capillary interactions at fluid interfaces. (i) Particles floating on a fluid interface cause its deformation, which triggers an attractive force. (ii) Hydrophilic particles adsorbed at a fluid interface. Immersion forces (in this case, attractive) result from the interface deformation that is caused by the formation of a finite particle contact angle. (B) “Collective sinking” mechanism. Numerical simulations showing the deformation of the fluid interface by clusters of adsorbed particles as a function of (i) the number of particles or (ii) the particle charge.  $x$  and  $y$  are coordinates along and perpendicular to the fluid interface. Reproduced from ref 68 with permission from the Royal Society of Chemistry. (C) Negatively charged particles at a fluid interface with their electric double layer (dashed lines) created by the accumulation of counterions around each particle. Eventual residual charges on the particle surface inside the nonpolar phase (in orange) contribute to the interparticle repulsion.

When two menisci approach each other, the fluid interface deforms in such a way that the total energy of the system decreases with decreasing interparticle distance. The larger the interfacial deformation created by the particles, the stronger the attractive lateral flotation force. The importance of lateral flotation forces can be estimated by knowing the interfacial tension of the fluid surface and the particle size. Such forces will be attractive if the liquid deformations created by two neighboring particles have the same orientation (i.e., both are concave) and repulsive if the surface deformations have a different orientation. Instead, in the case of particles adsorbed on the surface of water and for  $R_p < 5 \mu\text{m}$ , the particle weight is too low to deform the interface significantly. The lateral flotation forces become comparable to  $k_B T$ , and the physics of the system

is governed mainly by surface tension. We note that capillary forces are also important in governing assemblies of small particles in the case of particle networks and anisotropic objects (see below). Although for small, smooth, and spherical colloids lateral flotation forces are negligible, there is experimental evidence of long-range attraction in such systems. This is due to another type of capillary force, called the lateral immersion force.<sup>3</sup> A particle adsorbed at a fluid interface has a finite contact angle that can cause the deformation of the surrounding fluid and hence trigger lateral capillary attractions also in the case of NPs (Figure 6A, (ii)). Contrary to flotation forces, this attraction stems from the particles being partially immersed in the fluid. The local deformation of the interface responsible for the attraction between particles is in this case a consequence of their wetting properties and not of gravity. As for flotation forces, lateral immersion forces are attractive if the menisci have the same orientation, for instance, when particles with similar wetting properties interact, and repulsive if the particle menisci have opposite orientations.

Kralchevsky and Nagayama provided simple expressions to estimate flotation and immersion forces in the case of two identical interacting particles:<sup>3</sup>

$$F \propto \frac{R_p^6}{\gamma} K_1(qL) \text{ for the flotation force} \quad (11)$$

$$F \propto \gamma R_p^2 K_1(qL) \text{ for the immersion force} \quad (12)$$

where  $K_1$  is the modified Bessel function of the first order and  $qL$  is a dimensionless unit length with  $L$  being the center-to-center interparticle distance and  $q^2 = \Delta\rho g/\gamma$  or  $q^2 = (\Delta\rho g - \Pi')/\gamma$  in a thick or thin film, respectively ( $\Pi'$  is the derivative of the disjoining pressure with respect to the film thickness). Both flotation and immersion forces exhibit similar dependences on interparticle separation but display different dependences on the particle size and the interfacial tension. In particular, a  $\gamma$  increase causes a decrease in the flotation force, whereas the immersion force increases. For a detailed description of capillary forces, we refer the interested reader to comprehensive reviews on the subject (SI).<sup>3</sup>

It is worth noting that both natural and synthetic particles often have rough surfaces; consequently, wetting of the particle by the fluids cannot be uniform. This results in an irregular contact line and thus an uneven shape of the interfacial meniscus, irrespective of the wetting properties of the particles. Consequently, two interacting particles will optimize such a local surface deformation by adjusting their orientation and distance.<sup>69</sup> Notably, an irregular meniscus on the particle surface can arise not only from surface roughness but also from a spatially heterogeneous distribution of dissociable surface groups.<sup>70</sup> Between particles that cause similar interfacial deformations, capillary interactions are always attractive and therefore play a fundamental role in particle assembly at fluid interfaces. The deformation of the interface by nonspherical particles has a specific orientation, and this allows for producing assemblies with defined angular symmetries, dictated by anisotropic attractive capillary interactions. We refer the interested reader to articles on this very active research topic, which we summarize in the SI. In the case of spherical particles, the meniscus deformation is expected to be isotropic. Instead, due to both the presence of surface roughness and the formation of doublets and small aggregates, the resulting menisci are no longer isotropic. Consequently, such interactions are anisotropic

in the interface plane and add directionality to particle organization, which usually results in disordered assemblies and the formation of fractal aggregates.<sup>71,72</sup>

In summary, whereas both vdW and capillary interactions are typically attractive in interfacial particle assemblies, their effective range is different. van der Waals forces typically extend over a range of tens of nanometers for micrometer-sized particles. Instead, capillary interactions have a much longer range and in most cases are the main cause of particle aggregation.<sup>73</sup>

Notably, while lateral flotation forces are negligible for small particles, larger deformations of the fluid interface become important in dictating particle assembly when the behavior of groups of particles is considered. Vella et al.<sup>68</sup> used numerical simulations to study the assembly of particle ensembles adsorbed at a fluid interface. They described how collective effects significantly modify the simple pairwise interactions and become important at high particle number densities, dictating the deformation of the surrounding interface. This in turn affected the final particle organization through what they called a “collective sinking” mechanism, by modifying the interparticle distance (Figure 6B). Indeed, for ensembles composed of PS particles ( $D_p = 5 \mu\text{m}$ ) adsorbed at the air–water interface, it has been experimentally observed that the interparticle distance decreased upon increasing the cluster size.<sup>22</sup> Such an effect was also shown for smaller PS particles ( $D_p = 2 \mu\text{m}$ ) at the decane–water interface.<sup>68</sup>

**Repulsive Interactions.** Particles dispersed in water are usually stabilized by electrostatic repulsions, being either inherently charged, or after surface modification with charged or highly hydrated groups (Figure 6C). The surface charge will account for the two main repulsive contributions in the interparticle interaction potential: Coulomb and dipolar interactions. They arise from the formation of an electric double layer in aqueous solution and scale as  $e^{-\kappa d}$ . Between like-charged particles, this gives a long-range repulsion ( $\kappa^{-1}$  can reach about 680 nm in pure water due to the self-dissociation of water molecules), the magnitude of which can be easily tuned by changing the pH, ionic strength, or type of electrolyte (i.e., different valence or hydration properties) in solution.

Because of the interface discontinuity between the two fluids, the dissociation of the surface groups of the particles is asymmetric across the interface. At an air–water interface, the ionizable groups on the particle surface can dissociate only inside the aqueous phase (Figure 6C). This gives rise to the emergence of dipoles on all particles, which are oriented perpendicular to the interface, and leads to a repulsive electrostatic force. The magnitude of this dipolar interaction depends not only on the surface charge but also on the contact angle of the particles, with a maximum for  $\theta = 90^\circ$ . The picture is somewhat similar at an oil–water interface. The resulting electrostatic repulsive force is given by<sup>72</sup>

$$F_E = \frac{3\epsilon_2}{2\pi\epsilon_0\epsilon_1^2} \frac{q^2\kappa^{-2}}{L^4} \quad (13)$$

where indices 1 and 2 refer to the water and air/oil phases, respectively, and  $q$  is the particle charge.

Aveyard et al.<sup>74</sup> observed that PS particles with sulfate surface groups ( $D_p = 2.6 \mu\text{m}$ ) adsorbed at an octane–water interface and formed ordered hexagonal arrays with a much larger interparticle distance compared to that of the same particles at the air–water interface. To explain the difference in the strength



of the interparticle repulsion between the two systems, the authors proposed that water droplets trapped on the rough particle surface exposed to the oil side could give rise to surface charges at the portion of the particle in contact with the apolar phase. Because of the absence of counterions in the oil phase, these charges were not screened and were thus expected to stabilize the particles at longer separation distances. In a follow-up study,<sup>75</sup> the same group measured the magnitude of the particle–particle repulsion experimentally. It was further suggested that repulsion should be due to unscreened charge–charge interactions through the oil phase, combined with the interaction between the charge of one particle and the image charge (in the aqueous phase) of the other particle.<sup>75</sup> A repulsive interaction scaling as  $L^{-4}$  was also confirmed in a following study by Park et al.,<sup>72</sup> although its magnitude was smaller than that measured by Aveyard et al.<sup>75</sup> Interestingly, a significant variation of the measured forces for different pairs of particles necessitated the use of average force values to draw meaningful conclusions.<sup>72</sup>

Horozov et al. studied the influence of particle wettability on the structure of silica particles at an octane–water interface. The particle contact angle was varied by using a silanization reaction to replace surface silanol groups with hydrocarbon chains.<sup>76</sup> Very hydrophobic particles ( $\theta > 129^\circ$ ) were organized in well-ordered monolayers with  $L > 3D_p$  because of strong, long-ranged repulsions. Instead, particles with  $\theta < 115^\circ$  formed aggregates, resulting in disordered monolayers, indicating a weakening of the repulsive interactions with decreasing  $\theta$ . This was attributed mainly to Coulombic repulsion through the apolar phase, given that even the dissociation of a single polar group on the particle surface is enough to cause electrostatic repulsion stronger than  $100k_B T$ . Although the dipolar repulsion was too weak to explain their experimental observations, the authors mentioned that it could also contribute to the stability of the ordered monolayers. In a follow-up study,<sup>77</sup> these authors confirmed the same trend in particle interactions and ordering with particle hydrophobicity, explaining that less hydrophobic silica particles had considerably smaller charge density at the particle–oil interface that was not sufficient to prevent aggregation. The observed long-range attractive interaction between hydrophilic particles was attributed to capillary attraction caused by undulation of the three-phase contact line due to inhomogeneous wetting of the particles.

Especially for hydrophobic particles, several other experiments<sup>78,79</sup> reported that residual charges at the particle–oil interface are indeed the main cause of long-range interparticle repulsion. This repulsion remained essentially unaffected by varying the pH or salt concentration of the aqueous phase. It is important to note that Masschaele et al. proposed another phenomenon that could account for the observed long-range repulsion. The authors suggested the presence of a dipole moment at the fluid interface that was a consequence of the formation of an asymmetric dense counterion layer (Stern layer) surrounding the particle surface in the water phase, resulting from the finite size of the counterions. Although this layer was thin, the resulting dipole was of the right order of magnitude to explain the discrepancy between theory and experiments.<sup>80</sup> Notably, also the particle size seems to affect the strength of the various components of the electrostatic repulsion between adsorbed particles.<sup>81</sup> For particles larger than the Debye screening length (i.e.,  $\kappa R_p \gg 1$ ), the electrostatic interactions across the aqueous phase were negligible. For smaller particles instead, the interactions across the water phase became

significant. Overall, charges at both the particle–water<sup>72,80,82</sup> and particle–nonpolar fluid<sup>74,76</sup> interfaces can contribute to the effective dipole moment that accounts for the repulsion between like-charged particles.<sup>83</sup> Note that other interactions (such as electrocapillary attractions and hydrodynamic interactions) between interfacial particles can also exist (SI).

Another common way to stabilize particles is to adsorb polymers on their surface. This can be done through either chemical, irreversible grafting (chemisorption) or physical modification (physisorption). When two particles approach each other, the polymer chains exert a steric repulsion, the range of which is defined by the polymer layer thickness and the solvent quality.<sup>37</sup> At a fluid interface, the picture becomes more complicated because the layer thickness, which depends on the solvent characteristics, will be different in the two media.<sup>52</sup> Interestingly, steric repulsion can be engineered to stabilize particles at very short distances, as required for the development of many collective properties.<sup>42</sup> Moreover, choosing polymers that are responsive to external stimuli (e.g., temperature, pH) allows one to actuate the assembled structures. (See the SI for relevant examples.)

**Influence of Additives on the Interactions between Interfacial Particles.** Additives have multiple effects on the magnitude of both attractive and repulsive interactions, which then greatly influences the particle interaction potential and therefore the final self-assembled structures. Electrolytes are mainly used to tune the electrostatic interactions by modifying  $\kappa^{-1}$  (eq 13). The electrostatic repulsion can also be screened by changing the pH of the aqueous phase, in this case affecting the particle charge. Instead, surface-active molecules (surfactants, cosolvents) act at multiple levels. Charged surfactants can effectively act as electrolytes by binding to the particles and modifying their surface charge. Additionally, they can change the wetting properties of the particles ( $\theta$ ) and decrease the interfacial tension of the fluid interface. Generally, these changes are expected to affect both vdW (a  $\theta$  change will influence  $A_{\text{eff}}$  through  $f$ , eqs 9 and 10) and capillary forces (eqs 11 and 12). Furthermore, the induced screening of charges in the aqueous phase is expected to decrease the electrostatic repulsions between like-charged particles. Below, we discuss a few studies that investigated some of these effects; we refer the interested reader to comprehensive reviews on the topic.<sup>1,84</sup>

Direct force measurements between a pair of particles at the interface formed by water and alkanes have been obtained using optical tweezers.<sup>72,73,75</sup> The experimental procedure was the following (Figure 7A,B). Two particles adsorbed at the interface by means of spreading were initially trapped at a long separation; successively, one particle was displaced toward the second one, and the consequent perturbation at the position of the stationary particle was recorded. Using traps with calibrated stiffness, the force experienced by the particle at each interparticle distance  $L$  was measured. The force was repulsive and scaled as predicted, that is, as  $L^{-4}$  (Figure 7C and eq 13). Such a dependence on  $L$  was maintained in the presence of salts added to the aqueous phase. In this case, increasing the electrolyte concentration resulted in the expected decrease in the magnitude of the repulsive interactions, as measured for NaCl concentrations ranging from 0.01 to 250 mM.<sup>72,73</sup> The following work showed that this repulsive force was rather insensitive to the size and valence of the counterions added to the aqueous phase.<sup>82</sup> The authors used  $\text{MgCl}_2$  or  $\text{RbCl}$  instead of NaCl, which have substantially different ionic radii in water but identical anions. The concentration of these salts was chosen to have a constant

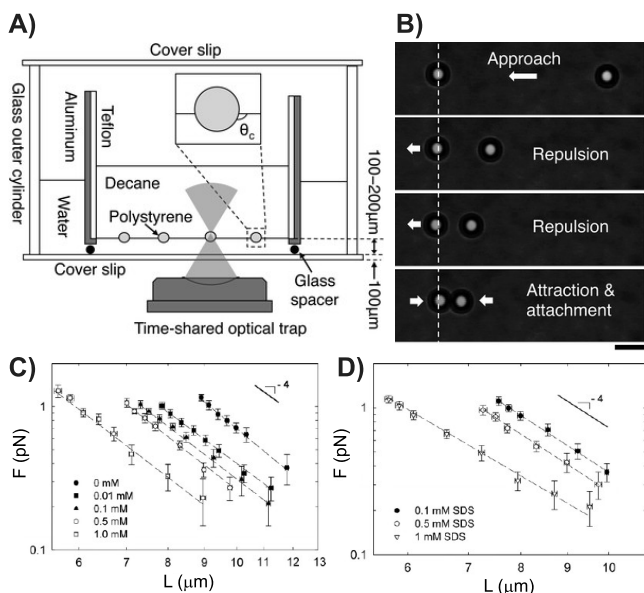


**Figure 7.** Direct measurements of the influence of additives on the interaction force between a pair of particles adsorbed at a fluid interface. (A) Experimental setup: particles at a decane–water interface are held individually by optical traps. The pair interaction force is measured as one particle is brought toward a stationary particle. (B) Snapshots of the experiment. The particle on the left is held in place while the second particle approaches. The displacement of the particle on the left with respect to its initial position (vertical dashed line) is recorded. Scale bar:  $5\ \mu\text{m}$ . (A, B) Reproduced from ref 73 with permission from the Royal Society of Chemistry. (C, D) Dependence of the interparticle force on the center-to-center distance ( $L$ ) of PS particles at the decane–water interface for different (C) NaCl or (D) SDS concentrations. Adapted with permission from ref 72. Copyright 2008 American Chemical Society.

Debye length. In all cases, the dependence of the repulsive force between a pair of particles scaled as  $L^{-4}$ .

The same technique was used to quantify the effect of surfactants on the interaction between two particles at the decane–water interface. The system investigated was composed of anionic PS particles ( $D_p = 3.1\ \mu\text{m}$ ) and anionic sodium dodecyl sulfate (SDS) at a concentration below the CMC.<sup>72</sup> The addition of a surfactant had a 2-fold effect: it acted as an electrolyte decreasing the Debye length, and it also changed the wetting properties of the particles. In this system, the addition of  $0.5\ \text{mM}$  SDS caused an increase in  $\theta$  from  $118$  to  $142^\circ$ , therefore pushing the hydrophobic particles more toward the oil side. Similar to increasing the salt concentration, the addition of SDS of up to  $1\ \text{mM}$  also caused weakening of the repulsion (Figure 7D). Additionally, for the higher  $C_s$  investigated, the force increase at shorter  $L$  was less pronounced. This was evidenced by the slight decrease in the scaling exponent, which deviated from the predicted value of  $-4$ . This suggested the onset of an attractive component in the interaction between the pair of particles. Interestingly, the combined effect of  $250\ \text{mM}$  NaCl and  $0.1\ \text{mM}$  SDS further weakened the strength of the repulsion, and particles jumped into contact at large separations ( $\sim 2\text{--}4\ \mu\text{m}$  for  $D_p = 3\ \mu\text{m}$ ), presumably due to lateral capillary attractions.<sup>73</sup> This attraction was much longer-ranged than expected for vdW forces, which typically extend over a range of tens of nanometers.

**Influence of Additives on Structural Organization.** The interaction between a pair of particles is the basis for

understanding and controlling the assembly of particle ensembles, where multiple interactions over different length scales come into play. Any additive introduced in a colloidal system, either deliberately or unintentionally, will affect the interactions between interfacial particles and hence the structural properties of the resulting assemblies.

**Additives in the Form of Unwanted Impurities.** Additives may be present as impurities in suspensions. Typically, the main sources of impurities are improper cleaning of the colloids after synthesis<sup>85</sup> (especially for surfactant-mediated synthesis), the release of unreacted monomers or un-cross-linked oligomers from the particles,<sup>86</sup> and chemicals unintentionally added during sample preparation.<sup>87,88</sup> Such impurities have been reported to have a profound effect on the interfacial particle organization. For example, Fernández-Toledano et al. discovered that loosely bound aggregates, chains, striations, and loops, which had been frequently observed after spreading particles at an air–water interface (Figure 8A), were actually a consequence of

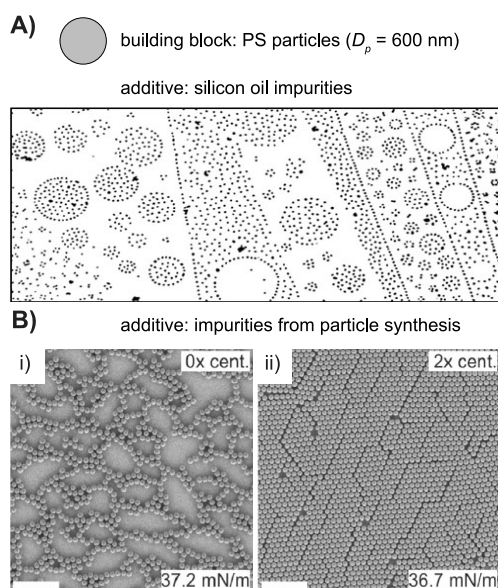


**Figure 8.** Influence of impurities on the structural organization of particles at fluid interfaces. (A) Various particle assemblies obtained after spreading a PS suspension in methanol at the air–water interface. Adapted with permission from ref 88. Copyright 2004 American Chemical Society. (B) SEM images of PS monolayers prepared at the air–water interface and transferred onto a solid substrate. Particle assembly obtained without cleaning the initial suspension (i). After washing the suspension with two steps of centrifugation and supernatant exchange, long-range hexagonally packed assemblies are obtained (ii). Scale bars:  $5\ \mu\text{m}$ . Adapted with permission from ref 86. Copyright 2019 American Chemical Society.

contamination from silicone oil. This was present in the coating of the needles and syringes used to spread the suspension onto the fluid interface.<sup>88</sup> Rey et al. found that the ordering of PS monolayers prepared at an air–water interface and transferred to a solid substrate was strongly affected by the washing procedure that involved the supernatant exchange from the suspension prior to sample preparation.<sup>86</sup> The monolayers exhibited long-range ordering if the suspension was subjected to at least two washing steps; otherwise, the ordering disappeared and the particles assembled into a chain-like network (Figure 8B). The authors attributed this perturbation of the assembly to the leakage of surface-active oligomeric species formed during

synthesis by emulsion polymerization from the particles during their storage. The fact that the purity of colloidal suspensions is linked to the interactions between interfacial particles, and consequently the derived self-assembled structures, is in agreement with other works that have shown that multiple centrifugation and redispersion steps resulted in stronger interparticle repulsions.<sup>85</sup>

**Modifying the Electrolyte Concentration or pH to Tune the Structural Organization.** Apart from the unintentional additive presence and its consequences discussed above, additives may be deliberately added to suspensions to affect the final particle organization. Electrolytes (typically NaCl) in the water subphase were used to suppress the electrostatic repulsion and induce particle aggregation at either the air–water<sup>74</sup> or oil–water interface.<sup>71</sup> In these cases, a transition of the monolayer structure from a hexagonally ordered array, first to clusters, followed by the emergence of interconnected aggregates, was observed. The exact amount of electrolyte required for particle aggregation depends on the particle and interface properties. For example, Aveyard et al. explored the influence of NaCl on the interactions between PS particles spread onto either air–water or alkane–water interfaces.<sup>74,75</sup> Interestingly, these authors could not efficiently spread the particles at the air–water interface when the NaCl concentration in the aqueous phase was less than 10 mM. At this salt content, particles experienced long-range repulsion, with  $L \approx 4D_p$ . Further NaCl addition significantly weakened the interparticle repulsion. At 100 mM, small aggregates and single particles coexisted, indicating a competition between screened repulsions and attractive interactions. At 1 M, interparticle attraction dominated, leading to an interconnected network. When using a divalent salt compared to a monovalent one, aggregation was obtained at a lower salt content.<sup>89</sup> This is in agreement with the DLVO theory that predicts that the transition from a charge-stabilized suspension to an unstable one in the presence of electrolytes occurs at a critical concentration inversely proportional to the counterion valence.<sup>37</sup> However, the DLVO theory alone cannot account for observations that larger amounts of salt (up to about 2 orders of magnitude) were required to induce interfacial particle aggregation compared to the critical concentrations for aggregation in the bulk.<sup>19</sup> This may be attributed to the fundamental differences between interparticle interactions in the bulk and at fluid interfaces, as analyzed earlier.

Electrolytes are nowadays routinely used to precisely control the interparticle distance in ordered structures.<sup>11,18,65</sup> Some examples, with an emphasis on using such additives for various applications, are illustrated in the last part of this Feature Article. Salts are an effective tool to control the lattice spacing through partial screening of the electrostatic interparticle repulsion. We note that this must be done in a very well controlled fashion so that short-range repulsion is still stronger than the attractive interactions.<sup>11</sup> Otherwise, the system quickly aggregates in an uncontrolled fashion. Electrolytes have also been used to control the structural organization of particles with charged polymers grafted on their surfaces.<sup>13</sup> For example, Srivastava et al. developed a platform to control the structure of Au NPs functionalized with single-stranded DNA (ssDNA) assembled at a fluid interface covered with cationic lipids.<sup>13</sup> The ssDNA chains acted as polyelectrolytes and formed a shell around the NPs that ensured their stabilization due to steric and electrostatic repulsions. When electrolytes (NaCl) were added to the aqueous phase, screening of the electrostatic repulsion between the ssDNA chains occurred, enabling the authors to

control the thickness of the shells. A decrease in the shell thickness at higher NaCl concentration resulted in an appreciable decrease in the interparticle distance in the monolayer. The interparticle spacing could be further controlled by changing *ex situ* the length of the DNA chains.

Notably, if the particles have surface groups, the charge dissociation of which depends on the pH, then tuning the pH of the aqueous phase also results in the modulation of the interparticle separation. In this case, the electrostatic repulsion is regulated by direct control of the effective charge of the particles. As an example, Retsch et al. studied the ordering of monolayers of anionic PS particles (carrying sulfate or carboxylic surface groups) at an air–water interface for different pH values.<sup>90</sup> At low pH, the assembly was composed of aggregated particles without spatial ordering. For both particles, the authors attributed this result to a screening of the particle charge, which was not enough to overcome attractive interactions stemming from capillary and vdW forces, as well as possible hydrogen bonding between the protonated acid groups. Conversely, highly ordered hexagonal structures were obtained at higher pH values (5.5 and 10.5) due to strong short-ranged electrostatic repulsions combined with long-range attractive capillary interactions. Alternatively, chemical modification of the particle surface with pH-responsive surface groups also allows for triggering particle organization by linking particles in a reversible manner, depending on the buffer used. This is exemplified by the reversible base-pairing between DNA chains grafted on neighboring NPs (under acidic conditions), as reported by Srivastava et al.<sup>91</sup>

Interestingly, it is possible to control the organization of particles at fluid interfaces not only with water-soluble electrolytes but also with electrolytes dissolved in the organic phase. Edel's group investigated the response of assemblies of Au NPs ( $D_p = 12.8$  nm) at a water–DCE interface upon addition of an organic electrolyte (tetrabutylammonium tetraphenylborate, TBA TPB).<sup>18</sup> Similar to the addition of NaCl in the aqueous phase, TBA TPB in the organic phase allowed for controlling the average spacing between adsorbed NPs, as evidenced by X-ray reflectivity and grazing incidence X-ray scattering. At higher electrolyte concentrations, the screening of the electrostatic interactions between particles increased, resulting in an increase in the interface surface coverage and a consequent decrease in the interparticle distance. This was also visualized by an increase in the overall reflected intensity from the particle monolayer and by the shift of the reflectance maximum toward longer wavelengths, obtained by increasing the TBA TPB concentration from 1 to 10 mM. Further experiments are required to understand the role of these organic ions in tuning interparticle organization<sup>18</sup> and to generalize their use with colloids with different bulk and surface properties.

**Tuning the Interfacial Organization with Surfactants.** As mentioned above, surfactants affect the interaction between particles on multiple levels. They have therefore been employed in various experimental formulations for different purposes (e.g., to screen or suppress the particle surface charge,<sup>24,27,58</sup> to facilitate transfer of the particle monolayer on solid substrates,<sup>90,92</sup> or to tune the particle wettability<sup>28</sup> and efficiently stabilize emulsions<sup>58</sup>).

Typically, surfactants have been used to reduce the order in monolayers of PS particles at the oil–water interface<sup>74</sup> and to control the aggregation kinetics<sup>71</sup> to produce structures with tailored rheological properties and interfacial rigidity.<sup>93</sup> This is a consequence of changes in both the wetting of the particles and

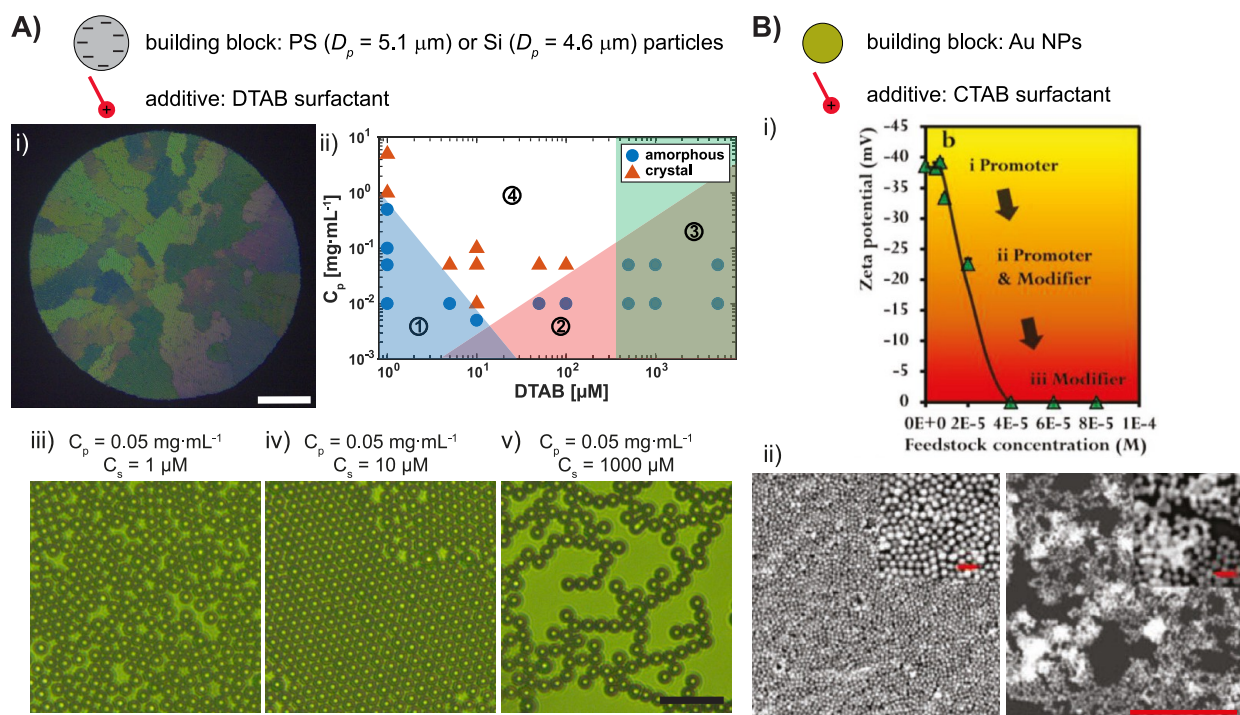


**Figure 9.** Control over the structural organization of interfacial particles by adding an oppositely charged surfactant. (A) PS or silica particles at the air–water interface. (i) A 2D polycrystalline structure obtained by mixing silica particles with  $10 \mu\text{M}$  DTAB. The borders between different structural colors indicate the grain boundaries. Scale bar:  $300 \mu\text{m}$ . (ii) Phase diagram of the 2D structure versus PS particle ( $C_p$ ) and DTAB ( $C_s$ ) concentrations. Symbols indicate an amorphous (circle) or a polycrystalline (triangle) state. The background colors qualitatively depict four zones. (See the main text.) (iii) Images of the different zones in (ii). Scale bar:  $25 \mu\text{m}$ . Adapted with permission from ref 22. Copyright 2018 American Chemical Society. (B) (i) Evolution of the  $\zeta$  potential of Au NPs as a function of the CTAB concentration. (ii) SEM images of Au NP monolayers at the water–DCM interface. At  $C_s = 7 \mu\text{M}$  (left), the monolayers are highly ordered, whereas at higher  $C_s$  ( $60 \mu\text{M}$ , right), the action of CTAB to modify the particle surface results in a disordered assembly comprising 3D aggregates. Scale bars:  $1 \mu\text{m}$  and  $50 \text{ nm}$  in the insets. Adapted with permission from ref 23. Copyright 2020 John Wiley and Sons.

the extent of the electrostatic repulsion, ultimately leading to destabilization of the monolayer. For example, Reynaert et al. studied the aggregation kinetics of ordered monolayers of PS particles formed by spreading them at the decane–water interface, not only in the presence of NaCl in the aqueous phase (as reported above) but also after the addition of SDS.<sup>71</sup> SDS caused both a decrease in  $\gamma$  and an increase in  $\theta$ , causing the particles to be pushed more into the oil phase. Consequently, the authors predicted a weakening of the lateral capillary interactions as well as of the double-layer electrostatic repulsion. Experimentally, they reported that SDS greatly reduced the time required to induce particle aggregation when salt was also present in solution. Conversely, the addition of SDS alone did not lead to pronounced aggregation but to a transition from a crystalline to a melted phase. They concluded that, to speed up the aggregation kinetics, an interplay of changes both in the electrostatic and wetting properties of the particles was required. Aggregation was promoted by an increased weakening of the electrostatic repulsion, while the directionality of particle aggregation was a consequence of the strength and anisotropy of the lateral capillary interactions. Such a strategy allowed the obtaining of percolating 2D colloid networks with reproducible structural features (i.e., particle coordination number, size of voids). This was later used to study the rheological properties and microstructural reorganization of aggregated monolayers subjected to interfacial shear flows.<sup>94</sup>

On the contrary, in experiments for producing ordered monolayers on solid substrates after transfer from the air–water interface, it was found that a small amount of SDS actually

increased the degree of order.<sup>90,95</sup> It should be noted that, in these examples, the structural organization of the assembly was characterized only *ex situ* after transferring onto a substrate. For  $C_s = 1 \text{ mM}$ , disordered structures of PS particles ( $D_p$  from  $0.18$  to  $1.12 \mu\text{m}$ ) were produced. Instead, for  $C_s = 0.1 \text{ mM}$ , an increased long-range order was observed with respect to the monolayer in the absence of SDS. This was attributed to a higher mechanical stability of the monolayer due to the presence of surfactant, which would help the transfer from the fluid interface onto the solid substrate. These experiments were done by spreading particle suspensions onto the fluid interface, usually in the presence of salts in the water subphase. This complicates the understanding of the role of surfactants in controlling particle assembly by introducing multiple parameters (e.g., the presence of spreading solvents, typically isopropanol, and of external forces and flows). The latter include Marangoni flows induced upon spreading, and the drying-induced compression of the fluid interface while transferring the monolayer onto solid substrates.

As discussed above, using surfactants of charge opposite to that of the particles at concentrations around the CMC to induce particle adsorption at fluid interfaces is nowadays a routinely applied process. The consequent particle neutralization induces aggregation and typically hinders the formation of structures with long-range positional order.<sup>96</sup> Indeed, long-ranged 2D crystals in the presence of surfactants have been found only in some special cases. For example, Velikov et al. studied the entrapment and organization of anionic PS particles ( $D_p = 7 \mu\text{m}$ ) confined in thin air–water–air films, produced out

of a reservoir of the suspension containing surface-active additives used as film stabilizers.<sup>97</sup> The interfacial behavior of particles upon thinning of the liquid film was observed, and different results were obtained depending on the additive used. In the presence of anionic SDS, the particles were pushed out of the water confined in the thinning film, presumably due to the electrostatic repulsion between the particles and the like-charged surfactants. Instead, in the presence of cationic DTAB at  $C_s = 6$  mM ( $\sim$ CMC/2), the partially hydrophobized particles adsorbed onto the film, first at the lower and then at the upper air–water interface, linking the two together. Successive cycles of opening and closing of the liquid film promoted the capture of an increased number of particles, up to complete surface coverage. Interestingly, under this condition the particles assembled into long-range 2D crystals. This was attributed to the combined effect of mechanical forces exerted on the monolayer and the fact that the particles were partially hydrophobized, which means that they could adsorb while maintaining 2D mobility within the interface plane. For  $C_s >$  CMC, the quality of the particle ordering inside the film was lower, while particles were also coagulating in suspension. Consequently, it was concluded that an important prerequisite to obtaining structures with long-range order was to use an appropriate surfactant at a concentration that caused particle hydrophobization but not bulk aggregation.

Another exceptional case of 2D colloid crystal formation, however of a smaller spatial extent and at a curved fluid interface, was demonstrated by Ramos et al.<sup>98</sup> These authors found that anionic PS particles ( $D_p = 0.83$ – $1$   $\mu$ m) could self-assemble in 2D crystals when adsorbed on the surface of oppositely charged vesicles prepared using mixtures of surfactants, having diameters from 100 nm to several micrometers. Under the appropriate surfactant composition (always above the CMC) and when the total charge on the vesicle was greater than the total particle charge, ordered 2D crystalline arrays formed on the surface of the vesicles. This process started with particle adsorption onto the fluid vesicle surface, which allowed particles to diffuse within its plane. The interfacial particles then assembled into 2D rafts, indicating a weak interparticle attraction. These rafts were initially amorphous, and their degree of order increased with time until particles were attached to each other and a 2D crystal was formed that then detached from the vesicle surface. The authors proposed a model that considered the total charge neutralization of particles in contact with the membrane and charge alterations along the membrane that involved the movement of counterions released by the particles and possible surfactant demixing.

Successive works focused instead on surfactant concentration ranges for which extensive particle hydrophobization was avoided. By using the flipping method described earlier, Anyfantakis et al.<sup>22</sup> discovered that when  $C_s \leq$  CMC  $\times 10^{-3}$ – $10^{-4}$ , monolayers of anionic PS particles with various degrees of order were formed at the air–water interface (Figure 9A). These assemblies were rationalized as a function of both surfactant ( $C_s$ ) and particle ( $C_p$ ) concentrations. The two main interactions at work were the electrostatic repulsion between like-charged particles and the collective deformation of the interface around particle clusters. The latter resulted in a long-range attractive potential that, at sufficient deformation, brought particles close to each other. For the whole  $C_s$  range analyzed, the particles maintained the same wetting properties ( $\theta \approx 30^\circ$ ). At low  $C_p$  and  $C_s$ , the number of adsorbed particles was small while the particles remained highly charged. These well-stabilized

interfacial particles assembled into a disordered phase (region (1) in Figure 9A (ii) and (iii)). Increasing  $C_p$  at low  $C_s$  promoted particle crystallization (region (4)) by the “collective sinking” mechanism: the particle assembly was large enough to induce a significant interface deformation that in turn facilitated particle packing. Increasing  $C_s$  (at constant  $C_p$ ) to up to 10  $\mu$ M promoted particle adsorption at the fluid interface by decreasing the adsorption barrier, without changing the particle charge (as evidenced by a constant  $\zeta$  potential in the bulk). Therefore, the slope of region (1) was negative and 2D crystals were obtained at lower  $C_p$  (Figure 9A (i–iv)). A further increase in  $C_s$  yielded screening of the particle charge and lowered the electrostatic interparticle repulsion, as surfactants started to adsorb significantly onto the oppositely charged particles. For  $C_s >$  10  $\mu$ M but low  $C_p$  (region (2)), particles did not form crystals because they were partially neutralized by the surfactants. Increasing  $C_p$  again promoted crystallization by increasing the long-range attractive potential, confining the particles in the center of the curved air–water interface. Finally, for  $C_s \geq$  500  $\mu$ M the surface charge was almost zero, leading to “sticky” particles which formed an amorphous gel-like structure regardless of the particle concentration (region (3), Figure 9A (v)). This interfacial crystallization mechanism was then generalized with the more hydrophobic CTAB surfactant and with silica and metallic NPs.<sup>12</sup>

Later on, Li et al. rationalized the role of CTAB in adsorbing anionic NPs at the DCM–water interface by combining  $\zeta$ -potential measurements with surface-enhanced Raman scattering (SERS) at the fluid interface.<sup>23</sup> In a typical experiment, aqueous suspensions of citrate-stabilized Au NPs containing CTAB were vigorously mixed with DCM. Particles adsorbed at the interface, as evident from the formation of a metal liquid-like film, for  $C_s$  ranging from 5 to 8  $\mu$ M, above which significant emulsification occurred. The SERS spectra were used to determine whether the surfactants were adsorbed onto the interfacial particles. At low  $C_s$ , particles remained charged ( $\zeta \leq -30$  mV, Figure 9B (i)) and the SERS spectra were dominated by the citric acid bound to the particles, with only a minor presence of CTAB bands. Instead, at  $C_s >$  20  $\mu$ M, a large amount of surfactants adsorbed onto the particles, as evidenced by the CTAB bands in the SERS spectra, and the  $\zeta$  potential reached a zero value. Surfactant adsorption onto the particles had a direct effect on the final organization at the interface. When the interfacial particles remained highly charged, they assembled into a close-packed monolayer. Conversely, particle neutralization led to the formation of 3D aggregates (Figure 9B (ii)).

These<sup>23</sup> and the previous results<sup>12,22</sup> emphasize the dual effect of cationic surfactant in adsorbing and organizing anionic particles at fluid interfaces. At low  $C_s$ , surfactants act as “promoters”, facilitating particle adsorption at the interface by decreasing the adsorption barrier. At the same time, the limited surfactant adsorption onto the particles leaves their surface properties unchanged, hence particles can form ordered 2D assemblies. Above a certain concentration threshold, dependent on the surfactant hydrophobicity (largely indicated by the CMC) and thus the extent of its adsorption onto the particles, surfactants act as “modifiers”. They adsorb significantly onto the particles, causing neutralization of the surface charge and inducing aggregation in the bulk and/or at the fluid interface.

**Other Additives Used to Tune the Structural Organization.** For the special case of Au NPs, Park’s group employed a specific additive, 1-dodecanethiol, to promote the formation of highly ordered monolayers at the hexane–water interface.<sup>32</sup> As already

mentioned, the addition of ethanol to the aqueous phase allowed for the destabilization of the suspension and consequently drove particle adsorption at the interface. In the absence of other additives, the formed monolayers were not ordered, presumably due to an electrostatic repulsive force between particles that was strong enough to prevent the formation of a close-packed film.<sup>32</sup> Instead, alkanethiols present in the hexane phase could adsorb onto the NP surface, causing their partial hydrophobization and consequently modifying the interparticle interactions at the interface (Figure 10A). At intermediate concentrations of 1-

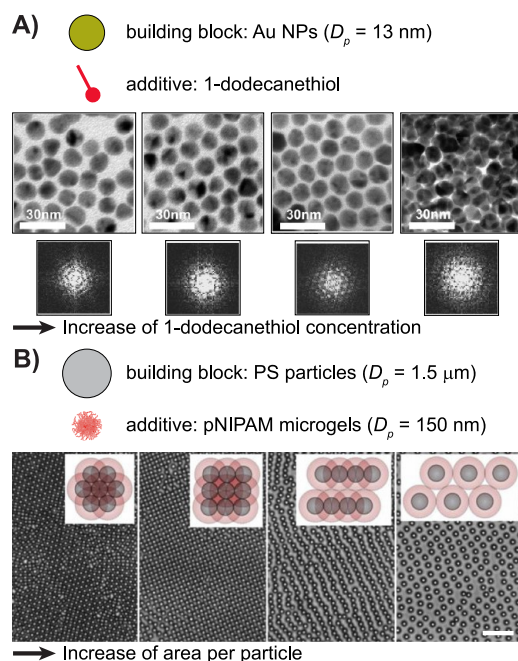


**Figure 10.** Employing reactive and polymeric additives to control the structural organization of adsorbed particles. (A) TEM images and corresponding fast Fourier transform of Au NPs adsorbed at the hexane–water interface in the presence of 1-dodecanethiol (0,  $4.17 \times 10^{-9}$ ,  $4.17 \times 10^{-7}$ , and  $4.17 \times 10^{-4}$  M from the left to the right image, respectively) in the hexane phase. Adapted with permission from ref 32. Copyright 2007 American Chemical Society. (B) PS particles and pNIPAM microgels adsorbed at the air–water interface. The microgels coat the PS particle surface and allow for tuning the structural organization at various surface compressions in a Langmuir trough. Scale bar:  $10 \mu\text{m}$ . Adapted with permission from ref 99. Copyright 2017 American Chemical Society.

dodecanethiol, its adsorption onto the NPs surface decreased the surface charge density. This led in turn to a further decrease in the electrostatic repulsion between the particles, thus favoring the formation of an ordered close-packed assembly. Instead, a higher 1-dodecanethiol concentration caused the formation of multilayers by the aggregation of NPs in the bulk.

New interesting directions for controlling particle assembly at fluid interfaces have been explored recently. One example exploited specific amphiphile/particle mixtures for promoting 2D organization into more complex geometries, including chain-like particle arrangement and square-packed arrays, and improved the control over the interparticle distance. Rey et al.<sup>99</sup> assembled mixtures of PS particles ( $D_p = 1.5 \mu\text{m}$ ) and soft pNIPAM microgels ( $D_p = 145 \text{ nm}$ ) at the air–water interface. The attractive interparticle interactions led to the *in situ* formation of a microgel corona around each PS particle at the interface. The microgels effectively acted as additives and

allowed the authors to assemble the PS particles into complex geometries upon compression of the fluid interface (Figure 10B). At maximum compression, PS particles arranged into a hexagonally close-packed crystal. Interestingly, relaxing the system by increasing the available area per particle caused the particles to assemble first into a phase with square symmetry, followed by distinct particle chains. Further increases of the available area resulted in a transition to a non-close-packed hexagonal arrangement with increased interparticle distance. The authors concluded that the microgel corona around the particles at the air–water interface added a soft, repulsive component to the interaction potential between the microspheres, which ultimately brought anisotropic interactions to the isotropic building blocks. At intermediate compressions, the system minimized its energy by fully compressing microgels in some directions to prevent the compression of the other microgels comprising the corona around the PS particles. Similar phase behavior was later obtained when mixing PS particles with smaller amphiphiles, such as block copolymers and proteins.<sup>100</sup>

**Rational Choice of Additives for Controlled Interfacial Particle Organization.** We earlier concluded that the appropriate choice of additives for efficiently adsorbing particles onto a fluid interface ultimately depends on the particle properties. A natural follow-up question is which type and amount of additive should one use to control the organization of interfacial particles? Our answer is in line with our earlier conclusion: it all depends on the physicochemical characteristics of the particles and the desired structural features of the resulting assembly. The strength and range of interactions responsible for interfacial colloid assembly primarily depend on the building blocks. As for bulk suspensions, particles adsorbed at fluid interfaces are stabilized by electric-double-layer repulsion due to ionizable surface groups and/or steric interactions in the case of polymer-grafted particles. Additional longer-range repulsions arise from electrostatic interactions between dipoles induced by the asymmetry in surface group dissociation across the interface. In the presence of residual charges in the apolar phase, Coulomb interaction between those charges also occurs, providing an additional long-range repulsion. These repulsive forces are counteracted primarily by attractive capillary forces, which, if predominant, dictate the directionality of the particle assembly and the formation of disordered, aggregated structures.

Additives influence the strength and range of interparticle interactions on *multiple* levels by varying several parameters, such as the electric double layer extent, the particle charge and wettability, and the fluid interfacial tension. Controlled interfacial particle organization is obtained only after carefully balancing both attractive and repulsive interactions. First, the particle number density must be high enough to promote self-assembly. Ordered structures spanning large areas are then obtained when particle–particle repulsive interactions are stronger than short-ranged attractions. This ensures adequate particle mobility within the interface plane, allowing for the rearrangement of particles into well-ordered assemblies. Additionally, a long-range attractive component or, alternatively, an external force that compresses the monolayer is usually required to accumulate and assemble all of the interfacial particles into the final structure.<sup>41,95,97</sup> The main role of additives in producing well-ordered arrangements is to tune the short-range attractive and repulsive forces. In most cases, the additive concentration should be chosen carefully so that it is below a given threshold, after which repulsive forces (typically electrostatic) are suppressed.<sup>22,23</sup> Such a threshold value primarily depends on the

additive chosen. Notably, within this concentration range, a careful screening of such repulsion also allows one to control the interparticle spacing in ordered structures.<sup>11,22</sup> Recent examples showed that soft repulsive interactions further allowed the promotion of anisotropy in the particle organization, leading to square-packed and chain-like assemblies.<sup>99</sup> Instead, to produce interfaces with tailored mechanical properties and shapes (e.g., planar<sup>94</sup> or arbitrarily<sup>30</sup> shaped networks, *bijels*<sup>7</sup>), interlocked structures with particles in strong contact are required. In such cases, the repulsive interactions are typically strongly suppressed at the concentration of additives used. All of these can be achieved by employing various additives (e.g., common salts, surfactants, polymers, or more particle-specific chemicals such as alkanethiols), which can be advantageously added to one or both fluid phases.

One may also wonder if a given additive is good enough to both facilitate particle adsorption and control self-assembly at a fluid interface. Here the answer is yes. A majority of additives have an effect on both particle–interface and particle–particle interactions in the bulk and at the interface. Fortunately, this usually takes place in a different concentration range. Particle adsorption and interactions among interfacial particles can be modulated even at additive concentrations low enough to maintain well-stabilized particles. This means that one does not necessarily need to work at high additive concentrations, which usually reduces the colloid stability and may lead to uncontrolled particle aggregation. Indeed, several works reported that a careful choice of the additive amount, within a narrow concentration window, allows one to control particle adsorption and organization at the same time. The acquired knowledge can be used to produce designed 2D structures simply by mixing, in the right amount, particles and additives. This has been generalized to different building blocks mainly for the case of minute amounts of surfactant in the aqueous phase<sup>12</sup> or for oil-soluble electrolytes.<sup>5</sup> The fact that the above additives are readily available and cost-effective adds a significant practical advantage to their use. Finally, we wish to highlight the importance of starting from a colloidal suspension, the composition of which is known precisely (i.e., devoid of unwanted impurities).

## ■ SPECIAL PROPERTIES AND APPLICATION POTENTIAL OF 2D COLLOID ASSEMBLIES

In this last part, we highlight a few recent examples of the application potential of 2D particle assemblies at fluid interfaces. In all cases, additives are a key component for producing the required structures. Self-assembled monolayers are exploited for various applications that make use of collective properties arising from the long-range and precisely controlled structural organization that can be attained by using several strategies.<sup>1,84</sup> To name a few examples, particle monolayers are used as masks for colloidal lithography,<sup>101</sup> for the fabrication of photonic crystals,<sup>102</sup> in plasmonic devices,<sup>6</sup> in coatings with specific wettability or reflection properties,<sup>103</sup> and as parts of complex materials that mimic natural structures.<sup>104</sup> In most cases, such applications require transferring the ordered assembly produced on fluid interfaces onto a solid substrate. Nonetheless, nowadays applications that make direct use of particles assembled at fluid interfaces are receiving increasing interest due to several advantages that they offer,<sup>105</sup> which will be highlighted throughout the text. These include the simplicity of their fabrication, their self-healing properties and responsiveness to external stimuli, and their ability to interact with traces of analytes soluble in either aqueous or organic phases.

Regardless of the exact properties desired, precise control over the adsorption and structural organization of the particle monolayer is of utmost importance because it directly affects the macroscopic material response. For example, defect-free ordered arrays are required for optical applications,<sup>12</sup> whereas interconnected networks are sought after for making rigid particle layers.<sup>30</sup> Here, we first discuss systems, the properties of which can be precisely modulated by the chemical composition of the system (e.g., pH and salt or surfactant content). We then go a step beyond and emphasize some remarkable responses of particle monolayers to external stimulation, of possible interest for future applications. Such stimuli can be either the addition of a specific chemical or the application of an external field, such as light or electric voltage. In these cases, the additives bring about responsiveness to external stimulation and allow for remotely tuning the structural organization and hence the functionality of the adsorbed particles.

**Additive-Controlled Interfacial Particle Assembly for Macroscopic Materials with Tailored Functionalities.** In this section, we discuss works in which additives have been used to prepare macroscopic colloid assemblies that are capable of performing specific tasks of practical interest. This is achieved by exploiting additives to precisely tune the nano- or micro-structure of the assemblies, which in turns leads to the emergence of remarkable physical and chemical properties.

*Preparing Materials with Unique Mechanical Behavior.* Russel and co-workers used polymeric surfactants as additives to control the structural and mechanical properties of liquid interfaces. Their system was composed of NH<sub>2</sub>-terminated PDMS chains dispersed in silicone oil and COOH-functionalized PS or silica NPs in the aqueous phase (as described above).<sup>29</sup> The NPs and the polymer chains diffused inside the fluids and met at the interface, where they electrostatically bound to each other to form an elastic skin of adsorbed particles. When  $C_p$  increased, the NPs underwent a transition from a liquid-like state to a solid-like state above a concentration threshold that yielded a percolating network.<sup>106</sup> Such an elastic network allowed locking in place the shape of the liquid interface by driving it to a kinetically trapped state. This system was used to print water in 3D shapes inside the oil phase (Figure 11A,B).<sup>30</sup> When the suspension was extruded through a needle, the NPs and the polymers assembled at the liquid interface into a percolating network. If the network was formed before the jet broke into droplets, then the shape of the water jet was kinetically trapped within the oil phase. Interestingly, the addition of multiple NH<sub>2</sub> functionalities on the polymer backbone caused cross-linking of the NP film, allowing the authors to tune the mechanical properties of the printed liquid shapes. The only requirement for an appropriate liquid surface coverage was the complementarity between the surface groups on the NPs and the functional groups on the polymer chains to ensure electrostatic binding. Therefore, numerous NPs have been used, including PS, silica, and Fe<sub>3</sub>O<sub>4</sub> nanocrystals.<sup>107</sup>

*Controlling the Deposition of Particles on Solid Surfaces by Suspension Drying.* Colloids find well-established applications as inks in the inkjet printing technology. In this case, particle-laden droplets (with a typical volume on the order of picoliters) are dispensed on a solid substrate, and particle deposition is accomplished after solvent evaporation. In most printing applications, homogeneous particle distribution across the substrate is required. An omnipresent obstacle in obtaining uniform deposits from any drying sessile drop of a colloidal suspension is the coffee-ring effect (Figure 3B).<sup>61</sup> To overcome

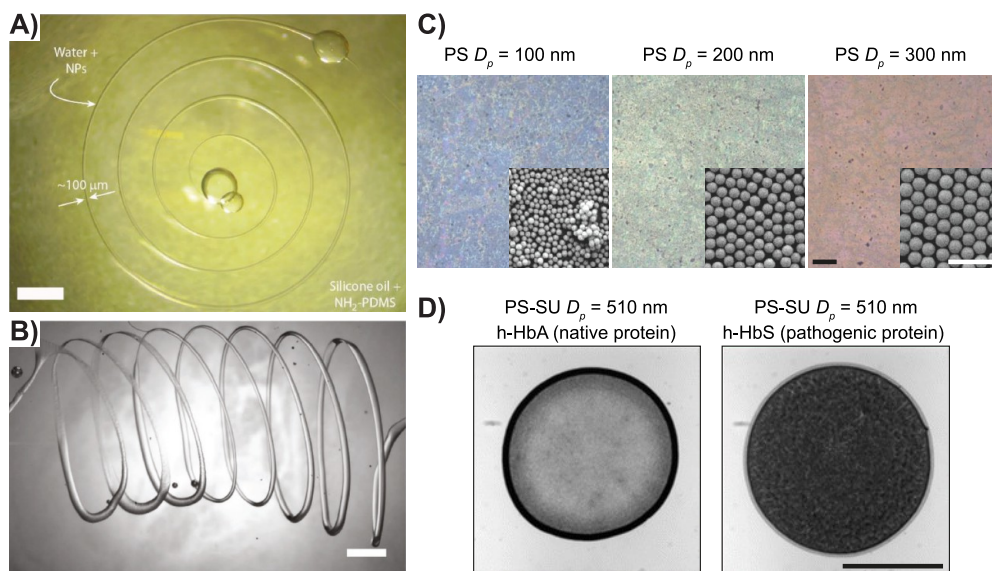


**Figure 11.** Control of particle adsorption at fluid interfaces for various applications: printing of liquid or solid structures and analyte detection. (A, B) Aqueous filaments printed in a silicon oil bath. COOH-functionalized silica NPs ( $D_p = 20$  nm) and  $\text{NH}_2$ -functionalized PDMS chains assemble with each other at the fluid interface to form a skin that locks in place the shape of the water jet. Scale bars: 2 mm. Adapted with permission from ref 30. Copyright 2018 John Wiley and Sons. (C) PS NP deposits obtained using the dual-droplet inkjet printing method. (See the main text.) The degree of order and the emergent structural color depend on the NP size (scale bar:  $50 \mu\text{m}$ ). (Inset) SEM images showing the structure of these deposits (scale bar:  $2 \mu\text{m}$ ). Adapted with permission from ref 109. Copyright 2018 John Wiley and Sons. (D) Deposits obtained from drying an aqueous drop containing sulfate-functionalized PS particles and human hemoglobin. The latter either was in its healthy native form (h-HbA) or underwent a pathogenic mutation (h-HbS). The difference in deposit morphology offers a simple, visual way of distinguishing the two protein forms. Scale bar: 1 mm. Adapted with permission from ref 60. Copyright 2016 American Chemical Society.

this, a major challenge in applying inkjet processes to the printing of functional materials is the design of appropriate “inks” that lead to homogeneous deposition. The formulation of suitable inks more often than not includes additives, which play a major role in dictating the colloid assembly after drying.<sup>108</sup> For example, additives such as cosolvents<sup>108</sup> are exploited to suppress the flow patterns within the drying droplets and realize uniform deposition thanks to a sol–gel transition that takes place. Although the descending surface of the droplet may cause a local increase in particle concentration yielding aggregation and in turn network formation, this mechanism does not involve particle adsorption onto the interface.<sup>108</sup>

Surprisingly, particle adsorption and self-assembly at fluid interfaces of printed droplets have rarely been exploited in inkjet printing to produce uniform deposits. A remarkable exception is the dual-droplet inkjet printing method developed by Al-Milaji et al.<sup>109</sup> This concept is based on the adaptation of the Langmuir–Blodgett method for picoliter droplets. A droplet of a high- $\gamma$  liquid (typically water) was first printed on the substrate. Successively, a second droplet (called the wetting droplet) of a particle suspension in a low- $\gamma$  solvent was dispensed on top of the first one. The particles spread over the underlying droplet and self-assembled at the liquid–liquid interface. Particle deposition on the supporting substrate took place after all solvents had evaporated, and the morphology of the dry pattern depended on the interactions between the particles and the fluid interface. When most particles adsorbed, well-ordered monolayers were obtained after drying. On the contrary, when particles diffused into the supporting droplet, disordered assemblies were formed. The particle–interface interaction and thus the structure of the dry deposits were dependent on various parameters, such as the solvent composition of the wetting droplet, the charge density of the particles, and the particle concentration. When the wetting droplet comprised

particles suspended in pure ethanol and their charge density was low, nearly 2D close-packed assemblies could be fabricated. The printed deposits displayed structural colors, which were dependent on the degree of order in the assembly and on the particle size (Figure 11C).<sup>109</sup> The same authors modulated the deposit morphology by changing the pH of the supporting droplet.<sup>110</sup> Carboxylated PS particles ( $D_p = 100$  nm) were organized into ring-like deposits and nearly monolayer films under acidic and basic conditions, respectively. On the contrary, PS particles with sulfate groups formed nearly monolayer assemblies in both low- and high-pH environments. These observations were explained on the basis of the pH-dependent affinity of particles for the bulk (for highly charged particles) or the fluid interface (upon charge decrease).

*Retrieving Microscopic Information from a Visual Inspection of Colloid Deposits.* Devineau et al. investigated the effect of proteins on the interaction between particles and the air–water interface of a drying sessile drop.<sup>60</sup> This was then exploited to develop a simple tool for detecting a single point mutation in a blood protein. The authors mixed PS NPs with different surface functionalizations with various proteins. The evolution of the morphology of deposits obtained after drying drops of mixtures of NPs with the globally negatively charged protein bovine serum albumin (BSA) was qualitatively similar to the case of particle/surfactant mixtures.<sup>24</sup> BSA adsorbed onto both anionic and cationic NPs via mostly hydrophobic and electrostatic interactions, respectively. However, the CRE was suppressed only for cationic NPs because the strong Coulomb attraction ensured that the amount of adsorbed proteins was large enough to make the NPs overall neutral. The situation was different with NP mixtures with the globally positively charged porcine hemoglobin (p-HbA). This protein adsorbed to a small extent onto cationic NPs, and as expected, the deposit morphology was always ring-shaped. Although p-HbA strongly



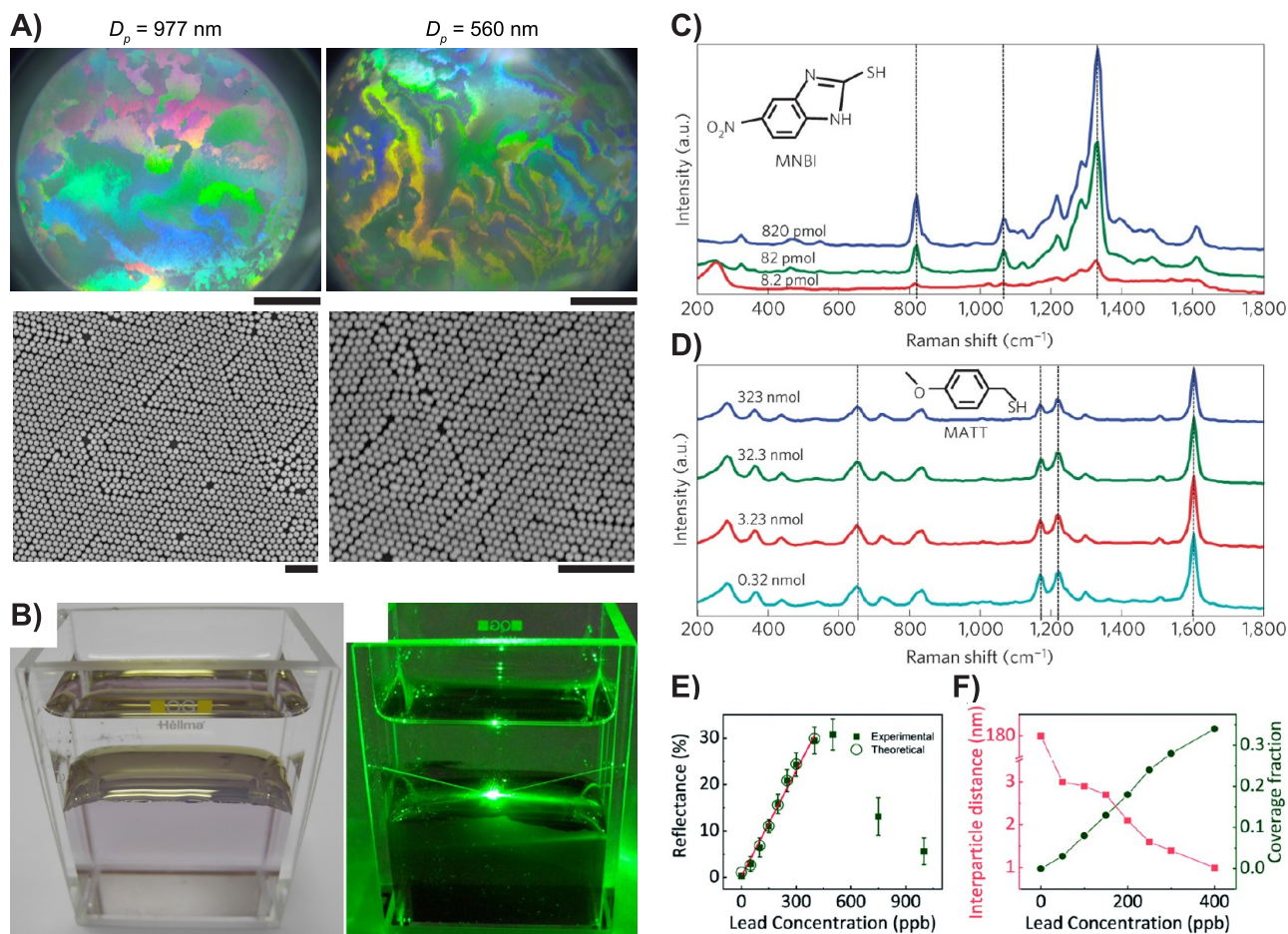


**Figure 12.** Applications based on the optical properties of particle assemblies at fluid interfaces. (A) Top row: structural colors resulting from the ordered assembly of silica particles at the air–water interface, promoted by adding  $5 \mu\text{M}$  DTAB (scale bar: 1 mm). Bottom row: SEM images of the particle assembly (scale bar:  $5 \mu\text{m}$ ). Reproduced from ref 12 with permission from the Royal Society of Chemistry. (B) Au NP ( $D_p = 60$  nm) film at the [heptane + DCE]–water interface. In the right image, the reflection of a laser beam from the interface is shown. Adapted with permission from ref 114. Copyright 2013 American Chemical Society. (C, D) SERS spectra from an Au NP monolayer at a water–DCE interface for different analyte concentrations. In (C), mercapto-5-nitrobenzimidazole was dissolved in the aqueous phase. In (D), 4-methoxy- $\alpha$ -toluenethiol was dissolved in the organic phase. Adapted with permission from ref 17. Copyright 2013 Springer Nature. (E) Maximum reflectance from a monolayer of glutathione-functionalized Au NPs at the water–DCE interface versus lead concentration in solution. (F) Calculated interparticle distance (red squares) and coverage fraction (green circles) versus lead concentration. (E, F) Reproduced from ref 115 with permission from the Royal Society of Chemistry.

adsorbed onto the anionic NPs, different deposit morphologies were obtained depending on the particle surface functionalization. Homogeneous patterns were observed only with NPs having sulfate groups, at p-HbA concentrations corresponding to charge neutralization. On the contrary, ring deposits were obtained with carboxylated NP at all of the studied p-HbA concentrations, despite NPs being overall neutralized at intermediate protein concentrations. This suggested that other effects, such as the reorganization of the proteins after they had adsorbed on the NPs, might play a significant role. Overall, the authors concluded that whenever NPs became hydrophobic they adsorbed at the air–water interface and formed an NP skin that was then homogeneously deposited on the substrate. On the contrary, when protein adsorption did not result in particle affinity for the fluid interface, NPs remain dispersed and the CRE yielded ring-shaped inhomogeneous deposits. On the basis of the above principles, the authors showed that a visual inspection of the deposit from a protein/NP mixture could distinguish healthy human hemoglobin (h-HbA) from its mutant form (differing by a single amino acid, h-HbS) that is responsible for sickle-cell anemia. Though both protein forms

adsorbed onto the NPs, it was only the adsorption of h-HbS that led to homogeneous NP deposits (Figure 11D). This confirmed that simple particle charge neutralization (which occurred only for h-HbA) due to protein adsorption could not always eliminate the CRE as in surfactant/particle mixtures. Instead, the required NP hydrophobicity was provided by the reorganization of the adsorbed h-HbS on the NP surface, which exposed hydrophobic protein moieties to the aqueous phase.

**Exploiting the Remarkable Optical Properties of Colloid Assemblies for Photonics and Sensing.** *Structural Colors from Ordered Interfacial Assemblies.* The emergence of structural color in soft matter is currently an active research topic in colloid science.<sup>102</sup> When a material is irradiated with white light, we perceive a particular color if light that reaches our eyes is within a narrow wavelength range. On the contrary to pigments and dyes, which prevent light of other wavelengths from reaching us due to absorption, structural color does not involve energy exchange between light and matter. Instead, phenomena such as refraction, scattering, and interference cause light to split into beams of different wavelengths, consequently resulting in the perceived color. These originate from a refractive

index periodicity in the material on the order of the wavelength of the incident light.<sup>102</sup> The vivid interest in structural colors stems in part from the quest to understand the interactions of light with the nanostructures responsible for the above phenomena and in their exploitation to create advanced coatings with vivid colors, which do not fade away (in contrast to colors from dyes and pigments). The fact that ordered 2D arrays of particles frequently display brilliant structural color, in conjunction with the relative ease of fabricating them on the macroscopic scale, highlights their application potential.

Structural colors are often observed in self-assembled monolayers of particles spread at the air–water interface.<sup>95,111</sup> Crystallization was achieved either by increasing the number of adsorbed particles by several additions of spread drops or by compressing the monolayer with moving barriers in a Langmuir–Blodgett trough. The resulting close-packed assemblies displayed brilliant structural colors, which were retained after transferring on a solid substrate. For example, Vogel et al. employed this to prepare binary colloid assemblies comprising close-packed monolayers of large particles with a superlattice of smaller particles positioned in the interstitial sites.<sup>95</sup> After compression was used to make this superstructure, the particle-laden fluid interface was lowered to deposit the monolayer onto a solid substrate. The authors could fabricate large 2D crystals, the size of which was limited only by the trough area, as demonstrated by a colored crystal that was deposited on a 6 in. silicon wafer. It consisted of centimeter-sized monocrystalline domains, distinguishable by their distinct coloration.

Besides spread monolayers, structural color has been observed in cases where 2D self-organization occurs with particles spontaneously adsorbing from the bulk. As already mentioned, Sekido et al. observed iridescent colors from monolayers of PDEA-stabilized PS particles at the air–water interface during suspension drying.<sup>21</sup> Colors at the fluid interface were observed for  $\text{pH} \geq 6.3$ , where the surface charge was reduced and particles were efficiently adsorbed (Figure 4C). Vialletto et al. extended the strategy of flipping a suspension upside down in the presence of cationic surfactants to allow the gravity-induced adsorption and control of the 2D assembly of silica NPs.<sup>12</sup> The addition of DTAB at  $C_s$  values of as low as 1–10  $\mu\text{M}$  promoted the complete adsorption of all NPs at the interface, allowing their assembly into a 2D crystalline monolayer. Upon side illumination with white light, vivid structural colors emerged (Figure 12A). When an increased amount of surfactant (1 mM) was used instead, aggregation of the adsorbed particles resulted in a disordered monolayer that appeared whitish under the same illumination conditions. A qualitatively identical picture emerged for NPs of various sizes ( $D_p = 304\text{--}977$  nm), showing that this method is applicable for preparing structurally colored 2D assemblies from different systems. Notably, this approach allows one to avoid wasting NPs in the bulk because of the high yield of particle adsorption to the interface, contrary to other methods. It is worth pointing out that, although common for submicrometer particles, structural colors have also been documented in 2D assemblies of micrometer-sized particles (e.g., at the air–water interface<sup>22</sup> or in dried particle-stabilized foams<sup>96</sup>). Although this may be attributed to the higher-order selective reflection of light,<sup>96</sup> further research is needed to clarify the underlying optical phenomena.

**Metal Nanoparticle Arrays Functioning as Optical Elements.** One of the most promising platforms with the potential for innovative applications is the assembly of metal

NPs at liquid–liquid interfaces,<sup>112</sup> which has been proposed for a range of applications, from photonics (e.g., liquid mirrors and filters) to photocatalysis and sensors. A layer of metal NPs at a fluid interface results in a film that maintains metallic properties such as high reflectivity, while it exhibits rheological properties similar to those of liquids; for instance, it can sustain waves, flow, and self-heal.<sup>113</sup> The reason for such remarkable optical responses lies in the unique properties that noble metal NPs (e.g., Au, Ag) inherently possess.<sup>112</sup> Single metal NPs have a strong absorption band in the visible that is absent in the bulk material. This is because the conduction band electrons undergo a coherent oscillation due to their interaction with the electromagnetic field of the incoming light wave. Light absorption occurs when the frequency of the incident photon matches that of the collective oscillation, and this effect is called surface plasmon resonance (SPR). The SPR can be tuned either at the single NP level, because it depends on NP properties such as size and shape, or in NP assemblies. In the latter case, the optical response of the assembly results from collective plasmonic effects, and it is sensitive to the interparticle spacing. It follows that the control of both the NP surface coverage and the interfacial organization is crucial to tuning the optical response of the functionalized interfaces, and it is currently a hot research field.<sup>112</sup> Such control has been advantageously realized by including additives in one of the two liquid phases.

In a seminal study, Yogeve and Efrima have shown that Ag films formed at the DCM–water interface exhibited high specular reflectivity and thus acted as liquid mirrors.<sup>113</sup> Later on, Fang et al. provided another clear demonstration of this, by showing that an Au NP film at a DCE–water interface can efficiently act as a mirror for a laser beam (Figure 12B).<sup>114</sup> In a following work, Girault's group developed a methodology for accumulating Au NPs at the fluid interface (described above),<sup>35</sup> which was then expanded by systematically studying the effect of the type of organic solvent and lipophilic molecules dissolved in it, for applications as liquid mirrors and filters. The authors investigated under which conditions an optimal surface coverage could be achieved so that the NPs would form a monolayer. They found that decreasing the presence of unwanted 3D aggregates below the interface would enhance its optical response. The nature of the organic solvent influenced the response of the particle layers only slightly, while replacing the lipophilic molecule tetrathiafulvalene with neocuproine resulted in a variation of the interparticle spacing, with a consequent modification of the optical behavior. Overall, interfacial films formed by small Au NPs ( $D_p = 12$  nm) performed well as liquid-based optical band-pass filters, capable of reducing green and red light while transmitting blue light. Instead, assemblies of larger Au NPs ( $D_p = 38$  nm) were used as liquid mirrors, with a strong reflectance for red and green light.<sup>36</sup> The authors also stressed the self-healing nature of such monolayers, where self-healing here means that the NP film retains its metallic properties after substantial perturbations (i.e., mechanical shaking of the covered liquid drops). It is important to note that tetrathiafulvalene prevented the irreversible aggregation of particles at the liquid interface, which would diminish the optical properties. Instead, this molecule acted as both a glue and a lubricant, keeping the particle film intact in the case of vigorous shaking.

**Retrieving Structural Information from Optical Phenomena in 2D Particle Assemblies.** As mentioned earlier, the collective SPR phenomenon exhibited by self-assembled particles can give rise to, or enhance, optical effects. This in

turn can be exploited to obtain qualitative or even quantitative information about phenomena that take place on the micro- or nanoscale. Here, we highlight an illustrative example that exploits this principle, which can be used for analyte detection. The optical reflectance of a fluid interface strongly depends on the NP surface coverage. Therefore, its magnitude can be modulated either by controlling the number of added particles<sup>114</sup> or by acting on the interparticle repulsion (e.g., by tuning the pH and the concentration of electrolytes in the aqueous phase<sup>11</sup>). This allowed Edel and co-workers to design a “plasmonic ruler” in which the localized SPR peak could be directly correlated to the interparticle distance in the monolayer at an oil–water interface. In particular, a plasmon resonance shift toward longer wavelengths was achieved by increasing the concentration of NaCl in the aqueous phase. This was ascribed to the increased number of adsorbed particles and the decrease in the interparticle distance at the liquid interface due to lowering of the electrostatic repulsion. An increase in salt concentration to above 150 mM caused a further red shift, which was attributed to NP aggregation and the emergence of inhomogeneities in the monolayer. This effect was also visible by the naked eye, as the film transitioned from a faint color (i.e., a weakly reflective surface) below 40 mM NaCl to a glossy, highly reflective surface (40–150 mM) and finally to a matte appearance above 150 mM due to more diffuse reflection. A similar effect was later obtained by systematically varying the ionic strength in the organic phase with oil-soluble electrolytes.<sup>18</sup>

**Detecting Trace Analytes with Optical Methods.** Promising applications rely on the use of metallic NP monolayers as sensors of trace analytes in the bulk of one of the two liquids. One option is to use these assemblies as SERS sensors.<sup>17</sup> A close-packed structure is ideal for SERS detection as the electromagnetic field is enhanced in the space between close-packed spheres, increasing the SERS signal. The addition of NaCl (20 mM), at the appropriate pH, enabled Cecchini et al. to produce close-packed particle monolayers of citrate-stabilized Au NPs ( $D_p = 43$  nm) at a water–DCE interface.<sup>17</sup> Notably, emulsification was used to accumulate particles at the liquid interface and, at the same time, allowed the particles to capture trace molecules in one of the two liquids. This is exemplified by the SERS spectra shown in Figure 12C,D, obtained after capturing analytes from either the aqueous or the organic phase. Visible Raman signals of the analytes under investigation could be obtained only when the distance between adsorbed particles was precisely controlled. Therefore, a fine-tuning of the solution pH and electrolyte concentration was of utmost importance.

Recording SERS spectra from 2D particle assemblies requires elaborate equipment. Instead, other optical responses of metallic monolayers are easier to detect. For example, one can measure the optical reflectivity of fluid interfaces decorated with metal NPs. The reflected signal is dependent on the interparticle distance and fades away when the NPs are positioned at distances larger than their diameter. On the basis of this principle, Ma et al. developed a sensor for measuring the concentration of lead in solution.<sup>115</sup> Interestingly, in this example the analyte to be detected was also the additive for controlling particle adsorption and organization. NPs functionalized with glutathione ligands were used because glutathione efficiently binds to lead ions. In the absence of lead, only a few NPs were captured at a water–DCE interface after shaking. On the contrary, in the presence of lead, an emulsion was readily formed which, after settling, gave rise to a reflective liquid

interface. In this process, the glutathione-functionalized NPs first harvested lead ions from the solution. This caused a reduction of the ligand charges on the NPs and promoted their accumulation at the liquid interface. Successively, the lead ions in between the particles linked the neighboring surfaces together through the glutathione–Pb–glutathione binding, creating a strongly reflective NPs skin. A linear relationship between the lead concentration and reflectance was obtained up to a Pb concentration of 400 ppb (Figure 12E), after which a higher concentration of lead caused unwanted 3D aggregation. This allowed the authors to determine the concentration of lead in solution. Additionally, fitting the experimental spectra with a theoretical model was used to estimate the interparticle distance in the assembly and the surface coverage, both of which were proportional to the Pb concentration (Figure 12F).

These examples highlight some of the advantages of exploiting additive-driven NP assemblies for optics and sensing, which stem from the nature of fluid interfaces. Regarding analyte detection, the transfer from 3D to 2D allows for concentrating both particles and analytes, thus more dilute samples are required and traces of analytes can be detected. Moreover, they are applicable to additives and analytes soluble in numerous solvents, as they can be present in either the aqueous or the organic phase or in the vapor phase and nonetheless can be captured at the interface. Notably, the use of simple transport methods to accumulate and assemble particles at fluid interfaces (e.g., hand shaking) advantageously allows for implementing these systems in in-the-field devices readily usable by non-specialists. Concerning photonic applications, a major advantage is the ease of preparing particle-laden interfaces even at large scales. Surfaces used for manipulating light must have a flatness on the order of a fraction of light wavelengths. For traditional optical materials such as glass, this is usually achieved by polishing, which is time-consuming and costly. Fluid interfaces, on the contrary, are inherently flat. In particle-laden interfaces, roughness is largely defined by the NP position, and for small NPs, it can be much smaller than visible wavelengths. This, combined with their enhanced reflectivity due to the collective SPR effect, makes them ideal for photonics. These unique features are accompanied by the possibility to make such assemblies responsive to external stimuli, which is discussed in the following section.

#### Dynamic Colloid Assembly at Fluid Interfaces.

Research is nowadays going a step beyond in developing materials that are responsive to external stimuli.<sup>116</sup> This requires designing systems that switch in a fast and reliable manner between two or more states characterized by different properties. Such an achievement will enable the development of novel adaptive materials, the response of which (e.g., reflectivity, coloration, or analyte detection) can be triggered on demand, without needing to change the system composition. Recent examples have shown proof of principles of such systems at fluid interfaces, in which stimuli-responsive processes or additives are incorporated into the system to convert an otherwise inert dispersion into a platform responsive to external stimuli. These novel research directions open the way to future applications, where the advantages of reconfigurable and dynamic particle assembly are combined with the inherent properties of 2D structures at fluid interfaces.

**Assemblies Responsive to Chemical Stimulation.** Sashuk et al. devised an elegant system in which Au NPs ( $D_p = 8$  nm), spread at an air–water interface, assembled in a dynamic fashion in response to a chemical stimulus.<sup>117</sup> Tetrahydrofuran (THF)

vapors injected above the water surface were used as an additive to control the surface tension of the interface locally. The THF-rich regions had a lower  $\gamma$  than the pure air–water interface. In response to such  $\gamma$  gradients, the NPs accumulated and were compressed into a dense monolayer in the higher  $\gamma$  zones. These dense structures were stable only in the presence of  $\gamma$  gradients. When an equilibrium in the vapor composition above the surface was reached, NPs returned to their initial homogeneously dispersed state. Surface tension gradients and therefore localized islands with a high density of NPs were produced either by locally introducing THF vapor above the air–water surface or by removing the organic solvent from a THF-rich vapor–water interface by locally blowing air. This strategy was used to control the spatial distribution of NP assemblies reversibly in response to additives present in the vapor phase. Notably, the characteristic response time of the system was on the order of a few seconds.

**Assemblies Responsive to Stimulation by External Fields.** Compared to using chemicals, stimulation using external fields might offer additional, unique advantages. These include more precise spatial and temporal control of the self-assembly process and the possibility of adapting these strategies to real-world devices. One of the most promising examples that falls within the above category was reported by Edel and co-workers, who employed an electric field that acted as a switch of the self-assembly process. They developed a switchable liquid mirror based on the voltage-controlled accumulation/depletion of anionic Au NPs at the interface between two immiscible electrolyte solutions.<sup>6</sup> They were composed of 10 mM NaCl in the aqueous phase and DCE with 10 mM tetrabutylammonium tetraphenylborate as the organic phase. A negative polarization of the aqueous solution with respect to the organic phase allowed the NPs to accumulate at the liquid interface and form a dense layer with high reflectivity. Instead, switching the polarity of the applied potential drop across the interface caused the removal of particles from the liquid surface and a consequent decrease in the reflectivity. This allowed the authors to build an interface that served as a switchable window/mirror. In the absence of an adsorbed NP layer, the liquid interface allowed light transmission. In this “window state”, the interface was transparent, and objects placed below it could be clearly seen. (See the currency note in Figure 13A.) Upon accumulation of NPs, the interface reached a mirror state, reflecting incoming light rays (see the reflected image of a coin placed above the interface in Figure 13A). It is worth noting that the reversible adsorption/desorption of NPs was possible due to their small size ( $D_p = 16$  nm) and thus the relatively small adsorption energy. The time response of this electro-tunable mirror was somewhat slow ( $\sim 1000$  s); hence, further research is required to further develop this exceptionally interesting concept.

Light-responsive surfactants are a very interesting class of responsive additives, able to modify the particle surface properties and/or the surface tension of a fluid interface remotely, upon light irradiation.<sup>118</sup> These are surfactants with a light-switchable moiety, the isomeric state of which can be controlled by the absorption of photons. The different isomers, due to their different polarity, have different affinities for solid and liquid interfaces, making them ideal candidates for tuning interfacial properties with an external stimulus. An example is AzoTAB<sup>118</sup> (azobenzene trimethylammonium bromide), a molecule with an azobenzene moiety in the hydrophobic tail that reversibly converts from trans to cis upon UV irradiation (Figure 13B). Back conversion occurs at ambient temperature,

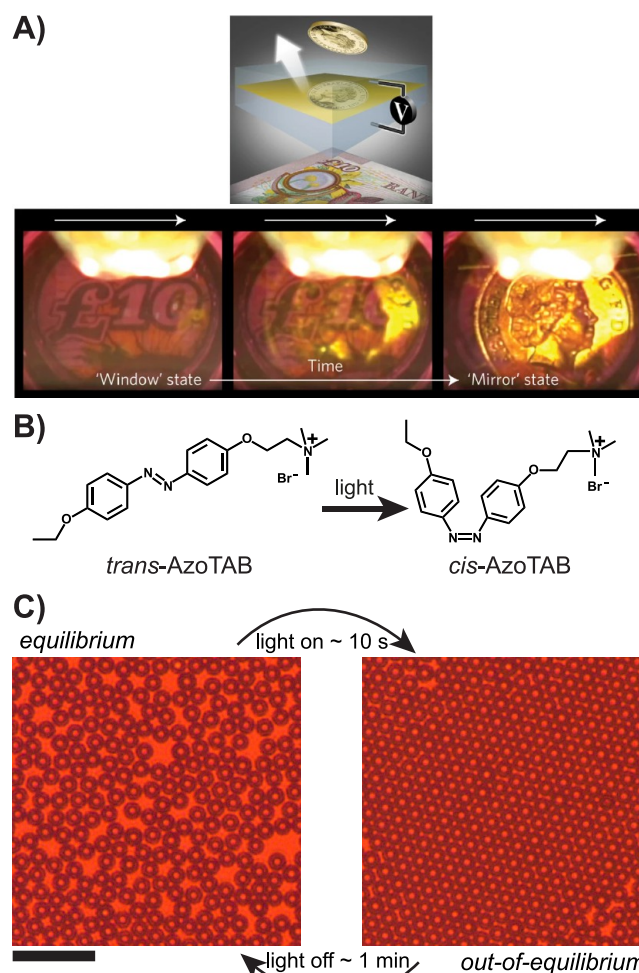


**Figure 13.** Reconfigurable 2D colloid assemblies: toward structures and functionality adaptable to external stimuli. (A) Top: schematic of an NP monolayer at the liquid interface in an electrochemical cell, with a currency note below and a coin above the interface. Bottom: images before (window state) and after (mirror state) the electrically induced assembly of the NPs at the interface. Adapted with permission from ref 6. Copyright 2017 Springer Nature. (B) Light-responsive surfactant AzoTAB. Light irradiation in the UV-blue range promotes isomerization from the trans to cis isomeric state. (C) Structure of a monolayer of anionic PS particles at the air–water interface, in the absence (left, equilibrium state) and presence (right, out-of-equilibrium crystalline state) of light irradiation. Scale bar: 25  $\mu\text{m}$ . (B, C) Adapted with permission from ref 9. Copyright 2019 John Wiley and Sons.

usually with slow kinetics, or is readily obtained with visible light irradiation. In the trans conformation, the surfactant tail is linear, and the molecule becomes apolar and hydrophobic. Instead, in the cis state the tail is bent and a dipole moment emerges, making AzoTAB polar and less hydrophobic.

By introducing AzoTAB into an aqueous suspensions of anionic NPs, Anyfantakis and Baigl developed a photosensitive colloidal system in which the tendency of the NPs to aggregate in the bulk and to adsorb at the air–water interface could be optically tuned on-demand.<sup>119</sup> This was achieved by irradiating these mixtures with light of different wavelengths, which reversibly (and dynamically) modulated the interactions between AzoTAB and the NPs. In the absence of UV light (dark state), different states of particle stickiness could be realized by varying the AzoTAB concentration. As for any oppositely charged surfactant/particle mixture (Figure 3), at

intermediate surfactant concentrations  $C_s$ , the surfactants adsorbed onto the particles, neutralizing them and causing a high affinity of the NPs for the fluid interface. Conversely, at lower or higher  $C_s$ , the particles were charged and tended to stay well dispersed. UV illumination reversibly shifted the behavior described above to higher surfactant concentrations because more *cis* than *trans* AzoTAB molecules were needed to achieve a certain number of surfactants adsorbed on the NPs. The particles were neutralized for  $C_s = 0.1$  and  $1$  mM for *trans*- and *cis*-AzoTAB, respectively. This was exploited to optically tune the CRE. The deposit obtained from a drying drop having constant particle and surfactant concentrations could have either a disk- or ring-shaped morphology, depending on the illumination conditions (UV irradiation versus dark state). For example, if the concentration of *trans*-AzoTAB was such that the particles adsorbed at the interface (neutral particles,  $C_s = 0.1$  mM  $\approx$  CMC  $\times 10^{-2}$ ), then the final deposit was a homogeneous disk. UV irradiation of the suspension prior to drying instead caused deposition into a ring shape due to an increase in the particle charge and consequent decreased affinity for the fluid interface.

Utilizing AzoTAB at micromolar concentrations ( $C_s = 0.01$  mM  $\approx$  CMC  $\times 10^{-3}$ ) allowed us to achieve, for the first time, the light-controlled dynamic assembly of PS particles at an air–water interface. We demonstrated that the 2D assembly could be reversibly switched between a disordered and a highly crystalline state upon on/off cycles of light irradiation (Figure 13C).<sup>9</sup> The surfactant concentration used was low enough to maintain highly charged particles. Prior to light excitation, an overall disordered aggregate was obtained by choosing a particle concentration below a given threshold to avoid 2D crystallization after particle adsorption at the fluid interface (cf. Figure 9A). Switching the light stimulus on induced desorption of the isomerized surfactants from the fluid interface, consequently increasing the electrostatic repulsion between particles. This in turn promoted particle crystallization due to confinement and local deformation of the liquid surface, with a characteristic time scale of  $\sim 10$  s. When the light was switched off, *trans*-AzoTAB from the bulk could adsorb again to repopulate the interface, decreasing the interparticle repulsion. As a result, the system transitioned to a disordered state triggered by interfacial particle diffusion that started at the location of the grain boundaries. This transition had a characteristic time scale of  $\sim 1$  min. This process, which is dependent on the dynamic adsorption/desorption of the surfactants at/from the air–water interface, could be cycled at will on a rapid time scale, independent of the kinetics of *trans*–*cis* and *cis*–*trans* isomerization. This is a remarkable paradigm of dissipative 2D colloid crystallization: the crystalline state is a metastable state reached only with a continuous energy supply provided by light irradiation, which depletes surfactants from the liquid surface.

Overall, further research is required to adapt these proof-of-principle systems to actual stimuli-responsive devices of practical interest. In particular, the systems responsive to external stimuli presented here, albeit showing very precise and not always straightforward responses to the external actuation, still need further development. This includes, for instance, the realization of the out-of-equilibrium crystallization of NPs commonly used for practical applications (e.g., metal NPs) or the implementation of much faster responses to the external stimulation. Nonetheless, they elegantly show how dynamic responses can be incorporated into colloid monolayers adsorbed at fluid interfaces, creating platforms with numerous

advantages compared to more conventional solid-state counterparts.

**Future Directions for Further Exploiting Additive-Controlled Colloid Organization at Fluid Interfaces for Practical Applications.** In the last part of this article, we focused on systems where additives (alone or combined with external fields) have been employed to drive the organization of particles into macroscopic materials with precisely tuned nanostructure and hence functionality. This general methodology fundamentally differs from the more common yet much more demanding strategy of using surface-modified particles to control their self-assembly.<sup>1</sup> Regardless of the particle surface properties, these systems are endowed with multiple advantages (highlighted above) with respect to similar solid-state devices, which stem from the employment of fluid interfaces.

However, tailoring on demand the surface properties of colloid particles necessitates excellent knowledge and the precise application of surface chemistry principles. Apart from requiring advanced experimental skills, such an approach may be costly, and it is usually hard to scale up for industrial-scale applications. In line with the emergent research direction of developing cost-effective and sustainable strategies for materials fabrication,<sup>120</sup> the use of additives can provide an interesting and efficient alternative. Considering the cost of materials, the addition of (small) amount of additives in colloidal suspensions is of particular interest because it allows for promoting the complete adsorption of particles to the fluid interface. This is an important achievement because it ensures that all particles are used to produce the desired structures, preventing material waste. Additionally, additives, by controlling particle–interface and particle–particle interactions, allow the obtaining of different functionalities in the final structures produced using the same building blocks. This is a concept of particular interest in materials science, as common materials may be used to produce a plethora of systems, from rigid interfaces for liquid printing<sup>30</sup> to films showing vivid structural colors.<sup>12,95</sup> Moreover, the shape of a fluid interface can be easily predefined (e.g., by choosing the appropriate experimental conditions<sup>22</sup>) or modified (e.g., by solvent evaporation<sup>96</sup>) to induce/modulate 2D colloid assembly. Therefore, combining interface shaping with the introduction of additives might open interesting avenues for fundamentally interesting and potentially useful paradigms of colloid self-organization.<sup>121</sup> Another step forward would be the implementation of stimuli-responsive additives,<sup>9,119</sup> which will enable the rational design of responsive assemblies. Instead of designing colloids with properties specific for each application, this may be possible using simple and already well-known building blocks.

In summary, these examples show that the additive-controlled self-organization of colloids in 2D can provide advantageous solutions to complex problems (e.g., inkjet printing,<sup>109</sup> light manipulation,<sup>36</sup> and analyte detection<sup>17</sup>). The multitude of intricate underlying phenomena calls for further investigation, making this topic exciting for fundamental research. At the same time, though, this strategy is in practice both simple and cost-effective, which may have a drastic impact in real-world applications.

## ■ CONCLUSIONS

As outlined in this Feature Article, controlling the adsorption and organization of colloid particles at fluid interfaces, by employing chemicals added in suspension, is receiving increasing attention not only in the field of foam/emulsion

stabilization<sup>10,53</sup> but also for fabricating 2D materials with precise order and composition. From a fundamental viewpoint, we underline the need to understand the rich physics and chemistry involved, especially in the presence of additives. This understanding is of paramount importance because it is a prerequisite for developing practical protocols for designing functional materials. From a materials science perspective, we envision the field developing in the following directions.

In phase with the esteemed development of “simple” material-fabrication techniques,<sup>120</sup> we believe that the discovery of formulations and methodologies that easily allow reaching such an objective will gain more and more interest, especially for nonspecialists. Understanding the precise effect of additives on particle–interface and particle–particle interactions can lead to preparing formulations that, combined with the most appropriate transport mechanism, allow for “simply mixing the suspension” to produce the desired materials. This is particularly useful when the colloid monolayer is just one out of many parameters in a given experiment. Having reliable formulations for producing such monolayers would allow researchers to focus on other aspects of their systems.<sup>104,122</sup> Additionally, it allows the easy implementation of these strategies for developing in-the-field devices.<sup>17</sup> The main advantage in this case is that accumulation and particle assembly into functional structures can be achieved by using simple procedures, such as mixing the suspension, or particle sedimentation.

Likewise, this acquired knowledge will open the way to developing methodologies and formulations applicable for industrial production, where reliable, fast, easy, and cheap strategies are always preferred. Specifically, spontaneous adsorption from a suspension is desirable for the continuous processing of particle monolayers, being a well-predicted and quantitative way to assemble the required materials. This will open the way to develop novel strategies applicable, for example, to the fabrication of surfaces endowed with a variety of properties (i.e., structural coloration, reflective, wetting, and adhesion) and of interest for different uses (i.e., coatings, sensing, and catalysis).

The field of dynamic self-assembly of particles at fluid interfaces, albeit providing substantial advantages and potential, is still in its infancy. Two recent Feature Articles reviewed the plethora of possibilities (from fundamental studies to applications) in reconfigurable and out-of-equilibrium colloidal assembly.<sup>116,123</sup> Combining such knowledge with the advantages that a fluid interface provides opens an avenue to novel exciting research directions. For instance, using photosensitive surfactants<sup>9</sup> to control the organization of NPs would be a straightforward way to produce assemblies with photoswitchable optical responses and thus novel reconfigurable photonic devices.

## ■ ASSOCIATED CONTENT

### SI Supporting Information

The Supporting Information is available free of charge at <https://pubs.acs.org/doi/10.1021/acs.langmuir.1c01029>.

Other mechanisms for transporting particles to a fluid interface; van der Waals interactions between suspended particles and a fluid interface; other interactions between suspended particles and a fluid interface; capillary interactions between nonspherical particles; and two-dimensional assemblies of polymer-stabilized particles at a fluid interface (PDF)

## ■ AUTHOR INFORMATION

### Corresponding Authors

**Jacopo Vialetto** – Laboratory for Soft Materials and Interfaces, Department of Materials, ETH Zürich, Zürich, Switzerland;

ORCID: [orcid.org/0000-0002-4617-4386](https://orcid.org/0000-0002-4617-4386);

Email: [jacopo.vialetto@mat.ethz.ch](mailto:jacopo.vialetto@mat.ethz.ch)

**Manos Anyfantakis** – Department of Physics and Materials Science, University of Luxembourg, Luxembourg L-1511,

Luxembourg; ORCID: [orcid.org/0000-0002-4572-5641](https://orcid.org/0000-0002-4572-5641);

Email: [anyfas.com@gmail.com](mailto:anyfas.com@gmail.com)

Complete contact information is available at:

<https://pubs.acs.org/10.1021/acs.langmuir.1c01029>

### Notes

The authors declare no competing financial interest.

### Biographies



Jacopo Vialetto studied chemistry (B.Sc.) at “La Sapienza” Univ. of Rome and photochemistry and molecular materials (M.Sc.) at the Univ. of Bologna (Italy). He received his Ph.D. from the École Normale Supérieure (Paris, France) under the supervision of Prof. Damien Baigl in 2018. Currently, he is a Marie Curie research fellow at ETH Zurich (Switzerland) in the laboratory of Prof. Lucio Isa. His research interests include the study of the interactions of hard and soft colloidal particles with and at fluid interfaces. In particular, he focuses on developing strategies to tailor colloidal self-assembly into functional structures through internal (added chemicals or tailored synthesis protocols) and/or external (light) control.



Manos Anyfantakis studied materials science (B.Sc.) and applied molecular spectroscopy (M.Sc.) at the University of Crete (UoC), Greece. He pursued his Ph.D. in polymer physical chemistry (2010) at UoC and the Max Planck Institute for Polymer Research, Germany, where he then returned for a postdoctoral position in interface science.

He next moved to ENS Paris, France, where he was a Marie Curie fellow with Prof. Baigl, working on various projects ranging from particle patterning to colloidal crystallization. He is now an independent FNR Core Jr fellow in the group of Prof. Lagerwall at the University of Luxembourg. His research lies at the boundary between curiosity-driven materials science and the exploitation of the emergent knowledge for practical solutions; he is currently interested in the self-organization of various soft, mesoscopic building blocks into macroscopic materials with tailored and/or tunable properties.

## ACKNOWLEDGMENTS

The authors thank Prof. Lucio Isa for fruitful discussions and comments on the manuscript. J.V. acknowledges funding from the European Union's Horizon 2020 research and innovation programme under Marie Skłodowska Curie grant agreement 888076. M.A. acknowledges support by the Luxembourg National Research Fund (CORE CORELIGHT grant, C18/MS/12701231).

## REFERENCES

- (1) Vogel, N.; Retsch, M.; Fustin, C.-A.; del Campo, A.; Jonas, U. Advances in Colloidal Assembly: The Design of Structure and Hierarchy in Two and Three Dimensions. *Chem. Rev.* **2015**, *115* (13), 6265–6311.
- (2) McGorty, R.; Fung, J.; Kaz, D.; Manoharan, V. N. Colloidal Self-Assembly at an Interface. *Mater. Today* **2010**, *13* (6), 34–42.
- (3) Kralchevsky, P. A.; Nagayama, K. Capillary Interactions between Particles Bound to Interfaces, Liquid Films and Biomembranes. *Adv. Colloid Interface Sci.* **2000**, *85* (2), 145–192.
- (4) Bresme, F.; Oettel, M. Nanoparticles at Fluid Interfaces. *J. Phys.: Condens. Matter* **2007**, *19* (41), 413101.
- (5) Xu, Y.; Konrad, M. P.; Trotter, J. L.; McCoy, C. P.; Bell, S. E. J. Rapid One-Pot Preparation of Large Freestanding Nanoparticle-Polymer Films. *Small* **2017**, *13* (2), 1602163.
- (6) Montelongo, Y.; Sikdar, D.; Ma, Y.; McIntosh, A. J. S.; Velleman, L.; Kucernak, A. R.; Edel, J. B.; Kornyshev, A. A. Electrotunable Nanoplasmonic Liquid Mirror. *Nat. Mater.* **2017**, *16* (11), 1127–1135.
- (7) Di Vitanonio, G.; Wang, T.; Haase, M. F.; Stebe, K. J.; Lee, D. Robust Bijels for Reactive Separation via Silica-Reinforced Nanoparticle Layers. *ACS Nano* **2019**, *13* (1), 26–31.
- (8) Binks, B. P. Particles as Surfactants—Similarities and Differences. *Curr. Opin. Colloid Interface Sci.* **2002**, *7* (1–2), 21–41.
- (9) Vialetto, J.; Anyfantakis, M.; Rudiuk, S.; Morel, M.; Baigl, D. Photoswitchable Dissipative Two-Dimensional Colloidal Crystals. *Angew. Chem., Int. Ed.* **2019**, *58* (27), 9145–9149.
- (10) Binks, B. P. Colloidal Particles at a Range of Fluid-Fluid Interfaces. *Langmuir* **2017**, *33* (28), 6947–6963.
- (11) Turek, V. A.; Cecchini, M. P.; Paget, J.; Kucernak, A. R.; Kornyshev, A. A.; Edel, J. B. Plasmonic Ruler at the Liquid-Liquid Interface. *ACS Nano* **2012**, *6* (9), 7789–7799.
- (12) Vialetto, J.; Rudiuk, S.; Morel, M.; Baigl, D. From Bulk Crystallization of Inorganic Nanoparticles at the Air/Water Interface: Tunable Organization and Intense Structural Colors. *Nanoscale* **2020**, *12* (11), 6279–6284.
- (13) Srivastava, S.; Nykypanchuk, D.; Fukuto, M.; Gang, O. Tunable Nanoparticle Arrays at Charged Interfaces. *ACS Nano* **2014**, *8* (10), 9857–9866.
- (14) Wang, H.; Singh, V.; Behrens, S. H. Image Charge Effects on the Formation of Pickering Emulsions. *J. Phys. Chem. Lett.* **2012**, *3* (20), 2986–2990.
- (15) Kaz, D. M.; McGorty, R.; Mani, M.; Brenner, M. P.; Manoharan, V. N. Physical Ageing of the Contact Line on Colloidal Particles at Liquid Interfaces. *Nat. Mater.* **2012**, *11* (2), 138–142.
- (16) Xu, Y.; Konrad, M. P.; Lee, W. W. Y.; Ye, Z.; Bell, S. E. J. A Method for Promoting Assembly of Metallic and Nonmetallic Nanoparticles into Interfacial Monolayer Films. *Nano Lett.* **2016**, *16* (8), 5255–5260.
- (17) Cecchini, M. P.; Turek, V. A.; Paget, J.; Kornyshev, A. A.; Edel, J. B. Self-Assembled Nanoparticle Arrays for Multiphase Trace Analyte Detection. *Nat. Mater.* **2013**, *12* (2), 165–171.
- (18) Velleman, L.; Sikdar, D.; Turek, V. A.; Kucernak, A. R.; Roser, S. J.; Kornyshev, A. A.; Edel, J. B. Tuneable 2D Self-Assembly of Plasmonic Nanoparticles at Liquid-Liquid Interfaces. *Nanoscale* **2016**, *8* (46), 19229–19241.
- (19) Williams, D. F.; Berg, J. C. The Aggregation of Colloidal Particles at the Air–Water Interface. *J. Colloid Interface Sci.* **1992**, *152* (1), 218–229.
- (20) Abdel-Fattah, A. I.; El-Genk, M. S. Sorption of Hydrophobic, Negatively Charged Microspheres onto a Stagnant Air/Water Interface. *J. Colloid Interface Sci.* **1998**, *202* (2), 417–429.
- (21) Sekido, T.; Kappl, M.; Butt, H.-J.; Yusa, S.; Nakamura, Y.; Fujii, S. Effects of PH on the Structure and Mechanical Properties of Dried PH-Responsive Latex Particles. *Soft Matter* **2017**, *13* (41), 7562–7570.
- (22) Anyfantakis, M.; Vialetto, J.; Best, A.; Auernhammer, G. K.; Butt, H.-J.; Binks, B. P.; Baigl, D. Adsorption and Crystallization of Particles at the Air–Water Interface Induced by Minute Amounts of Surfactant. *Langmuir* **2018**, *34* (50), 15526–15536.
- (23) Li, C.; Xu, Y.; Li, X.; Ye, Z.; Yao, C.; Chen, Q.; Zhang, Y.; Bell, S. E. J. Unexpected Dual Action of Cetyltrimethylammonium Bromide (CTAB) in the Self-Assembly of Colloidal Nanoparticles at Liquid-Liquid Interfaces. *Adv. Mater. Interfaces* **2020**, *7* (14), 2000391.
- (24) Anyfantakis, M.; Geng, Z.; Morel, M.; Rudiuk, S.; Baigl, D. Modulation of the Coffee-Ring Effect in Particle/Surfactant Mixtures: The Importance of Particle-Interface Interactions. *Langmuir* **2015**, *31* (14), 4113–4120.
- (25) Binks, B. P.; Rodrigues, J. A.; Frith, W. J. Synergistic Interaction in Emulsions Stabilized by a Mixture of Silica Nanoparticles and Cationic Surfactant. *Langmuir* **2007**, *23* (7), 3626–3636.
- (26) Binks, B. P.; Kirkland, M.; Rodrigues, J. A. Origin of Stabilisation of Aqueous Foams in Nanoparticle-Surfactant Mixtures. *Soft Matter* **2008**, *4* (12), 2373.
- (27) Deleurence, R.; Parneix, C.; Monteux, C. Mixtures of Latex Particles and the Surfactant of Opposite Charge Used as Interface Stabilizers – Influence of Particle Contact Angle, Zeta Potential, Flocculation and Shear Energy. *Soft Matter* **2014**, *10* (36), 7088–7095.
- (28) Maestro, A.; Guzmán, E.; Santini, E.; Ravera, F.; Liggieri, L.; Ortega, F.; Rubio, R. G. Wettability of Silicananoparticle-Surfactant Nanocomposite Interfacial Layers. *Soft Matter* **2012**, *8* (3), 837–843.
- (29) Cui, M.; Emrick, T.; Russell, T. P. Stabilizing Liquid Drops in Nonequilibrium Shapes by the Interfacial Jamming of Nanoparticles. *Science* **2013**, *342* (6157), 460–463.
- (30) Forth, J.; Liu, X.; Hasnain, J.; Toor, A.; Miszta, K.; Shi, S.; Geissler, P. L.; Emrick, T.; Helms, B. A.; Russell, T. P. Reconfigurable Printed Liquids. *Adv. Mater.* **2018**, *30* (16), 1707603.
- (31) Reincke, F.; Hickey, S. G.; Kegel, W. K.; Vanmaekelbergh, D. Spontaneous Assembly of a Monolayer of Charged Gold Nanocrystals at the Water/Oil Interface. *Angew. Chem., Int. Ed.* **2004**, *43* (4), 458–462.
- (32) Park, Y.-K.; Yoo, S.-H.; Park, S. Assembly of Highly Ordered Nanoparticle Monolayers at a Water/Hexane Interface. *Langmuir* **2007**, *23* (21), 10505–10510.
- (33) Li, Y.-J.; Huang, W.-J.; Sun, S.-G. A Universal Approach for the Self-Assembly of Hydrophilic Nanoparticles into Ordered Monolayer Films at a Toluene/Water Interface. *Angew. Chem., Int. Ed.* **2006**, *45* (16), 2537–2539.
- (34) Bigioni, T. P.; Lin, X.-M.; Nguyen, T. T.; Corwin, E. I.; Witten, T. A.; Jaeger, H. M. Kinetically Driven Self Assembly of Highly Ordered Nanoparticle Monolayers. *Nat. Mater.* **2006**, *5* (4), 265–270.
- (35) Smirnov, E.; Scanlon, M. D.; Momotenko, D.; Vrabel, H.; Méndez, M. A.; Brevet, P.-F.; Girault, H. H. Gold Metal Liquid-Like Droplets. *ACS Nano* **2014**, *8* (9), 9471–9481.
- (36) Smirnov, E.; Peljo, P.; Scanlon, M. D.; Gumy, F.; Girault, H. H. Self-Healing Gold Mirrors and Filters at Liquid-Liquid Interfaces. *Nanoscale* **2016**, *8* (14), 7723–7737.
- (37) Berg, J. C. *An Introduction to Interfaces and Colloids*; World Scientific: Singapore, 2009; pp 1–804.

- (38) Abdel-Fattah, A. I.; El-Genk, M. S. On Colloidal Particle Sorption onto a Stagnant Air–Water Interface. *Adv. Colloid Interface Sci.* **1998**, *78* (3), 237–266.
- (39) Duan, H.; Wang, D.; Kurth, D. G.; Möhwald, H. Directing Self-Assembly of Nanoparticles at Water/Oil Interfaces. *Angew. Chem., Int. Ed.* **2004**, *43* (42), 5639–5642.
- (40) Li, Y.; Yang, Q.; Li, M.; Song, Y. Rate-Dependent Interface Capture beyond the Coffee-Ring Effect. *Sci. Rep.* **2016**, *6* (1), 24628.
- (41) Lin, X.; Fang, G.; Liu, Y.; He, Y.; Wang, L.; Dong, B. Marangoni Effect-Driven Transfer and Compression at Three-Phase Interfaces for Highly Reproducible Nanoparticle Monolayers. *J. Phys. Chem. Lett.* **2020**, *11* (9), 3573–3581.
- (42) Garbin, V.; Crocker, J. C.; Stebe, K. J. Nanoparticles at Fluid Interfaces: Exploiting Capping Ligands to Control Adsorption, Stability and Dynamics. *J. Colloid Interface Sci.* **2012**, *387* (1), 1–11.
- (43) Deshmukh, O. S.; van den Ende, D.; Stuart, M. C.; Mugele, F.; Duits, M. H. G. Hard and Soft Colloids at Fluid Interfaces: Adsorption, Interactions, Assembly & Rheology. *Adv. Colloid Interface Sci.* **2015**, *222*, 215–227.
- (44) Israelachvili, J. N. *Intermolecular and Surface Forces*, 3rd ed.; Elsevier, 2010; pp 1–706.
- (45) Chaplin, M. Theory vs Experiment: What Is the Surface Charge of Water? *Water* **2009**, *1*, 1–28.
- (46) Ciunel, K.; Armélin, M.; Findenegg, G. H.; von Klitzing, R. Evidence of Surface Charge at the Air/Water Interface from Thin-Film Studies on Polyelectrolyte-Coated Substrates. *Langmuir* **2005**, *21* (11), 4790–4793.
- (47) Marinova, K. G.; Alargova, R. G.; Denkov, N. D.; Velev, O. D.; Petsev, D. N.; Ivanov, I. B.; Borwankar, R. P. Charging of Oil-Water Interfaces Due to Spontaneous Adsorption of Hydroxyl Ions. *Langmuir* **1996**, *12* (8), 2045–2051.
- (48) Mishra, H.; Enami, S.; Nielsen, R. J.; Stewart, L. A.; Hoffmann, M. R.; Goddard, W. A.; Colussi, A. J. Bronsted Basicity of the Air–Water Interface. *Proc. Natl. Acad. Sci. U. S. A.* **2012**, *109* (46), 18679–18683.
- (49) Williams, D. F. *Aggregation of Colloidal Particles at the Air–Water Interface*; University of Washington, 1991; pp 1–141.
- (50) Leunissen, M. E.; van Blaaderen, A.; Hollingsworth, A. D.; Sullivan, M. T.; Chaikin, P. M. Electrostatics at the Oil–Water Interface, Stability, and Order in Emulsions and Colloids. *Proc. Natl. Acad. Sci. U. S. A.* **2007**, *104* (8), 2585–2590.
- (51) Garbin, V.; Crocker, J. C.; Stebe, K. J. Forced Desorption of Nanoparticles from an Oil–Water Interface. *Langmuir* **2012**, *28* (3), 1663–1667.
- (52) Isa, L.; Amstad, E.; Schwenke, K.; Del Gado, E.; Ilg, P.; Kröger, M.; Reimhult, E. Adsorption of Core-Shell Nanoparticles at Liquid–Liquid Interfaces. *Soft Matter* **2011**, *7* (17), 7663.
- (53) Tran, L.; Haase, M. F. Templating Interfacial Nanoparticle Assemblies via in Situ Techniques. *Langmuir* **2019**, *35* (26), 8584–8602.
- (54) Binks, B. P.; Rodrigues, J. A. Double Inversion of Emulsions by Using Nanoparticles and a Di-Chain Surfactant. *Angew. Chem., Int. Ed.* **2007**, *46* (28), 5389–5392.
- (55) Ravera, F.; Santini, E.; Loglio, G.; Ferrari, M.; Liggieri, L. Effect of Nanoparticles on the Interfacial Properties of Liquid/Liquid and Liquid/Air Surface Layers. *J. Phys. Chem. B* **2006**, *110* (39), 19543–19551.
- (56) Gonzenbach, U. T.; Studart, A. R.; Tervoort, E.; Gauckler, L. J. Ultrastable Particle-Stabilized Foams. *Angew. Chem., Int. Ed.* **2006**, *45* (21), 3526–3530.
- (57) Binks, B. P.; Murakami, R. Phase Inversion of Particle-Stabilized Materials from Foams to Dry Water. *Nat. Mater.* **2006**, *5* (11), 865–869.
- (58) Binks, B. P.; Isa, L.; Tyowua, A. T. Direct Measurement of Contact Angles of Silica Particles in Relation to Double Inversion of Pickering Emulsions. *Langmuir* **2013**, *29* (16), 4923–4927.
- (59) Costa, L.; Li-Destri, G.; Thomson, N. H.; Konovalov, O.; Pontoni, D. Real Space Imaging of Nanoparticle Assembly at Liquid–Liquid Interfaces with Nanoscale Resolution. *Nano Lett.* **2016**, *16* (9), 5463–5468.
- (60) Devineau, S.; Anyfantakis, M.; Marichal, L.; Kiger, L.; Morel, M.; Rudiuk, S.; Baigl, D. Protein Adsorption and Reorganization on Nanoparticles Probed by the Coffee-Ring Effect: Application to Single Point Mutation Detection. *J. Am. Chem. Soc.* **2016**, *138* (36), 11623–11632.
- (61) Deegan, R. D.; Bakajin, O.; Dupont, T. F.; Huber, G.; Nagel, S. R.; Witten, T. a. Capillary Flow as the Cause of Ring Stains from Dried Liquid Drops. *Nature* **1997**, *389* (6653), 827–829.
- (62) Kettlewell, S. L.; Schmid, A.; Fujii, S.; Dupin, D.; Armes, S. P. Is Latex Surface Charge an Important Parameter for Foam Stabilization? *Langmuir* **2007**, *23* (23), 11381–11386.
- (63) Fujii, S.; Mochizuki, M.; Aono, K.; Hamasaki, S.; Murakami, R.; Nakamura, Y. PH-Responsive Aqueous Foams Stabilized by Hairy Latex Particles. *Langmuir* **2011**, *27* (21), 12902–12909.
- (64) Chai, Y.; Lukito, A.; Jiang, Y.; Ashby, P. D.; Russell, T. P. Fine-Tuning Nanoparticle Packing at Water–Oil Interfaces Using Ionic Strength. *Nano Lett.* **2017**, *17* (10), 6453–6457.
- (65) Nayak, S.; Fieg, M.; Wang, W.; Bu, W.; Mallapragada, S.; Vaknin, D. Effect of (Poly)Electrolytes on the Interfacial Assembly of Poly(Ethylene Glycol)-Functionalized Gold Nanoparticles. *Langmuir* **2019**, *35* (6), 2251–2260.
- (66) Kang, D. W.; Lim, J. H.; Park, B. J. Heterogeneous Interface Adsorption of Colloidal Particles. *Soft Matter* **2017**, *13* (36), 6234–6242.
- (67) Kim, K.; Han, H. S.; Choi, I.; Lee, C.; Hong, S.; Suh, S.; Lee, L. P.; Kang, T. Interfacial Liquid-State Surface-Enhanced Raman Spectroscopy. *Nat. Commun.* **2013**, *4* (1), 2182.
- (68) Lee, D.-G.; Cicuta, P.; Vella, D. Self-Assembly of Repulsive Interfacial Particles via Collective Sinking. *Soft Matter* **2017**, *13* (1), 212–221.
- (69) Stamou, D.; Duschl, C.; Johannsmann, D. Long-Range Attraction between Colloidal Spheres at the Air–Water Interface: The Consequence of an Irregular Meniscus. *Phys. Rev. E: Stat. Phys., Plasmas, Fluids, Relat. Interdiscip. Top.* **2000**, *62* (4), 5263–5272.
- (70) Chen, W.; Tan, S.; Ng, T.-K.; Ford, W. T.; Tong, P. Long-Ranged Attraction between Charged Polystyrene Spheres at Aqueous Interfaces. *Phys. Rev. Lett.* **2005**, *95* (21), 218301.
- (71) Reynaert, S.; Moldenaers, P.; Vermant, J. Control over Colloidal Aggregation in Monolayers of Latex Particles at the Oil–Water Interface. *Langmuir* **2006**, *22* (11), 4936–4945.
- (72) Park, B. J.; Pantina, J. P.; Furst, E. M.; Oettel, M.; Reynaert, S.; Vermant, J. Direct Measurements of the Effects of Salt and Surfactant on Interaction Forces between Colloidal Particles at Water–Oil Interfaces. *Langmuir* **2008**, *24* (5), 1686–1694.
- (73) Park, B. J.; Furst, E. M. Attractive Interactions between Colloids at the Oil–Water Interface. *Soft Matter* **2011**, *7* (17), 7676.
- (74) Aveyard, R.; Clint, J. H.; Nees, D.; Paunov, V. N. Compression and Structure of Monolayers of Charged Latex Particles at Air/Water and Octane/Water Interfaces. *Langmuir* **2000**, *16* (4), 1969–1979.
- (75) Aveyard, R.; Binks, B. P.; Clint, J. H.; Fletcher, P. D. I.; Horozov, T. S.; Neumann, B.; Paunov, V. N.; Annesley, J.; Botchway, S. W.; Nees, D.; Parker, A. W.; Ward, A. D.; Burgess, A. N. Measurement of Long-Range Repulsive Forces between Charged Particles at an Oil–Water Interface. *Phys. Rev. Lett.* **2002**, *88* (24), 246102.
- (76) Horozov, T. S.; Aveyard, R.; Clint, J. H.; Binks, B. P. Order-Disorder Transition in Monolayers of Modified Monodisperse Silica Particles at the Octane–Water Interface. *Langmuir* **2003**, *19* (7), 2822–2829.
- (77) Horozov, T. S.; Aveyard, R.; Binks, B. P.; Clint, J. H. Structure and Stability of Silica Particle Monolayers at Horizontal and Vertical Octane–Water Interfaces. *Langmuir* **2005**, *21* (16), 7405–7412.
- (78) Law, A. D.; Buzza, D. M. A.; Horozov, T. S. Two-Dimensional Colloidal Alloys. *Phys. Rev. Lett.* **2011**, *106* (12), 128302.
- (79) Dietrich, K.; Volpe, G.; Sulaiman, M. N.; Renggli, D.; Buttinoni, I.; Isa, L. Active Atoms and Interstitials in Two-Dimensional Colloidal Crystals. *Phys. Rev. Lett.* **2018**, *120* (26), 268004.
- (80) Masschaele, K.; Park, B. J.; Furst, E. M.; Franssaer, J.; Vermant, J. Finite Ion-Size Effects Dominate the Interaction between Charged



Colloidal Particles at an Oil–Water Interface. *Phys. Rev. Lett.* **2010**, *105* (4), 048303.

(81) Danov, K. D.; Kralchevsky, P. A. Forces Acting on Dielectric Colloidal Spheres at a Water/Nonpolar Fluid Interface in an External Electric Field. 2. Charged Particles. *J. Colloid Interface Sci.* **2013**, *405*, 269–277.

(82) Wirth, C. L.; Furst, E. M.; Vermant, J. Weak Electrolyte Dependence in the Repulsion of Colloids at an Oil–Water Interface. *Langmuir* **2014**, *30* (10), 2670–2675.

(83) Petkov, P. V.; Danov, K. D.; Kralchevsky, P. A. Surface Pressure Isotherm for a Monolayer of Charged Colloidal Particles at a Water/Nonpolar-Fluid Interface: Experiment and Theoretical Model. *Langmuir* **2014**, *30* (10), 2768–2778.

(84) Lotito, V.; Zambelli, T. Approaches to Self-Assembly of Colloidal Monolayers: A Guide for Nanotechnologists. *Adv. Colloid Interface Sci.* **2017**, *246*, 217–274.

(85) Park, B. J.; Vermant, J.; Furst, E. M. Heterogeneity of the Electrostatic Repulsion between Colloids at the Oil–Water Interface. *Soft Matter* **2010**, *6* (21), 5327.

(86) Rey, M.; Yu, T.; Guenther, R.; Bley, K.; Vogel, N. A Dirty Story: Improving Colloidal Monolayer Formation by Understanding the Effect of Impurities at the Air/Water Interface. *Langmuir* **2019**, *35* (1), 95–103.

(87) Ghezzi, F.; Earnshaw, J. C.; Finnis, M.; McCluney, M. Pattern Formation in Colloidal Monolayers at the Air–Water Interface. *J. Colloid Interface Sci.* **2001**, *238* (2), 433–446.

(88) Fernández-Toledano, J. C.; Moncho-Jordá, A.; Martínez-López, F.; Hidalgo-Álvarez, R. Spontaneous Formation of Mesostructures in Colloidal Monolayers Trapped at the Air–Water Interface: A Simple Explanation. *Langmuir* **2004**, *20* (17), 6977–6980.

(89) Vialetto, J. *Interface-Driven Soft Matter Systems: From 2D Particle Crystallization and Light-Responsive Assemblies to Magnet-Guided Fluid Transport*; Sorbonne Université: Paris, 2018; pp 1–226.

(90) Retsch, M.; Zhou, Z.; Rivera, S.; Kappl, M.; Zhao, X. S.; Jonas, U.; Li, Q. Fabrication of Large-Area, Transferable Colloidal Monolayers Utilizing Self-Assembly at the Air/Water Interface. *Macromol. Chem. Phys.* **2009**, *210* (3–4), 230–241.

(91) Srivastava, S.; Fukuto, M.; Gang, O. Liquid Interfaces with PH-Switchable Nanoparticle Arrays. *Soft Matter* **2018**, *14* (19), 3929–3934.

(92) Lotito, V.; Zambelli, T. Self-Assembly of Single-Sized and Binary Colloidal Particles at Air/Water Interface by Surface Confinement and Water Discharge. *Langmuir* **2016**, *32* (37), 9582–9590.

(93) Maestro, A.; Deshmukh, O. S.; Mugele, F.; Langevin, D. Interfacial Assembly of Surfactant-Decorated Nanoparticles: On the Rheological Description of a Colloidal 2D Glass. *Langmuir* **2015**, *31* (23), 6289–6297.

(94) Masschaele, K.; Franssaer, J.; Vermant, J. Direct Visualization of Yielding in Model Two-Dimensional Colloidal Gels Subjected to Shear Flow. *J. Rheol.* **2009**, *53* (6), 1437–1460.

(95) Vogel, N.; de Viguier, L.; Jonas, U.; Weiss, C. K.; Landfester, K. Wafer-Scale Fabrication of Ordered Binary Colloidal Monolayers with Adjustable Stoichiometries. *Adv. Funct. Mater.* **2011**, *21* (16), 3064–3073.

(96) Fujii, S.; Ryan, A. J.; Armes, S. P. Long-Range Structural Order, Moiré Patterns, and Iridescence in Latex-Stabilized Foams. *J. Am. Chem. Soc.* **2006**, *128* (24), 7882–7886.

(97) Velikov, K. P.; Durst, F.; Velev, O. D. Direct Observation of the Dynamics of Latex Particles Confined inside Thinning Water–Air Films. *Langmuir* **1998**, *14* (5), 1148–1155.

(98) Ramos, L. Surfactant-Mediated Two-Dimensional Crystallization of Colloidal Crystals. *Science* **1999**, *286* (5448), 2325–2328.

(99) Rey, M.; Law, A. D.; Buzzza, D. M. A.; Vogel, N. Anisotropic Self-Assembly from Isotropic Colloidal Building Blocks. *J. Am. Chem. Soc.* **2017**, *139* (48), 17464–17473.

(100) Rey, M.; Yu, T.; Bley, K.; Landfester, K.; Buzzza, D. M. A.; Vogel, N. Amphiphile-Induced Anisotropic Colloidal Self-Assembly. *Langmuir* **2018**, *34* (34), 9990–10000.

(101) Isa, L.; Kumar, K.; Müller, M.; Grolig, J.; Textor, M.; Reimhult, E. Particle Lithography from Colloidal Self-Assembly at Liquid–Liquid Interfaces. *ACS Nano* **2010**, *4* (10), 5665–5670.

(102) von Freymann, G.; Kitaev, V.; Lotsch, B. V.; Ozin, G. A. Bottom-up Assembly of Photonic Crystals. *Chem. Soc. Rev.* **2013**, *42* (7), 2528–2554.

(103) Vogel, N.; Belisle, R. A.; Hatton, B.; Wong, T.-S.; Aizenberg, J. Transparency and Damage Tolerance of Patternable Omniphobic Lubricated Surfaces Based on Inverse Colloidal Monolayers. *Nat. Commun.* **2013**, *4* (1), 2176.

(104) Kolle, M.; Salgard-Cunha, P. M.; Scherer, M. R. J.; Huang, F.; Vukusic, P.; Mahajan, S.; Baumberg, J. J.; Steiner, U. Mimicking the Colourful Wing Scale Structure of the Papilio Blumei Butterfly. *Nat. Nanotechnol.* **2010**, *5* (7), 511–515.

(105) Edel, J. B.; Kornyshev, A. A.; Urbakh, M. Self-Assembly of Nanoparticle Arrays for Use as Mirrors, Sensors, and Antennas. *ACS Nano* **2013**, *7* (11), 9526–9532.

(106) Toor, A.; Forth, J.; Bochner de Araujo, S.; Merola, M. C.; Jiang, Y.; Liu, X.; Chai, Y.; Hou, H.; Ashby, P. D.; Fuller, G. G.; Russell, T. P. Mechanical Properties of Solidifying Assemblies of Nanoparticle Surfactants at the Oil–Water Interface. *Langmuir* **2019**, *35* (41), 13340–13350.

(107) Zhang, Z.; Jiang, Y.; Huang, C.; Chai, Y.; Goldfine, E.; Liu, F.; Feng, W.; Forth, J.; Williams, T. E.; Ashby, P. D.; Russell, T. P.; Helms, B. A. Guiding Kinetic Trajectories between Jammed and Unjammed States in 2D Colloidal Nanocrystal–Polymer Assemblies with Zwitterionic Ligands. *Sci. Adv.* **2018**, *4* (8), No. eaap8045.

(108) Shi, J.; Yang, L.; Bain, C. D. Drying of Ethanol/Water Droplets Containing Silica Nanoparticles. *ACS Appl. Mater. Interfaces* **2019**, *11* (15), 14275–14285.

(109) Al-Milaji, K. N.; Secondo, R. R.; Ng, T. N.; Kinsey, N.; Zhao, H. Interfacial Self-Assembly of Colloidal Nanoparticles in Dual-Droplet Inkjet Printing. *Adv. Mater. Interfaces* **2018**, *5* (10), 1701561.

(110) Al-Milaji, K. N.; Radhakrishnan, V.; Kamekar, P.; Zhao, H. PH-Modulated Self-Assembly of Colloidal Nanoparticles in a Dual-Droplet Inkjet Printing Process. *J. Colloid Interface Sci.* **2018**, *529*, 234–242.

(111) Zhang, L.; Cha, D.; Wang, P. Remotely Controllable Liquid Marbles. *Adv. Mater.* **2012**, *24* (35), 4756–4760.

(112) Scanlon, M. D.; Smirnov, E.; Stockmann, T. J.; Peljo, P. Gold Nanofilms at Liquid–Liquid Interfaces: An Emerging Platform for Redox Electrocatalysis, Nanoplasmonic Sensors, and Electrovariable Optics. *Chem. Rev.* **2018**, *118* (7), 3722–3751.

(113) Yogeve, D.; Efrima, S. Novel Silver Metal Liquidlike Films. *J. Phys. Chem.* **1988**, *92* (20), 5754–5760.

(114) Fang, P.-P.; Chen, S.; Deng, H.; Scanlon, M. D.; Gummy, F.; Lee, H. J.; Momotenko, D.; Amstutz, V.; Cortés-Salazar, F.; Pereira, C. M.; Yang, Z.; Girault, H. H. Conductive Gold Nanoparticle Mirrors at Liquid/Liquid Interfaces. *ACS Nano* **2013**, *7* (10), 9241–9248.

(115) Ma, Y.; Sikdar, D.; He, Q.; Kho, D.; Kucernak, A. R.; Kornyshev, A. A.; Edel, J. B. Self-Assembling Two-Dimensional Nanophotonic Arrays for Reflectivity-Based Sensing. *Chem. Sci.* **2020**, *11* (35), 9563–9570.

(116) Solomon, M. J. Tools and Functions of Reconfigurable Colloidal Assembly. *Langmuir* **2018**, *34* (38), 11205–11219.

(117) Sashuk, V.; Winkler, K. Ž.; Ywociński, A.; Wojciechowski, T.; Górecka, E.; Fiałkowski, M. Nanoparticles in a Capillary Trap: Dynamic Self-Assembly at Fluid Interfaces. *ACS Nano* **2013**, *7* (10), 8833–8839.

(118) Baigl, D. Photo-Actuation of Liquids for Light-Driven Microfluidics: State of the Art and Perspectives. *Lab Chip* **2012**, *12* (19), 3637.

(119) Anyfantakis, M.; Baigl, D. Dynamic Photocontrol of the Coffee-Ring Effect with Optically Tunable Particle Stickiness. *Angew. Chem., Int. Ed.* **2014**, *53* (51), 14077–14081.

(120) Tian, X.; Lind, K. R.; Yuan, B.; Shaw, S.; Siemianowski, O.; Cademartiri, L. Simplicity as a Route to Impact in Materials Research. *Adv. Mater.* **2017**, *29* (17), 1604681.

(121) Ershov, D.; Sprakel, J.; Appel, J.; Cohen Stuart, M. a.; van der Gucht, J. Capillarity-Induced Ordering of Spherical Colloids on an

Interface with Anisotropic Curvature. *Proc. Natl. Acad. Sci. U. S. A.* **2013**, *110* (23), 9220–9224.

(122) Grillo, F.; Fernandez-Rodriguez, M. A.; Antonopoulou, M.-N.; Gerber, D.; Isa, L. Self-Templating Assembly of Soft Microparticles into Complex Tessellations. *Nature* **2020**, *582* (7811), 219–224.

(123) van Ravensteijn, B. G. P. P.; Voets, I. K.; Kegel, W. K.; Eelkema, R. Out-of-Equilibrium Colloidal Assembly Driven by Chemical Reaction Networks. *Langmuir* **2020**, *36* (36), 10639–10656.